

The zebrafish (*Danio rerio*) as a model system to investigate *Candida albicans* device-associated infections

Shannen Deconinck

Promotor: Prof. P. Van Dijck

Co-promotor: Dr. Soňa Kucharikova

Proefschrift ingediend tot het

behalen van de graad van

Master of Science in Biochemie/biotechnologie

Academiejaar 2014-2015

© Copyright by KU Leuven

Without written permission of the promotors and the authors it is forbidden to reproduce or adapt in any form or by any means any part of this publication. Requests for obtaining the right to reproduce or utilize parts of this publication should be addressed to KU Leuven, Faculteit Wetenschappen, Geel Huis, Kasteelpark Arenberg 11 bus 2100, 3001 Leuven (Heverlee), Telephone +32 16 32 14 01.

A written permission of the promotor is also required to use the methods, products, schematics and programs described in this work for industrial or commercial use, and for submitting this publication in scientific contests.

Acknowledgements

First of all, I would like to thank Prof. Dr. Patrick Van Dijck for giving me the opportunity to do my master thesis in his research group. I was very pleased to work on this exciting project and thanks to his feedback during the weekly *Candida* meetings, we all had a boost of positive energy to continue our experiments. I also would like to thank Prof. Dr. Johan Thevelein for making use of the Molecular Cell Biology facilities to execute my experiments. Furthermore, I would like to thank both of my readers, Prof. Dr. Joris Winderickx and Dr. Mekonnen Demeke for reading and judging my project.

A very special word of thanks goes to my co-promotor Dr. Soňa Kucharíková who taught me a lot of new techniques. Her patience is admirable and because of her friendliness it was a pleasure to work with her. She shared all her ideas and knowledge with me and corrected my drafts very carefully.

The researchers, staff and my fellow students also receive a huge word of thanks for making the working environment a thousand times more pleasant. They helped me whenever I was desperate. I also want to thank them for their patience when I took possession of the confocal microscope, often for days long.

For making use of the equipment of the aquatic facility, I would like to thank Dr. Kathleen Lambaerts. She guided us through the whole zebrafish injection process and was available to answer our questions.

Last but not least, I also want to thank the most important people in my life, my family and my boyfriend for their enormous patience and support during this exciting but sometimes quite exhausting period.

List of Abbreviations

ALS: Agglutinin- Like Sequence

C. albicans: *Candida albicans*

CFU: colony forming units

CLSM: confocal laser scanning microscopy

CWPs: Cell Wall Proteins

Dpf: day(s) post fertilization

FBS: fetal bovine serum

GPI: glycosylphosphatidylinositol

GUT: gastrointestinal induced transition

HGC1: Hyphal G cyclin 1

Hpf: hour(s) post fertilization

Hpi: hour(s) post injection

HWP: Hyphal Wall Protein

HYR: hyphally upregulated protein

IFF: IPF family F

MTL: mating- type locus

PBS: phosphate buffered saline

pc: compensation pressure

pi: injection pressure

PLs: phospholipases

Rpm: revolutions per minute

RPMI: Roosevelt Park Memorial institute

Saps: secreted aspartyl proteases

ti: injection time

WT: wild type

XTT: 2, 3-bis (2-methoxy-4-nitro-5-sulfophenyl)-2H-tetrazolium-5-carboxanilide

YPD: yeast peptone dextrose

Table of contents

Literature study.....	1
1. Main characteristics of <i>Candida albicans</i>	1
2. <i>C. albicans</i> virulence factors.....	2
2.1. Iron acquisition.....	3
2.2. Yeast-to-hyphae transition.....	3
2.3. Adhesins.....	4
2.4. Phenotypic switching.....	6
2.5. Hydrolytic enzymes.....	7
3. <i>C. albicans</i> biofilm development.....	8
4. Models to study <i>C. albicans</i> biofilm formation <i>in vitro</i> and <i>in vivo</i>	10
4.1. <i>In vitro</i> model systems.....	10
4.2. <i>In vivo</i> model systems.....	11
5. The zebrafish (<i>Danio rerio</i>) as a host model organism to study infections caused by <i>C. albicans</i>	13
5.1. Life cycle and developmental stages.....	13
5.2. Advantages of the zebrafish.....	16
5.3. Disadvantages of the zebrafish.....	18
5.4. The zebrafish as a host model to study <i>Candida albicans</i> infection.....	18
5.5. Routes of administration.....	21
Aims.....	23
Materials.....	24
1. Media.....	24
1.1. YPD media.....	24
1.1.1. YPD (yeast peptone dextrose) medium.....	24
1.1.2. YPD medium with penicillin/streptomycin cocktail.....	24
1.2. Glucose (40%).....	24
1.3. Roosevelt Park Memorial Institute Medium (RPMI- 1640 medium) buffered with 0.165 mol/L MOPS.....	24
1.4. 10 x PBS buffer (Phosphate Buffered Saline).....	25
1.5. 1 x PBS buffer (Phosphate Buffered Saline).....	25
1.6. Egg water (system water with methylene blue).....	25
1.7. Anesthesia and euthanasia of zebrafish larvae.....	25
Methods.....	26
1. <i>In vitro</i> experimental procedures.....	26
1.1. <i>C. albicans</i> cells and microspheres enumeration using a hemocytometer.....	26
1.2. Preparation of microspheres.....	26

1.2.1.	Types of microspheres	26
1.2.2.	Preparation of microspheres for <i>in vitro</i> experiments	27
1.2.3.	Preparation of microspheres for <i>in vivo</i> experiments.....	28
1.3.	Preparation of <i>Candida</i> strains.....	28
1.3.1.	<i>C. albicans</i> strains used in this study.	28
1.3.2.	Preparation of <i>C. albicans</i> strains for <i>in vitro</i> experiments.....	28
1.3.3.	Preparation of <i>C. albicans</i> strains for <i>in vivo</i> experiments.....	29
1.4.	Detection of fluorescence signal intensity of microspheres and <i>C. albicans</i> strains.....	29
1.5.	<i>In vitro C. albicans</i> biofilm formation on borosilicate chambers and on polyethylene discs in the presence or absence of microspheres.....	29
2.	<i>In vivo</i> experimental procedure.....	29
2.1.	Zebrafish lines	29
2.2.	Zebrafish maintenance and care.....	29
2.3.	Zebrafish injection.....	32
2.3.1.	Pulling the capillaries	32
2.3.2.	Open the capillaries	33
2.3.3.	Calibration of the needles	33
2.3.4.	Injection of <i>C. albicans</i> cells and microspheres into zebrafish embryos	34
2.3.5.	Survival of zebrafish larvae.....	36
3.	<i>In vitro</i> biofilm quantification methods.....	36
3.1.	Biofilm formation on 96-well plate	36
3.2.	XTT.....	36
3.3.	Confocal laser scanning microscopy (CLSM).....	37
4.	<i>In vivo</i> biofilm quantification methods	37
4.1.	Confocal laser scanning microscopy.....	37
4.2.	Homogenization and CFUs.....	37
4.3.	Statistics	38
Results	39
1.	Determination of the fluorescence signal of red and green microspheres	39
2.	Characterization of the fluorescence signal of <i>C. albicans</i> GFP- and yCherry- tagged strains with and without microspheres.....	39
3.	<i>In vitro</i> biofilm formation on 96 well polystyrene plate	42
4.	<i>In vitro</i> biofilm formation of <i>C. albicans</i> strains on polyethylene discs in the presence or absence of fluorescent microspheres.....	43
5.	Unravel the injection volume and the size of microspheres.....	48
6.	Zebrafish survival upon injection of microspheres at different concentrations into the yolk.....	49

7. <i>C. albicans</i> injection and follow-up of the survival of zebrafish embryos	52
8. <i>C. albicans</i> device-associated infection in zebrafish embryos.....	59
Discussion.....	67
References.....	75
Addendum A: Risk analysis	A-1
Addendum B: Additional figures of dead embryos upon WT-GFP and <i>bcr1Δ/bcr1Δ</i> -GFP injection into the yolk of 1-cell stage zebrafish embryos.	B-3
Addendum C: Statistical significance after 1 and 2 days of <i>Candida</i> -yCherry and spheres and <i>Candida</i> -GFP and spheres injection into 1- cell stage zebrafish embryos.....	C-4
Addendum D: Survival experiment of <i>Candida</i> -yCherry and microspheres injection.....	D-5
.....	D-6
.....	D-6

Samenvatting

In de natuur komen micro-organismen zelden voor als planktoncellen, maar vormen liever driedimensionale, beschermende structuren, biofilms genaamd. Eén van de meest voorkomende humane pathogenen is *Candida albicans* (*C. albicans*) en dit organisme is in staat om biofilms te vormen op verscheidene biotische en abiotische substraten. In ziekenhuizen kan de vorming van biofilms op medische apparatuur zoals vasculaire katheters, dialyse katheters in het buikvlies en oculaire lenzen leiden tot een disseminatie in de bloedstroom met hoge mortaliteit tot gevolg.

Deze huidige studie focuste vooral op *C. albicans* apparatuur-geassocieerde infecties ontwikkeld in de zebravis als een model organisme. De zebravis biedt tal van voordelen zoals de transparantie en de aanwezigheid van een aangeboren en verworven immuunsysteem. Dankzij de aanwezigheid van immuniteit, kan de menselijke omgeving nagebootst worden.

Onze resultaten toonden aan dat de zebravis larven geschikte modelorganismen zijn om op grote schaal apparatuur-geassocieerde infecties te bestuderen. Een interessant aspect was dat deze larven niet meteen onderhevig waren aan de infectie en zelfs in sommige gevallen tot 6 dagen lang konden overleven. We hebben ook ontdekt dat de larven sneller stierven wanneer we mutante *C. albicans* stammen in combinatie met de microsferen van polystyreen injecteerden, dan wanneer we stammen injecteerden zonder de microsferen. Daarnaast hebben we ook nog één experiment uitgevoerd met als doel de immunrespons van de zebravis larven op de apparatuur-geassocieerde infecties te bestuderen. Deze preliminaire data toonden aan dat macrofagen in staat waren om de gistcellen te fagocyteren maar konden de infectie veroorzaakt door hyfen niet elimineren. Verder onderzoek zal cruciaal zijn om de rol van het immuunsysteem tijdens *C. albicans* apparatuur-geassocieerde infecties verder op te helderen.

Summary

In nature, microorganisms exist rarely as planktonic cells and prefer to create three-dimensional, protective structures also known as biofilm. One of the most prevalent human fungal pathogens is *Candida albicans* (*C. albicans*). This organism is capable of forming biofilms on a variety of biotic and abiotic substrates. In a hospital setting, the formation of biofilms on medical devices such as vascular catheters, peritoneal dialysis catheters and ocular lenses leads to dissemination of *C. albicans* into the bloodstream causing systemic infections with high mortality.

The present study mainly focused on *C. albicans* device-associated infections developed inside the zebrafish as a host model organism. The zebrafish offers a lot of advantages, one of them is its transparency and the presence of an innate and adaptive immune system. The presence of the immunity strongly mimics the situation in the human body.

Our results indicated that zebrafish larvae are suitable model organisms for studying high-throughput device-associated infections. Interestingly, the larvae did not immediately succumb to the infection, and in some cases they survived up to 6 days. Moreover, we discovered that when injecting *C. albicans* mutant strains together with a substrate such as polystyrene microspheres, the larvae died more rapidly than in the absence of microspheres. Additionally, we performed one experiment to check the immune response of the zebrafish larvae to a *Candida* device-associated infection. These preliminary data showed that macrophages are able to phagocytose yeast cells but are not capable of eliminating an infection caused by *Candida* hyphal cells, which disseminated inside the embryo. Further data and experiments will be crucial to elucidate the role of the immune system during *C. albicans* device-associated infections.

Literature study

1. Main characteristics of *Candida albicans*

C. albicans belongs to the *Saccharomycetaceae* family of ascomycete fungi and is distantly related to *Saccharomyces cerevisiae* (*S. cerevisiae*). An abnormality in its genetic code, in which the CUG codon encodes for serine instead of leucine, makes this species together with other related species, such as *Candida parapsilosis* (*C. parapsilosis*) and *Candida tropicalis* (*C. tropicalis*), genetically distinctive. *C. albicans* is a commensal fungal species colonizing human mucosal surfaces such as the gastrointestinal tract, oral and vaginal mucosa (Kim & Sudbery, 2011). However, in patients with impaired immune system (e.g. HIV infection), it can become an opportunistic pathogen, causing mucosal and life-threatening disseminated infections with high mortality rate (Shirliff et al., 2009; Mayer et al., 2013). Together with *Staphylococcus aureus* (*S. aureus*), *Candida* belongs to the leading nosocomial (hospital-acquired) pathogens causing high morbidity and mortality (Peters et al., 2012). Among all *Candida* species, *C. albicans* is one of the best-studied human fungal pathogens.

C. albicans is known to grow in three distinctive morphological structures: yeast, pseudohyphae and true hyphae (Kim & Sudbery, 2011). Both hyphae and pseudohyphae (i.e. filamentous forms) are invasive, which can further promote tissue penetration during the early stages of infection (Sudbery et al., 2004; Mayer et al., 2013). Because hyphae have the tendency to adhere and penetrate to host tissue, they are more responsible for mucosal infections (e.g. oral candidiasis) (Peters et al., 2012). Moreover, these filamentous forms are also important for the colonization of organs, for example kidneys, causing deep-seeded infections. The yeast form, on the contrary might be more suited for dissemination in the bloodstream and systemic disease (Sudbery et al., 2004). Bloodstream infection caused by *C. albicans* is called 'candidemia'. Such an infection may further lead to the colonization of internal organs, a condition that is known as 'disseminated candidiasis'. Both of them represent extremely serious medical and clinical problems (Kim & Sudbery, 2011). Most dimorphic fungal pathogens, with a life cycle that includes a saprophytic environmental phase (such as *Histoplasma capsulatum*, *Paracoccidioides brasiliensis*, *Penicillium marneffei* and *Blastomyces dermatitidis*) exist as filamentous fungi in the external environment, whereas in infected tissues they proliferate by budding. *C. albicans*, on the contrary, has no terrestrial life cycle and can grow as a yeast and/or filamentous form in the host (Gow et al, 2012).

Another important feature of *C. albicans* represents a lack of a complete sexual cycle (no conventional meiosis has been observed) and until recently it was thought that *Candida* exists only as an obligate diploid organism (Forche et al., 2008). However, a robust mating system has been discovered in *C. albicans* (figure 1), in which mating occurs between mating type-like a and α strains leading to an a/α tetraploid strain (Forche et al., 2008).

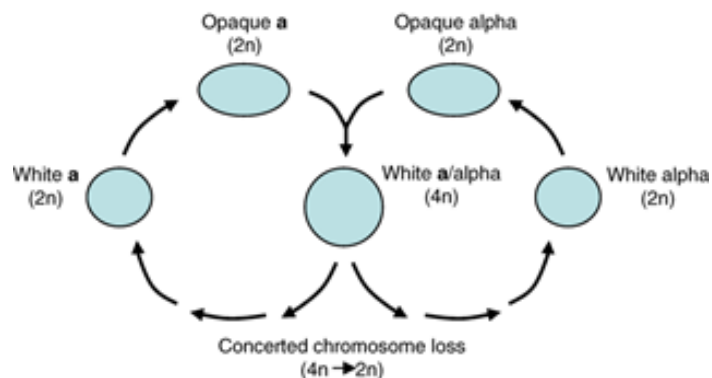


Figure 1: *Candida albicans* parasexual cycle. First, white MTL α and MTL a switch to the opaque state upon mating and formation of a tetraploid a/α cell. Mating in *C. albicans* is regulated by phenotypic switching, whereby MTL homozygous *C. albicans* cells can reversibly switch between the white and opaque state. This physiological switch from the standard ‘white’ (oval form) to the ‘opaque’ (oblong form) phase is a requirement in order to have diploid mating, leading to tetraploids. Under some stress conditions, tetraploid strains could return to the diploid state via a parasexual mechanism, accompanied with chromosome loss. Many of the progeny strains are aneuploid strains (often trisomic for one or more chromosomes) rather than true diploids (Forche et al., 2008; Berman, 2012).

The homozygous cells for the mating- type locus (MTL) have the potential to mate after the switch from ‘white’ to ‘opaque’ phase. The alteration of generations from diploids to tetraploids and reverse to diploids without the usual meiosis, is known as the parasexual cycle (Berman, 2012).

Among the *Candida* species and next to *C. albicans*, *C. glabrata* together with *C. parapsilosis* and *C. tropicalis*, are responsible for approximately 65%-75% of all systemic diseases (Brunke & Hube, 2013). *C. glabrata* is more closely related to the baker’s yeast *S. cerevisiae* and unlike *C. albicans*, only appears in the yeast form (Brunke & Hube, 2013).

2. *C. albicans* virulence factors

C. albicans virulence factors include the host recognition and binding of the latter organism to host cells and host proteins reduces the extent of clearance by the host (Calderone & Fonzi, 2001). The factors that enable *C. albicans* to switch from commensal to pathogen include host recognition biomolecules (adhesins), morphogenesis, secreted aspartyl proteases (Saps), phospholipases (PLs) and phenotypic switching (Calderone & Fonzi, 2001; Kuo et al., 2013; Demuyser et al., 2014). Among these factors, the yeast-to-hyphae transition is considered as one of the most crucial virulence factors for *C. albicans* pathogenesis (Kuo et al., 2013). The

development of mechanisms to acquire or reduce access to metals also contributes to the pathogenicity of *C. albicans*.

2.1. Iron acquisition

The ability of *C. albicans* to acquire iron from the host tissues is a major contributing factor to the virulence of pathogenic microorganisms. To date, iron is the most widely investigated transition metal (Mayer et al., 2013). *C. albicans* is able to utilize hemin and hemoglobin as iron sources (Kuo et al., 2013). Studies have shown that pre-treatment of endothelial cells with an iron chelator can diminish *C. albicans* damage (Kuo et al., 2013). Another study of iron acquisition during an oral infection, indicated that *C. albicans* utilizes the host ferritin as an iron source. Moreover, only the hyphae and not the yeast cells were found to bind ferritin and this binding was crucial for iron acquisition of ferritin (Jacobsen et al., 2012).

2.2. Yeast-to-hyphae transition

As it has been already stated above, *C. albicans* is known to undergo yeast-to-hyphae transition (Bonhomme & d'Enfert, 2013). The phenomenon described as reversible transition between unicellular yeast cells and filamentous growth forms - pseudohyphae and hyphae- is called morphogenesis (Calderone & Fonzi, 2001) (Figure 2).

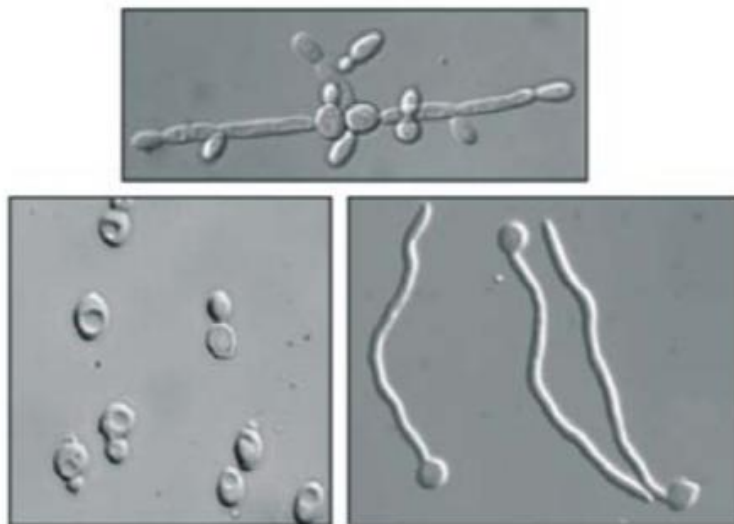


Figure 2: Light microscopy images of cells with hyphae (bottom right), pseudohyphae (top) and yeast morphologies (bottom left) (Kim & Sudbery, 2011).

As it is shown in figure 2, unicellular yeasts grow by budding while in the case of pseudohyphae, the daughter cell remains attached to the mother cell. This results in filaments composed of elongated cells with restrictions at the septa. In comparison with pseudohyphae,

true hyphae have no restrictions at the septal junctions and consist out of chains of tube-like cells (Kim & Sudbery, 2011).

Hyphal growth is promoted by a number of environmental factors such as 37 °C growth temperature, the presence of serum, neutral pH, high CO₂, growth in embedded conditions and N-acetylglucosamine (Kim, 2011 and Mayer, 2013). Yeast cells prefer to grow at 30°C and in acidic pH (pH 4.0). Pseudohyphal growth occurs at conditions such as 35°C or pH 5.5 (Kim & Sudbery, 2011; Mayer et al., 2013).

Hyphal growth is characterized by the expression of several genes. The main hyphae-specific genes are *HGC1* (Hyphal G Cyclin 1), *UME6*, *ALS3* (Agglutinin- Like sequence 3), *HWP1* (Hyphal Wall Protein 1) and *ECE1*. *HGC1* is important in polarized growth and is necessary for hyphal morphogenesis. Deletion of *HGC1* results in the failure of *Candida* to form hyphae and thus the cells only grow as a yeast form (Mayer et al., 2013). In a mouse model of systemic infection, the *hgc1* Δ/Δ mutant was attenuated supporting the hypothesis that hyphal formation is an important virulence property (Mayer et al., 2013). *ALS3* encodes a cell wall surface protein and is highly expressed in the hyphal stage of growth. *HWP1* is essential for normal growth of the mycelium. Both *ALS3* and *HWP1* are important genes during biofilm formation (see section 2.3). *ECE1* is a specific hyphal gene encoding a membrane protein and is expressed during the growth of the mycelium (Fan et al., 2013). One of the transcription factors that is activated by a signal transduction pathway and that regulates the morphological outcome is *UME6*. Down-regulation of *UME6* results in pseudohyphal growth, while up-regulation induces hyphal growth (Kim & Sudbery, 2011). In addition, *C. albicans* strains lacking both *CPH1* and *EFG1* are unable to form hyphae or pseudohyphae and are avirulent in a mouse model (Lo et al., 1997). A reduced *EFG1* expression resulted in a failure to form true hyphae but not pseudohyphae (Lo et al., 1997). Moreover, there are three well-known hyphae-related pathways; MAP kinase and cyclic AMP signalling pathways and the polarized cell growth pathway (Kuo et al., 2013).

2.3. Adhesins

Adhesins represent a class of Cell Wall Proteins (CWPs), which are crucial for a host pathogen interaction and for an attachment of a microorganism to biotic or abiotic surfaces (Demuyser et al., 2014). CWPs, found on the outer layer of the cell wall, are attached to the inner layer (which contains chitin and β -1, 3-glucan) predominantly by glycosylphosphatidylinositol (GPI) remnants, which are linked to the skeletal polysaccharides through β -1,6-glucan (Gow et al., 2012). Adhesins promote the adherence of *C. albicans* to host cells or host ligands (Calderone & Fonzi, 2001) and they have two distinct domains: the N-terminus, which mediates the

interaction with other molecules and the C-terminus, which attaches the protein indirectly to the glucan moiety of the cell wall (Demuyser et al., 2014).

The most studied adhesin gene families are *ALS* (Agglutinin- Like Sequence), *HWP* (Hyphal Wall Protein) and *IFF/HYR* (IPF family F/ hyphally up-regulated protein). The *ALS* gene family contains eight agglutinin-like sequence (Als) proteins (ALS1 - ALS7 and ALS9), which play very important roles in biofilm formation and in adherence to abiotic surfaces (Liu & Filler, 2011; Demuyser et al., 2014). Als1, Als3 and Als5 are involved in attachment of *Candida* cells to multiple host constituents including oral epithelial cells, while Als6 and Als9 do not (Zhu & Filler, 2010). *C. albicans* ALS3 (key target under the control of BCR1) showed to play an important role in *in vitro* biofilm formation, because an *als3/als3* mutant produced rudimentary biofilms on catheters (Nobile et al., 2006; Liu & Filler, 2011). Moreover, the *als3/als3* deletion strain was not defective in hyphal formation under hyphae inducing conditions (Nobile et al., 2006). However, this deletion strain was able to form sufficient biofilms in a rat central venous catheter model indicating that Als3 is not absolutely required for biofilm formation *in vivo* (Nobile et al., 2006). Some other functions are cell-cell interactions, invasion of host tissue and iron acquisition, in which Als3 is the only involved as transferrin receptor (Demuyser et al., 2014). ALS1, another member of the *ALS* gene family, has been described as a cell surface protein, which may affect *C. albicans* filamentation process (Fu et al., 2002). An *als1/als1* mutant produced substantial biofilm *in vitro* and *in vivo* (Nobile et al., 2006; Nobile et al., 2008). Strains lacking all functional ALS1 and ALS3 alleles (*als1/als1 als3/als3*), failed to produce any adherent cells in an *in vivo* catheter model and simultaneous observations were observed for an *in vitro* model indicating that *C. albicans* needs at least two functional ALS1 or ALS3 alleles to produce biofilm (Nobile et al., 2008).

Another important adhesin represents Hwp1p. *HWP1* has a significant role in adhesion and biofilm development and is expressed on the surface of *C. albicans* hyphae (Zhu & Filler, 2010; de Groot et al., 2013). It has been shown that the *hwp1/hwp1* mutant has a partial biofilm defect *in vitro* and a severe biofilm defect *in vivo* (Nobile et al., 2008). Moreover, the mutant displayed reduced virulence in a mouse model of disseminated candidiasis (Mayer et al., 2013). *HWP1* encodes for an outer surface mannoprotein (Calderone & Fonzi, 2001) and is well known as a substrate for the host transglutaminases and as such permits covalent attachment of *C. albicans* to epithelial cells (Nobile et al., 2008; Zhu & Filler, 2010).

The last class of the three most studied adhesin gene families is the Iff/Hyr family. This family is also important in adhesion process because up-regulation of *IFF4*, for example, led to increased adherence of *C. albicans* to plastic and epithelial cells. In addition, both up-regulation and down-regulation of *IFF4* resulted in an attenuation of virulence in animal models, suggesting the requirement of a specific expression level for maximal virulence. Iff11 and Hyr1

are two hyphae specific proteins, whereby deletion of *IFF11* results in cell wall alterations, therefore indicating its role in cell organization and/or enzymatic function. The molecular substrates of the Iff/Hyr family have not been identified, yet. Finally, Hyr1 seems to play a role in resistance to neutrophil killing and the use of anti-Hyr1 antibodies resulted in immunity to disseminated candidiasis in mice (de Groot et al., 2013).

2.4. Phenotypic switching

One of the most well-characterized phenotypic switch in *C. albicans* is a transition from the white state to the opaque state. Strains that are homozygous for the MTL undergo a switch between smooth, white colonies and flat, grey (opaque) colonies (Sudbery et al., 2004). This process is believed to be under the epigenetic control (Sudbery et al., 2004; Kim & Sudbery, 2011). The two colony types differ in several characteristics; white cells are round, while opaque cells are elongated, opaque cells have pimples on the cell wall surface and are twice the size of the white-phase cells and white cells germinate at 37°C, pH 6.7, but opaque cells do not. Freshly isolated strains from vaginitis or systemically infected patients have higher frequency of switching, but the role of phenotypic switching in the virulence of *C. albicans* remains doubtful (Calderone & Fonzi, 2001). *C. albicans* pathogenicity, mating behaviour and biofilm formation is influenced by the differential regulation of more than 450 genes between white and opaque states. White cells, for example, have shown to be more virulent in a mouse tail-vein systemic infection model, while opaque cells colonize the skin in a cutaneous infection model more efficiently (Alby & Bennett, 2009). Moreover, white and opaque cells behave differently in their interaction with immune cells. In comparison with opaque cells, white cells do secrete a chemo-attractant for leukocytes. Furthermore, there seems to be a difference in the level of phagocytosis for both white and opaque cells and hence the white-opaque switching may be a possible mechanism for *C. albicans* to circumvent the host immune system (Alby & Bennett, 2009). Pande et al. (2013) showed that the *C. albicans* transition from commensal to pathogenic state is not only the consequence of an impaired immune system, but also the change of cell identity seems to play a role in the infection process. Additionally, they described a new cell type, under the control of *WOR1* (a transcription factor and master regulator of white-opaque switch), which is responsible for the commensal lifestyle of *C. albicans*. The passage of *C. albicans* wild-type cells through the mouse gastrointestinal tract triggers the expression of *WOR1* and consequently causing a developmental switch to a commensal cell type, named GUT (gastrointestinal induced transition). These GUT cells differ from the previous defined cell types (such as white and opaque cells) in morphology and functionality. There seems to be an optimization of the GUT cell metabolism upon encountering the mammalian digestive tract, which contributes to the success of the commensal lifestyle of *C. albicans* (Pande et al., 2013).

2.5. Hydrolytic enzymes

Secreted hydrolases are virulence factors that contribute to invasion of host tissues and avoidance of host defence mechanisms. In addition, their secretion is proposed to facilitate the extracellular nutrient acquisition (Schaller et al., 2005; Mayer et al., 2013). It is also known that such enzymes are able to attack the host immune system, thereby leading to antimicrobial resistance. Most of these enzymes are secreted extracellularly by the fungus. The Saps are the most crucial hydrolytic enzymes, whereas only little is known about the physiological role of the PLs. Saps invade host tissue by digesting or destroying cell membranes and by degrading the host surface molecules (Schaller et al., 2005). These proteases enable the pathogen to use protein as a sole source of nitrogen. The role of Saps as a virulence factor was proven by the fact that fungal isolates from individuals with oral diseases showed higher Sap activity than that recorded for isolates from healthy individuals (Schaller et al., 2005). In *Candida*, around 10 *SAP* genes have been identified. Sap 2, for example, is able to degrade extracellular matrix and host surface proteins such as fibronectin, collagen, mucin and laminin. In addition, Sap2 can also hydrolyse several host defence proteins (e.g. salivary lactoferrin, enzymes of the respiratory burst of macrophages and almost all immunoglobulins). In *C. albicans*, distinct differences in pH optima were found between the proteases.

A second group hydrolytic enzymes are the PLs. These enzymes have the ability to hydrolyse one or more ester linkages in glycerophospholipids. They consist out of four different classes (A, B, C and D) and only the five members of the B class (PLB1-5) are extracellular and may contribute to pathogenicity by host membrane disruption (Mayer et al., 2013). Phospholipids are the major components of biological membranes and are a target for various PLs (Schaller et al., 2005). The role of PLs during *Candida* infection tends to be host cell penetration and membrane damage, adhesion to epithelial cells, penetration and possibly also an interaction with the host signal transduction pathway (Schaller et al., 2005; Mohandas & Ballal, 2011).

A last group that contributes to the infection process represents the lipases and esterases. The lipases consist of 10 members (LIP1-10). A mutant strain *lip8* Δ/Δ had reduced virulence in a mouse model of systemic infection, indicating that the lipases play a role in *C. albicans* pathogenicity (Mayer et al., 2013). Esterases and lipases are able to catalyse the hydrolysis of ester bonds of mono-, di- and triacylglycerols or even phospholipids (Schaller et al., 2005). However, they differ in their ability to act on soluble substrates. Lipases hydrolyse ester bonds at the interface between the insoluble triacylglycerol phase and the aqueous phase in which the enzyme is dissolved, while esterases act on soluble substrates (Schaller et al., 2005).

3. *C. albicans* biofilm development

Another important virulence factor represents the ability of *C. albicans* to develop biofilms (Mayer et al., 2013). In comparison with planktonic (“free-living”) cells, biofilms are communities of microorganisms that proliferate on living or inert surfaces and are enclosed in an extracellular matrix, forming a three-dimensional architecture (Bonhomme & d'Enfert, 2013). *C. albicans* is able to form biofilms on abiotic surfaces, as well as on the host tissue causing an array of infections (Demuyser et al., 2014). Biofilm infections can be caused by either single microbial species or by a mixture of bacterial and fungal species. It is estimated that around 65-80% of all infections are biofilm-related (Coenye & Nelis, 2010; Bonhomme & d'Enfert, 2013). Biofilm formation on medical devices such as catheters, ocular lenses, prosthetic heart valve and joint replacements, allow the fungus to gain access to the bloodstream resulting in dissemination and systemic disease (Douglas, 2003; Ricicova et al., 2010; Demuyser et al., 2014). A well-known example of a natural biofilm is dental plaque on tooth surfaces (Douglas, 2003). However, biofilms can cause also detrimental effects on environment as their formation in drinking water reservoirs and distribution systems impedes the system’s efficiency (Coenye & Nelis, 2010). The first step of biofilm formation is the adherence of yeast cells to a solid surface (figure 3). Next, basal layers of yeast microcolonies are formed which anchor each microcolony to the surface. After morphogenesis has occurred, a dense layer of cells of mixed morphology, embedded in extracellular polymeric substances, is produced. The last step of biofilm formation is the maturation in a three-dimensional structure and cell dispersion (Douglas, 2003; Bonhomme & d'Enfert, 2013).

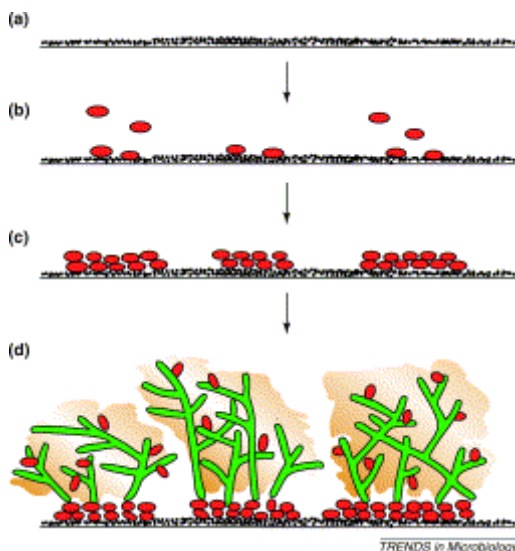


Figure 3: Formation of a *C. albicans* biofilm on a polyvinylchloride (PVC) catheter surface. (a) A film of host proteins is formed on the catheter surface. (b) Adhesion of yeast cells to the surface. (c) Formation of basal layers of yeast microcolonies. (d) Formation of the extracellular matrix and maturation into a three-dimensional structure with water channels allowing circulation of nutrients (Douglas, 2003).

Cells in a biofilm display phenotypes distinct from free-floating cells, including their reduced susceptibility to antimicrobial agents (Kucharikova et al., 2013, Kucharikova et al., 2011 and Nobile et al., 2006). Studies have shown that the biofilm extracellular matrix plays an important role in the tolerance to antifungals such as azoles and polyene classes (Nett et al., 2010b; Bonhomme & d'Enfert, 2013; Mitchell et al., 2015). Other processes that play a role in tolerance are cell density, overexpression of drug targets, expression of efflux pumps or the occurrence of persister cells (phenotypic variants of the wild type (WT) that are highly tolerant) (LaFleur et al., 2006; Bonhomme & d'Enfert, 2013). The production of persister cells together with the withstanding of host immune responses, has made the need for improved drug therapies crucial (Christensen et al., 2007; Shirliff et al., 2009). Despite of the increased tolerance to antifungals, some anti-biofilm activity with the liposomal formulation of amphotericin B (Ramage et al., 2013) and two echinocandins (caspofungin and micafungin) has been demonstrated (Douglas, 2003; Kucharikova et al., 2010; Kucharikova et al., 2013).

Because of the presence of different cell types (yeast, hyphae and pseudohyphae) in a biofilm and the three-dimensional structure, fungal biofilms are assumed to be heterogeneous environments. Biofilms of *C. albicans* create a hypoxic environment and adaptation to hypoxia is a necessity for biofilm formation (Bonhomme & d'Enfert, 2013). It has also been observed that cells in the deepest layer of the biofilm survive starvation or oxidative stress due to changes in sulfur assimilation as sulfur amino acids contribute to the synthesis of antioxidant molecules (Bonhomme & d'Enfert, 2013).

Gene expression analyses and microarray studies revealed some genes, which were highly expressed in this process. For example, transcription factor *BCR1* has been shown to play a significant role in *C. albicans* biofilm development (Nobile et al., 2006). Deletion strain *C. albicans bcr1Δ/bcr1Δ* formed only rudimentary biofilm *in vitro* and also *in vivo* (Nobile et al., 2006). More importantly, this strain did not demonstrate any difficulties to switch from yeast-to-hyphae. Further studies have indicated that the surface protein Als3 (known as an adhesin) is a Bcr1 target and that absence of Als3 causes a biofilm defect *in vitro* and not *in vivo* (Nobile et al., 2005). Moreover, deletion of the Tec1p transcription factor, results in a defect in producing hyphae *in vitro* and in biofilm formation (Nobile et al., 2006). Moreover, the deletion of two transcription factors *EFG1* and *CPH1*, which are involved in *C. albicans* morphogenesis (Chao et al., 2010), exhibited only monolayers of elongated yeast cells scattered on the surface (Lo et al., 1997).

4. Models to study *C. albicans* biofilm formation *in vitro* and *in vivo*

4.1. *In vitro* model systems

As *C. albicans* biofilms are often considered to be the reason for an increased tolerance of device-associated cells to antimicrobial agents, biofilm model systems are essential to gain better insights in the mechanisms involved in biofilm formation (Coenye & Nelis, 2010; Tournu & Van Dijck, 2011). Several *in vitro* and *in vivo* models have been introduced including both advantages and disadvantages. So far, there is no single, ideal model system (McBain, 2009). *C. albicans* can colonize and develop biofilms on a variety of prosthetic materials such as polystyrene, polyvinylchloride (PVC), silicon and polycarbonate surfaces (Shinde et al., 2011). The frequent use of prosthetic devices in immunocompromised patients resulted in increased incidence of device-related biofilm infections caused by *C. albicans*. These infections may further lead to deep-seeded bloodstream infections (Shinde et al., 2011). It should be emphasized that the physical and chemical nature of the contact surface is also an important factor, besides the cell properties, as it is known to influence adhesion as well as biofilm formation (Shinde et al., 2011).

A most common *in vitro* biofilm model system is the flat bottom 96-well polystyrene plate. Inside polystyrene wells, biofilms can grow on either the walls or on the bottom of the plate. Eventually, substrate made of different material, such as catheters, discs and beads can be placed inside the wells of the microtiter plate (Pierce et al., 2008; Coenye & Nelis, 2010). Quantification of the biofilm is achieved after a washing step to remove non-device-associated cells (Mc Bain, 2009). This system provides numerous advantages e.g. they are user-friendly, cheap and a large number of tests can be performed simultaneously. Disadvantageous remains the fact that microtiter plates are closed systems lacking a natural flow in or out the plate consequently causing changes in the environment surrounding the cells (depletion of nutrients, accumulation of molecules, etc.) during the experiment. This problem can be partially solved by refreshing the medium regularly or by using flow displacement systems, for example BioFlux system (Coenye & Nelis, 2010). These latter systems are 'open' systems allowing growth medium with nutrients to be continuously added and waste products to be continuously removed.

As mentioned earlier, biofilms can also be formed on biotic surfaces such as mucosal surfaces (Kim & Sudbery, 2011). Although it is very difficult to mimic this situation it can be partially studied by using human cell lines. *C. albicans* can be inoculated on reconstituted human epithelia and as a consequence a biofilm-like structure will be formed on top of the epithelial layer resulting in a superficial tissue infection model (Coenye & Nelis, 2010). To mimic systemic infections, an *in vitro* flow adhesion assay has been set up. Immortalized human microvascular endothelial cells were coated on a glass slide and placed in a flow chamber that is perfused

with a *C. albicans* suspension. This situation mimicked the flow, which occur within blood vessels (Coenye & Nelis, 2010).

A disadvantage of the systems mentioned above is the absence of the commensal flora and the lack of the immune response to the biofilm-associated infections. Therefore, several *in vivo* biofilm models have been established to study *C. albicans* biofilm development. These models are discussed below.

4.2. *In vivo* model systems

In vitro biofilm assays can't mimic a complex *in vivo* environment (Brothers & Wheeler, 2012), so it is critical to find a proper model system to perform biofilm infection studies.

The murine and rat models are the most commonly used small animals for *C. albicans* biofilm research (Coenye & Nelis, 2010). A first vertebrate biofilm model system is the central venous catheter (CVC) system (Andes et al., 2004, Lazzell et al., 2009). It has been demonstrated that biofilm formation on CVCs can lead to considerable morbidity and mortality with the dissemination into the blood and kidneys. With this model, small catheter pieces are inserted into the jugular vein of rats or mice. These models have been used to study *in vivo* susceptibility and molecular response to fluconazole treatment, the effect of amphotericin B and of various antifungal compounds (caspofungin, chitosan) (Coenye & Nelis, 2010; Lazzell et al., 2009).

A second model, a rodent oral denture model, was established by Nett et al. (2010a) and mimicks human denture stomatitis. Denture stomatitis is the most common form of oral candidiasis and involves biofilm growth on oral prosthetic surfaces. This model was used to characterize biofilm formation, architecture, and drug resistance of *C. albicans* and mixed oral bacterial species. Next to the oral denture model, Nett et al. (2014) also set-up a rodent model to study urinary catheter associated *C. albicans* biofilm formation and utilized this model to test the efficacy of antifungals.

A fourth model that has been adapted is the subcutaneous foreign body infection model (Riccova et al., 2010). In this model, materials, e. g. small catheter pieces can either be infected prior to the implant or the animals can be infected post-implant. Importantly, up to 9 catheter fragments can be implanted per rat (Riccova et al., 2010). In comparison with the CVC model, which is based on the catheter implant of one single piece of plastic, subcutaneous model allows us to study 9 devices. When using the subcutaneous model, the limited factors remain: the lack of blood flow and the incidence of the inflammatory response associated with surgery in the presence of the foreign body (Coenye & Nelis, 2010). This may lead to the inhibition of the *C. albicans* biofilm development. In order to diminish such response

and to allow *Candida* cells to proliferate and to form biofilms, we often impair the immune system by partial immunosuppression of the animals (presence of dexamethasone in the drinking water) (Racicova et al., 2010). This model has been also successfully used to test the effect of novel and existing compounds on early and later stages of biofilm development (Bink et al., 2012; Kucharikova et al., 2010; Kucharikova et al., 2013). Subcutaneous foreign body infection models are particularly established to study the effect of substrates on biofilm formation.

Next to these models, a murine peritonitis model was optimized to assess the effect of monomicrobial versus polymicrobial infection with two commonly isolated peritonitis pathogens, *C. albicans* and *S. aureus*. Peritonitis is an inflammatory disease caused by insertion of medical devices such as peritoneal dialysis catheters (Peters & Noverr, 2013).

Irrespective of the numerous murine model systems, the need of other vertebrate models has become of great importance. It is impossible to perform high-throughput screening when using small laboratory animals. Moreover, the use of these model systems requires biofilm analysis post-mortem and consequently a large number of animals are sacrificed per experiment. In our laboratory, we have partially solved a problem of animal sacrifice when studying certain time points of biofilm development by bioluminescence imaging (BLI). For these experiments the *Gaussia princeps* gene (*gLUC*) has been successfully transformed to *C. albicans* (Vande Velde et al., 2014; Kucharikova et al., 2015) and has made BLI of *C. albicans* biofilms. The *in vivo* biofilm development has been explored in a subcutaneous catheter model. They could successfully monitor and quantify the *in vivo* biofilm development on the implanted catheters, indicating that BLI can be used as an easy, cost-effective and rapid screening method. Recently, the zebrafish (*Danio rerio*) has been increasingly used for *C. albicans* research and allows for easy spatio-temporal imaging (Chao et al., 2010; Gratacap et al., 2014).

Some additional models that have been established to study *C. albicans* systemic disease are the wax moth (*Galleria mellonella*), the fruit fly (*Drosophila melanogaster*), and the nematode (*Caenorhabditis elegans*) (Chao et al., 2010). These systems have several advantages in common, such as conserved innate immunity, advanced molecular tools, inexpensive housing, and a high-throughput drug-screening platform (Chao et al., 2010). These minihosts have been used to unravel the virulence mechanism of *C. albicans* disseminated infection. However, such model organisms have major differences when compared with the human immune system, for example the lack of adaptive immunity (Chao et al., 2010). Accordingly, there is a need for other models to reveal the complex mechanisms of fungal pathogenesis.

5. The zebrafish (*Danio rerio*) as a host model organism to study infections caused by *C. albicans*

5.1. Life cycle and developmental stages

The zebrafish (*Danio rerio*) is a tropical freshwater fish belonging to the minnow family (Cyprinidae) of the order Cypriniformes (ray-finned fish) (Reed & Jennings, 2011). The name zebrafish is derived from the stripes that are present on the side of the body. The fishes have five alternating blue-black and silver-yellow stripes containing two types of pigment cells, melanophores and iridophores and xantophores and iridophores, respectively (Reed & Jennings, 2011). The zebrafish has a total lifespan of 5.5 years and is widely distributed in shallow, slow-flowing waters on the Indian subcontinent (EOL Encyclopedia of life, 2015). Male fish have a yellowish belly and are leaner than females, which are more silver-like. The zebrafish expressed rapid development and a short generation time of 3 to 4 months. The life cycle of zebrafish is demonstrated on figure 4.

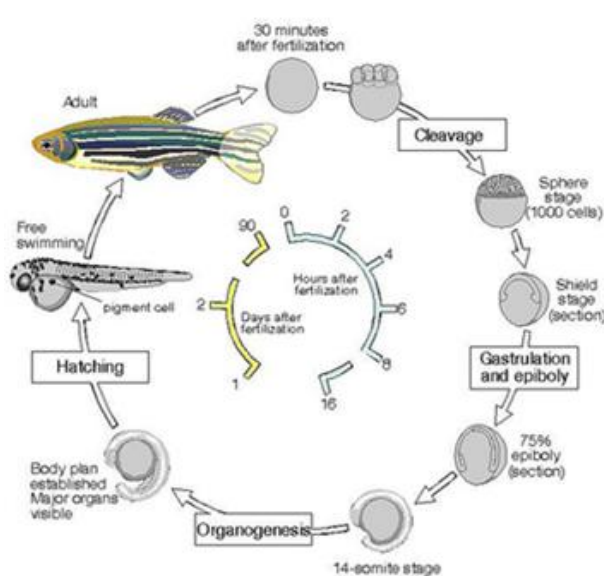


Figure 4: Zebrafish life cycle. Zebrafish have a short generation time of approximately 3 months. In the first 24 h after fertilization, all major organs are formed and within 3 days the fishes hatch and initiate the search for food. After 3-4 months, the fishes are sexually mature and can generate new offspring (Bopp et al., 2006; Staveley, 2015).

Zebrafish are known to have high fertility and fertilization occurs externally (Bopp et al., 2006). When the egg was not fertilized, the growth stopped after the first few cell divisions and they appeared more turbid. Fertilized eggs immediately became transparent, which makes the zebrafish a very useful research model organism (Chao et al., 2010). Females can spawn every 2 to 3 days and large progeny sizes are achieved (up to hundreds of eggs per clutch) (Reed & Jennings, 2011). The eggs have a diameter of 0.6 - 0.7mm, while the length of the

larvae can vary between 3.5 and 6 mm. In terms of size, adult fish are still small organisms ranging from 3-4 cm long (Bopp et al., 2006; EOL Encyclopedia of life, 2015).

In the past decade, the zebrafish became a very popular model organism for several research fields, for example developmental biology, toxicology, oncology, etc. Prof. George Streisinger is considered as the founding father of zebrafish and description of its developmental stages and genetic background (Sullivan & Kim, 2008). In 1981, Streisinger et al. developed methods to produce homozygous strains and performed mutagenesis studies. These findings led to the increased usage of zebrafish embryos in different research areas (EOL Encyclopedia of life, 2015).

Zebrafish are very useful organisms for genetic studies, because the existence of morpholino – antisense technology was used to reduce expression of the particular gene (Chao et al., 2010). Moreover, the construction of transgenic lines of zebrafish to study the function of specific genes is considered as an easier procedure. Furthermore, mutagenesis screens have led to the identification of hundreds of genes controlling vertebrate development (EOL Encyclopedia of life, 2015).

Kimmel et al. (1995) described a series of stages for the development of the embryo. These stages are grouped into larger time-blocks, which are called periods. There are seven broad periods of embryogenesis defined; the zygote, cleavage, blastula, gastrula, segmentation, pharyngula, and hatching periods. The different developmental stages of zebrafish are demonstrated in figure 5.

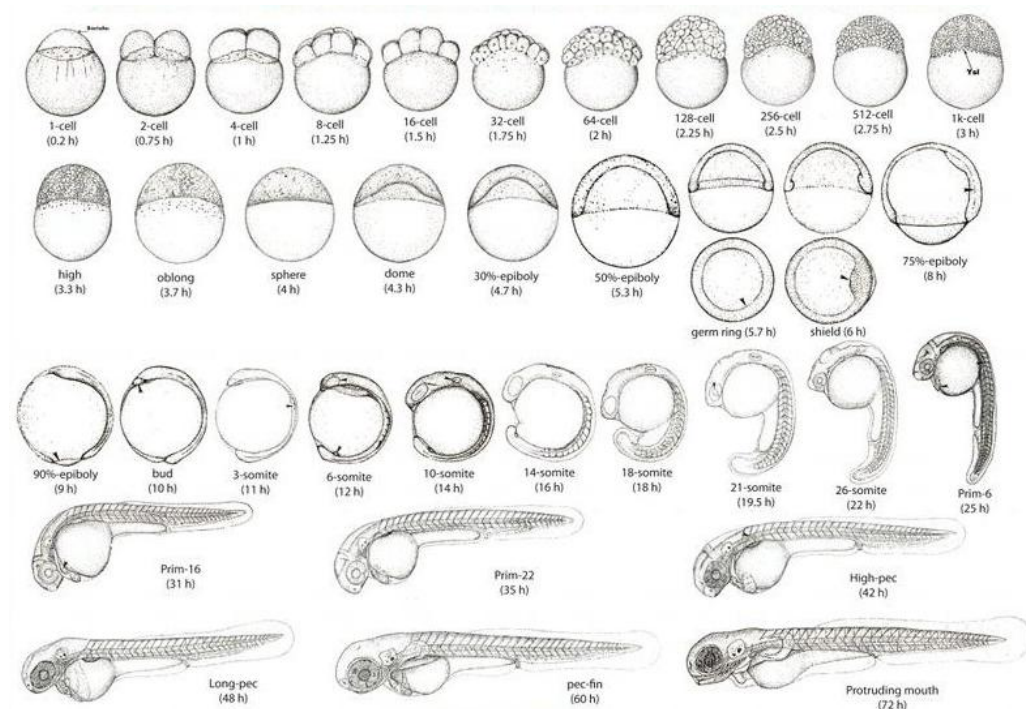


Figure 5: Developmental stages of the zebrafish (Fashion Cloud, 2015).

A fertilized egg is in the zygote period until the first cleavage occurs (about 40 minutes after fertilization). Only one single stage, the one cell stage, is included. During this stage, the chorion swells and lifts away from the newly fertilized egg. Fertilization also activates cytoplasmic movements. Subsequent to the zygote period is the cleavage period (3/4 h). After the first cleavage, the cells or blastomeres, divide at about 15-minute intervals. During the cleavage period, six cleavages (2-4-8-16-32-64- cell stage) occur at regular orientations. Following the first cleavage, additional cleavages are strictly oriented relative to the first one.

After the cleavage, the following period is called the blastula (2^{1/4} h). Blastula refers to the period when the blastodisc (embryo-forming portion appearing as a small disc on the upper surface of the yolk mass) begins to look ball-like, at the 128-cell stage and until the time of onset of gastrulation. During the blastula period, the yolk syncytial layer (YSL) is formed and epiboly (thinning and spreading of the YSL and the blastodisc over the yolk cell) begins which continues during the gastrula period.

The late blastula period is also characteristic for the beginning of the expression of genes that encode for regionally localized putative transcription factors. The gastrula period (5^{1/4} h) is defined as the period where epiboly continues and the production of primary germ layers and the embryonic axis occurs. For the onset of gastrulation, an organ- and tissue map has been set up (Figure 6).

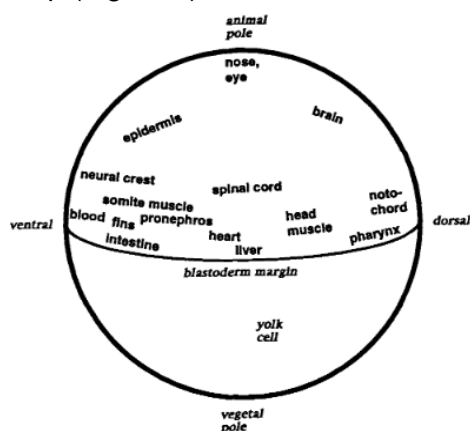


Figure 6: Organ and tissue-level fate map. Ectodermal fates map nearest the animal pole, mesoderm maps in a broad marginal ring, and endoderm overlaps this ring just at the blastoderm margin. Stomach, pancreas and swim bladder map laterally, near the liver and smooth muscle maps near the heart. The median and pectoral fins both map to or near the same ventral location (Kimmel et al., 1995).

The gastrula period ends when epiboly is completed and the tail bud has been formed. The end of the gastrulation period is followed by the advent of the segmentation period (10 h). During this period, a variety of morphogenetic movements occur. The somites start to develop, the rudiments of the primary organs are appearing, the tail bud becomes more prominent and

the embryo elongates. During this period, the first body movements are visible and the body length of the embryo increases very rapidly.

The pharyngula period (24 h) is referred to the time of development when one can compare the morphologies of embryos of different vertebrates (for the zebrafish, the 2nd of the 3 days of embryonic development). During this period, the pharyngeal arches develop rapidly and the brain consists out of 5 lobes. Moreover, the head straightens out, fins begin to form, pigment cells differentiate, the circulatory system is formed and the heart begins to beat just at the onset of the period. There is also a marked behavioral development characterized by rhythmic movements of swimming.

The animals are called embryos until the 3rd day, whereas after this period they are considered as larvae, regardless of whether they hatched or not. The period when the embryo is devoided from the chorion, is called the hatching period (48 h). In a zebrafish clutch, the hatching occurs asynchronously. During this period, morphogenesis of the rudimentary organs is rather completed except for the gut and its associated structures. The cartilage develops in the head and pectoral fin and later on also in the jaw. Furthermore, the circulation in the pharyngeal arch region is becoming more complex with the onset of gill filament development.

By the 3rd day of development, the hatched larva has completed most of its morphogenesis and it continues to grow rapidly. One of the prominent changes during the early larval period (72 h) is the inflation of the swim bladder. During this last period, the larva begins to swim actively, whereas during the hatching period the embryo is usually resting. It also moves its jaws, eyes and pectoral fins and starts to seek for a pray.

5.2. Advantages of the zebrafish

The zebrafish represents a vertebrate organism, which shares about 70 % homology with humans (Chao et al., 2010; Howe et al., 2013). The development of the zebrafish is very similar to the embryogenesis in higher vertebrates, including humans. The whole zebrafish genome has been sequenced by the Sanger institute. In addition, the zebrafish immune system is very similar to the human immune system. Zebrafish and human share a similar developmental program, a comparable set of specialized T and B immune cells and similar immune signaling molecules (Tobin et al., 2012). Zebrafish have both innate and adaptive immunity. The innate immune system of the zebrafish embryo starts developing during the first day post fertilization (dpf) but the adaptive arm of immunity takes longer (van der Sar et al., 2006 and Tobin et al., 2012). Therefore, innate immunity is the sole protector of young fish for the first 30 days of development. This characterization serves as an advantage during the studies dedicated to initial stages of host-pathogen interactions (Tobin et al., 2012). The use of transgenic larvae with fluorescing innate immune cells allows to identify specific cell types involved in infections

(Brothers & Wheeler, 2012). Reverse genetics with morpholinos, and zinc finger nucleases enable examination of the roles of specific genes during infection (Tobin et al., 2012).

Zebrafish are small animals, therefore in one study it is possible to use more than 100 organisms at once (Bopp, 2006) and they are very easy to handle and maintain (Levraud et al., 2014). The excessive experimental costs that are obtained when working with mice (Chao et al., 2010) are extremely reduced by the use of this minivertebate. In addition, anesthesia and euthanasia are easy to execute in zebrafish (Levraud et al., 2014).

Another advantage of this species is its high fertility. One pair of adult fish is capable of laying around 200 eggs per day and this yield can be achieved every 5-7 days. This supports a possibility to use embryos for high-throughput screening platform (Chao et al., 2010), as a zebrafish embryo is small enough to develop in a well of a 384-well plate (Tobin et al., 2012). The external fertilization ensures that embryos are more accessible for manipulation (EOL Encyclopedia of life, 2015) and together with the optical clarity during embryogenesis, visual analysis of early developmental processes can be facilitated. Moreover, the rapid maturation of zebrafish enables the performance of transgenic studies. After around 100 days, zebrafish can be utilized in e.g. mutagenesis analyses (Bopp et al., 2006).

Thanks to the short generation times genetic analyses are promoted. Large-scale genetic screens have resulted in the identification of more than 500 mutant phenotypes in various aspects of early development. This helps to identify issues of organogenesis, complex disease and other vertebrate processes on the basis of function without a priori knowledge of the genes involved (Dooley & Zon, 2000).

As already mentioned before (section 4.2), a number of in vivo models have been introduced for *Candida* infection such as the CVC model in rats and in mice. The major disadvantage of the usage of such models is that they require biofilm burden analyses post-mortem. More importantly, the histological examination of biopsies is time consuming and does not allow to follow the infection process over time (Veneman et al., 2013). As a consequence, high-throughput screening in rodents is not feasible and even with the use of bioluminescence and fluorescence imaging, high challenge doses are required to visualize colonization. Therefore, the zebrafish at the embryonic and larval stages provide an ideal model. Because of its transparency and possibility of fluorescently labeled immune cells, obtained by transgenic zebrafish lines, *Candida* cells causing infection process can be imaged microscopically in real time (Veneman et al., 2013). Pigmentation in the embryos starts only about 30-72 hours post fertilization (hpf) (Bopp et al., 2006). Therefore, changes in the morphology within their early-stage development can be easily observed under the microscope (Bopp et al., 2006).

Moreover, another important characteristic of the zebrafish is that the mutant zebrafish embryos with strong morphological malformations or with an organ dysfunction, are still able to survive certain period of time. In contrast, malformed embryos of rodents die mostly *in utero* (Bopp et al., 2006).

5.3. Disadvantages of the zebrafish

Many of the above mentioned advantages fade as larvae grow and become juveniles. Morpholinos or mRNAs injected at the one-cell stage become diluted and degraded so their effect lasts only for few days (Levraud et al., 2014). The adult zebrafish model organism does not permit real-time visualization of e.g. infections and morpholino- directed gene knockdown is not applicable in the adult zebrafish (Brothers et al., 2011). When using larvae older than 30-72 hpf, their pigmentation could prevent microscopic observation. However, this could be circumvented by the addition of melanin synthesis inhibitor to the water or by using mutants with no pigmentation. Moreover, juvenile or adult zebrafish have problems with the recovery after longer anesthesia (Levraud et al., 2014).

Although the development of zebrafish and humans is very similar, there are some crucial anatomical differences between zebrafish and mammals, such as gills instead of lungs, hematopoiesis in the anterior kidney instead of bone marrow, lack of discernable lymph nodes and a different reproductive system (Tobin et al., 2012).

Although, zebrafish embryos and larvae develop well at 22 °C – 33 °C, this particular feature has not been demonstrated as a problem during the host pathogen interaction studies. Zebrafish do not possess an adaptive immune system until 1 month post fertilization which limits the possibility of examining innate-adaptive crosstalk in the transparent embryo (Tobin et al., 2012).

In comparison to the more traditional used model system i.e. the mouse, there is a lack of antibody reagents that act specifically against zebrafish proteins. There are only few antibodies to immunity-related proteins available, which makes the imaging more difficult. However, antibodies against well-conserved mammalian proteins often demonstrate cross-reactivity with zebrafish orthologues (Tobin et al., 2012).

5.4. The zebrafish as a host model to study *Candida albicans* infection

The zebrafish is more closely related to humans than for example *Drosophila melanogaster* or *Caenorhabditis elegans*. Therefore it is a powerful vertebrate model organism to explore human diseases, for example hematopoietic and cardiovascular disorders. It has emerged as a popular model organism in toxicological, teratogenic and cancerogenic studies (Dooley & Zon, 2000; Bopp et al., 2006). The identification of mutant zebrafish phenotypes (Dooley & Zon, 2000), aids in the deciphering of complex biological pathways which are often disturbed

in the above mentioned diseases. Next to that, the zebrafish is often used as a host for several infection studies to address questions about immunity and disease. The zebrafish offers a high- throughput screening platform and thanks to its transparency, infection studies can be followed in real time. Murine models, on the other hand, require analyses of the infection *post mortem*.

The pathogenesis of several microorganisms, which cause infections in human, including those caused by bacteria (*Escherichia coli*, *Mycobacterium marinum*, *S. aureus* etc.) or viruses (Herpes simplex virus type- 1, Chikungunya virus) have been well studied by utilizing the zebrafish (Kuo et al., 2012). To address the spread of a viral infection throughout the body, there was taking advantage of time-lapse imaging of the transparent zebrafish larvae (Levraud et al., 2014). By injecting fluorescently tagged viruses, it was possible to determine the time of appearance and death of infected cells (Levraud et al., 2014). Veneman et al. (2013) established a zebrafish embryo infection model of *Staphylococcus epidermis* (*S. epidermis*) and *Mycobacterium marinum* (*M. marinum*) to assess bacterial proliferation and to identify the zebrafish genes that serve as a marker for *S. epidermis* infection. Furthermore, they compared the transcriptome response of infection with *S. epidermis* and *M. marinum*. It was discovered that first *S. epidermis* bacteria grew for 2 to 3 days inside the yolk of the embryos, while from 3 and 4 days post injection, the bacteria invaded the whole body provoking a strong response of many immune related genes (cytokines, heat shock proteins, leukocytes etc.). Moreover, when comparing the transcriptome responses of *S. epidermis* with those of *M. marinum*, it was shown that *M. marinum* has a stronger effect on host gene regulation and that some genes specifically responded to *S. epidermis* and not to *M. marinum*.

The focus of this project lies on the infection of *C. albicans* in the zebrafish as a host model. As it was already stated above, *Candida* is able to form biofilms on several medical devices leading to systemic diseases with high mortality. Therefore it is crucial to find a model organism to study *C. albicans* device- associated infections.

The zebrafish has already been used in several *C. albicans* infection studies (Chao et al., 2010; Brothers et al., 2011). In the study of Chao et al. (2010), adult zebrafish were anesthetized and then intraperitoneally injected with different concentrations of *C. albicans* (1×10^8 , 1×10^9 , and 1×10^{10} cells/ml). It was demonstrated that *C. albicans* can invade and colonize the zebrafish at multiple anatomical sites including the liver, gastrointestinal tract, and muscle and kill the fish in a dose-dependent manner. In addition, filamentation at multiple loci has been reported suggesting that the zebrafish is an ideal model for studying virulence factors (such as morphogenesis), which contribute to *C. albicans* pathogenesis (Chao et al., 2010). In the same study it has also been tested whether the yeast-to-hyphae transition plays a central role in *C. albicans* infection. Therefore, the pathogenicity of two mutant strains defective for filamentation

(*cph1/cph1 efg1/efg1* double mutant and *hgc1/hgc1*) were compared with the WT strain. The mutant strains were attenuated in virulence compared with the WT. These data confirmed other existing data that morphogenesis is important for *C. albicans* virulence (Chao, 2010). Kuo et al. constructed an integrated intercellular protein- protein interaction network between the hyphal proteins of *C. albicans* and the zebrafish proteins during infection to understand the mechanisms responsible for *C. albicans* pathogenicity and the host immune responses. Therefore they used adult zebrafish and injected them intraperitoneally with 1×10^8 CFUs (colony forming units) *C. albicans* cells. Several important proteins related to *C. albicans* infection were identified such as Ubi4 (Ubiquitin 4) and Act1 (Actin 1) which play the most important roles in hyphal growth and development.

The zebrafish is a powerful model for non-invasive visualization and understanding the interactions of pathogens such as *C. albicans* with the innate immune system. For the first 4 weeks of development, zebrafish have only developed innate immune defenses and this simplifies the study of diseases such as disseminated candidiasis, which is highly dependent on innate immunity (Brothers, 2011).

Invading and disseminating *Candida* cells primarily encounter phagocytic cells such as macrophages and neutrophils which efficiently phagocytose *C. albicans* yeast cells and short hyphae (Jacobsen, et al., 2012). The first macrophage precursors are already present as early as 20 hpf (Torraca et al., 2014). Neutrophils are identifiable from around 48 hpf and are from that point the dominant leukocytes in zebrafish larvae (Renshaw et al., 2006; Renshaw & Trede, 2012).

Brothers et al (2014) established a successful hindbrain ventricle *C. albicans* infection in a zebrafish larva. At 5 hpi (hours post injection), *C. albicans* was engulfed by macrophage- like cells (these cells exhibit overall characteristics most similar to macrophages) in the hindbrain ventricle. By 24 hpi, *Candida* already disseminated throughout the tail, since *Candida* was present inside macrophage-like cells in the dorsal tail tissue (Brothers & Wheeler, 2012). In another study of Brothers et al. (2011), the zebrafish was microinjected in the prim25 stage with a 1×10^7 /ml *C. albicans* suspension through the otic vesicle (ear) of the hindbrain. Their study, showed that both macrophage-like cells and neutrophils engulf *C. albicans* during infection. Furthermore, they investigated how fungi fare inside phagocytes. *In vitro*, *C. albicans* germinates inside macrophages but not in neutrophils. By using their zebrafish *in vivo* model, they revealed that neutrophils phagocytosed a limited number of *C. albicans* yeast cells and remained highly motile post phagocytosis while on the other hand, macrophage-like cells phagocytosed more *C. albicans* yeast cells but had a reduced motility. In addition, they found out that neutrophils may have a greater capacity to kill *C. albicans* and inhibit growth (including

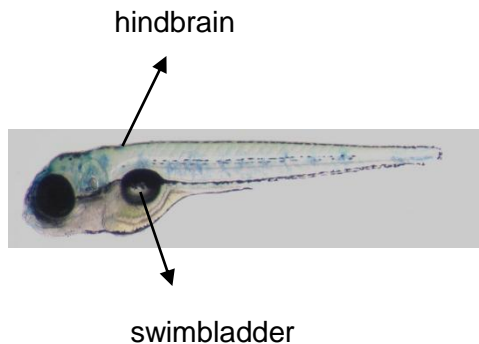
the yeast-to-hyphae transition) than macrophages in the intact host. This implicates that hyphal transition is a critical event for escaping the phagocytes (Brothers et al., 2011).

The phagocyte NADPH oxidase complex (NOX2 or phagocyte oxidase), expressed in both macrophages and neutrophils, is also one of the key mediators of *C. albicans* innate immunity. NADPH oxidase catalyzes the production of microbicidal reactive oxygen and nitrogen species and is required for neutrophils to inhibit the *C. albicans* yeast-to-hyphae switch *in vitro*. By using a *C. albicans* strain (called WT-OXYellow) that has constitutive expression of yCherry (a codon optimized form of mCherry (Keppler-Ros et al., 2008)) and oxidative stress-inducible expression of EGFP (enhanced GFP), Brothers et al. (2011) found that the host NADPH oxidase is the major cause of oxidative stress in *C. albicans* during infection and is of vital importance in limiting fungal proliferation and filamentous growth (Brothers et al., 2011).

5.5. Routes of administration

Adult zebrafish are usually injected intraperitoneal or intramuscular but these methods are not very suitable for high-throughput screening. Another commonly used infection method that is applied on adult fish, is bath immersion. With this method however, variable mortality rates were achieved (Meijer & Spaink, 2011). The conventional infection method for zebrafish embryos is injection of pathogens into the caudal vein or the common cardinal vein (Duct of Cuvier, a bilaterally paired longitudinal vein) (Meijer & Spaink, 2011; Veneman et al., 2013). This injection method however results in high mortality, is labor intensive and is consequently not high-throughput (Brothers et al., 2011; Veneman et al., 2013). Therefore, Veneman et al. (2013) developed and validated a high-throughput yolk infection model using *M. marinum* and a microinjector. They used this automated microinjection system to develop a high-throughput system for quantitating infection with *S. epidermis* (figure 7).

Injection of *Candida albicans*



Injection of *Staphylococcus epidermis*

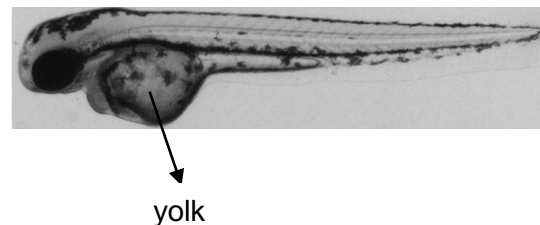


Figure 7: Several routes of pathogen administration in the zebrafish. The conventional infection method is caudal vein injection but this results in high mortality and is labor intensive. Veneman et al. (2013) developed a high-throughput yolk infection model to quantitate infection with *S. epidermis*. In the past, a successful hindbrain ventricle *C. albicans* infection was established (Brothers et al., 2011; Brothers & Wheeler, 2012) and recently a mucosal infection in zebrafish larvae was created by direct injection of *C. albicans* in the swimbladder (Gratacap et al., 2014).

Meijer & Spink (2011) found that *M. marinum* yolk injection during the first hours of embryogenesis does not interfere with embryo development and that bacteria disseminate from the yolk into the tissues (Meijer et al., 2011). Brothers et al. (2011) demonstrated consistent injection of 15-20 yeast cells through the otic vesicle into the hindbrain ventricle of 36 to 48 hpf larvae (prim25 stage). By using this infection model, there is an initial local infection that spreads throughout the body by 24 hpi. In the study of Gratacap et al. (2014), mucosal candidiasis is modelled in zebrafish larvae by swimbladder injection (homologue of the mammalian lung). Their method ensured for injection of a consistent dose of *C. albicans* cells and accurate and reproducible infection of the swimbladder. In addition, the method permitted a non-invasive temporal documentation of infection dynamics which aids in the understanding of the role of the innate immune system during *C. albicans* mucosal infection (Gratacap et al., 2014).

Aims

The first main aim of this project was to use the zebrafish (*Danio rerio*) as a host model to study *C. albicans* device-associated infections. In the past, zebrafish larvae have been used as hosts for *C. albicans* infection studies with planktonic cells, but one of the innovative aspects is the development of *C. albicans* infections on polystyrene microspheres. We were the first to use optically transparent zebrafish larvae to follow non-invasively the infection of fluorescently tagged *C. albicans* cells on microspheres in real time. We made use of a WT GFP- or yCherry-tagged *C. albicans* strain and a *bcr1Δ/bcr1Δ* –GFP and *efg1Δ/Δ cph1Δ/Δ*-yCherry strain as a control. The application of zebrafish larvae to study *C. albicans* device-associated infections provides several advantages, for example its small size and transparency, permitting high-throughput screens and chemical genetic screens. If successful, this novel model will provide an easier tool to study *C. albicans* device-associated infections over time within the same animal.

C. albicans is able to invade and colonize different types of tissues due to its ability to switch from the yeast to the more virulent hyphal form. Therefore, upon microspheres and *C. albicans* injection, we expected that the *Candida* cells would colonize the microspheres and that, simultaneously, *Candida* would disseminate into different compartments of the host. So the second main aim consisted out of the examination of *C. albicans* dissemination into additional organs and to show the importance of *C. albicans* morphogenesis as a crucial phenomenon in the development of an infection.

Finally, we wanted to explore the role of the host innate immune system in the device-associated infection development in the above mentioned model system. Zebrafish have both innate and adaptive immunity but the adaptive branch develops only 30 days post fertilization. Until now, not so much is known about the role of the immune system during early stages of *C. albicans* infection. Innate immunity as a sole protector of young fish, allowed us to look at initial host-pathogen interactions and to investigate the role of macrophages and neutrophils as a first line of defense. Therefore, we made use of a transgenic *fli:GFP* fish line with GFP-expressing macrophages and a yCherry expressing *C. albicans* strain. The *efg1Δ/Δ cph1Δ/Δ*-yCherry strain was used as a control. The main issue was whether the immune system could cope and combat the device-associated infection.

Materials

1. Media

1.1. YPD media

1.1.1. YPD (yeast peptone dextrose) medium

- 10 g of yeast extract (Merck)
- 20 g of Bacteriological peptone (OXOID)
- For solid medium: 15 g of Agar granulated (Difco)
- Dilute with 950 ml of Milli-Q water

Autoclave at 120 °C for 20 min at 120kPa.

- Add 50 ml of 40% D-Glucose solution (for final concentration of 2%)

Solid YPD medium was used for CFUs enumeration and liquid YPD for overnight culture of *C. albicans*.

1.1.2. YPD medium with penicillin/streptomycin cocktail

- YPD solid medium was prepared as described above and supplemented with 10 ml of the penicillin-streptomycin cocktail (Sigma Aldrich, USA). Penicillin-streptomycin solution contains 10,000 units of penicillin and 10 mg of streptomycin/mL. Plates were used for CFUs determination of the *C. albicans* cells retrieved from homogenized zebrafish embryos.

1.2. Glucose (40%)

- 440 g of 10% stock concentration of D-glucose (Sigma-Aldrich)
- Adjust to 1L with Milli-Q water.

Glucose was added to YP medium after autoclaving.

1.3. Roosevelt Park Memorial Institute Medium (RPMI- 1640 medium) buffered with 0.165 mol/L MOPS

- 10,4 g powdered RPMI 1640 medium (with glutamine and phenol red, without bicarbonate) (Sigma-Aldrich)
- 34,53 g MOPS (3-[N-morpholino] propanesulfonic acid) buffer (Sigma-Aldrich)
- 950 ml Milli-Q

Adjust the pH to 7.0 at 25°C by using 1 mol/L NaOH- tablets (Merck)

- Add additional 100 mL of water to a final volume of 1 L. Filter sterilize by using a Fast PES filter unit (Nalgene- Thermo scientific) and store at 4 °C before use.

This medium was used for the formation of biofilms on chambers (see description at 5) or on polyethylene discs (see description at 5).

1.4. 10 x PBS buffer (Phosphate Buffered Saline)

- 2 g KCl (VWR international)
- 80 g NaCl (Merck)
- 14,4 g Na₂HPO₄ (Merck)
- 2,4 g KH₂PO₄ (Merck)

Autoclave at 120°C for 20 min at 120 kPa.

1.5. 1 x PBS buffer (Phosphate Buffered Saline)

- Add 50 ml of 10X PBS stock solution to 450 ml of Milli-Q water

Autoclave at 120 °C for 20 min at 120 kPa.

1.6. Egg water (system water with methylene blue)

- 58 mM NaCl
- 0.7 mM KCl
- 0.4 mM MgSO₄ (x7 H₂O)
- 0.6 mM Ca(NO₃)₂ (x4 H₂O)
- 5 mM HEPES

Stock solution	Per 1 L	concentration
NaCl	101.7 g	1740 mM
KCl	1.56 g	21 mM
MgSO ₄ .7H ₂ O	2.96 g	12 mM
Ca(NO ₃) ₂ .4H ₂ O	4.25 g	18 mM
HEPES buffer	35.75 g	150 mM

The pH was adjusted to 7.6 and from this stock, final concentration of egg water can be 0.3 x or 1.0 x (for higher buffering capacity). Consequently, 2 ml of methylene blue was added to avoid mold growth.

1.7. Anesthesia and euthanasia of zebrafish larvae

Tricaine (3-amino benzoic acid ethyl ester or ethyl m-aminobenzoate) stock solution (4 mg/ml):
CAS 886-86-2

400 mg tricaine powder

97.9 ml DD water

~ 2.1 ml 1 M Tris (pH 9)

Components are mixed in a glass bottle with screw cap and adjusted to pH 7 with 1M Tris pH 9. This solution should be kept refrigerated and in the dark (covered by aluminium foil) and replaced every month.

Tricaine working solution (0.168 mg/ml):

4.2 ml tricaine stock solution for 100 ml system water

Aliquots of 1 ml were made by adding 420 µl of the tricaine stock solution to 10 ml of system water.

Two days old zebrafish were anesthetized with tricaine prior to homogenization and screening of the embryos by means of confocal scanning laser microscopy (see section 4.1). Six days after injection, the larvae were sacrificed by given them an overdose of ethanol.

Methods

1. *In vitro* experimental procedures

1.1. *C. albicans* cells and microspheres enumeration using a hemocytometer

The amount of *Candida* cells and microspheres was counted by using a Bürker chamber (BLAUBRAND®, counting chamber 0,100 mm depth) counting grid. The total amount of cells or microspheres per 1 mL was calculated via the following formula:

$$\frac{\sum_{\text{small squares}} \text{cells}}{\text{\#small squares}} * 25 * 10^4 * \text{dilution}$$

Afterwards, the total amount of *Candida* cells was adjusted to 1 mL including the dilution factor.

1.2. Preparation of microspheres

1.2.1. Types of microspheres

Microspheres (latex beads or latex particles) are spherical particles that are formed from an amorphous polymer such as polystyrene. They are biologically inert and are loaded with a dye to create highly fluorescent beads. For the *in vitro* and *in vivo* experiments, the following microspheres were used:

Table 1: An overview of the microspheres used for the *in vitro* and *in vivo*

Type of microspheres	Experiment
Red microspheres (580/605 nm) 10 micron (life technologies, carboxylate-modified FluoSpheres® polystyrene)	<i>In vitro</i> experiments
Yellow-green microspheres (505/515 nm) 10 micron (life technologies, carboxylate-modified FluoSpheres® polystyrene)	<i>In vitro</i> experiments
Red microspheres (580/605 nm) 4 micron (life technologies, FluoSpheres® Sulfate)	<i>In vivo</i> experiments
Yellow-green microspheres (505/515 nm) 4 micron (life technologies, FluoSpheres® Sulfate)	<i>In vivo</i> experiments

All types of microspheres were ordered from Life technologies, stored in the refrigerator (2-8°C) and protected from light. During the experiments, all actions were executed in the dark.

1.2.2. Preparation of microspheres for *in vitro* experiments

Red or yellow-green microspheres (10 µm diameter) were vortexed and transferred to a 1.5 ml low adhesion microcentrifuge tube. Low adhesion material was used to avoid adherence of the microspheres to the walls of the tube. Subsequently, microspheres were washed twice with Milli-Q water and centrifuged for 2 min, 22°C at 8 000 rpm (revolutions per minute). This step is crucial in order to avoid traces of the solution, which is used to maintain microspheres (sodium azide and antibiotic - 0.02% thimerosal). After the last washing step, microspheres were submerged in 1 ml of fetal bovine serum (FBS, Sigma Aldrich), sonicated for 10 min at 40 000 Hz to assure that the beads are in suspension. Subsequently, the beads were incubated at 37 °C, overnight. The FBS will promote the adherence of *C. albicans* cells to the substrate (in our case, the microspheres). Afterwards, tubes containing microspheres were centrifuged for 2 min, 22°C at 8000 rpm and submerged in RPMI – MOPS, pH 7.0. Next, the amount of microspheres was enumerated by using a hemocytometer (Bürker chamber). The final concentrations of microspheres were adjusted to 1×10^4 microspheres/well of UV sterilized borosilicate chamber (Lab-Tek® Chambered #1.0 Borosilicate Coverglass system, Nunc™) or to a polystyrene 24-well plate (24 Well Cell Culture Plate, CELLSTAR®, Greiner Bio-One).

1.2.3. Preparation of microspheres for *in vivo* experiments

Red or yellow-green microspheres (4 µm diameter) were prepared as described above but they were not submerged in FBS before use.

1.3. Preparation of *Candida* strains

1.3.1. *C. albicans* strains used in this study.

C. albicans GFP-expressing strains (*C. albicans* MLR62-GFP and CJN750-GFP) were kindly provided by Prof. Aaron Mitchell (Carnegie Mellon University, Pittsburgh, USA). Two additional strains, fused to yCherry (a codon optimized version of mCherry) were kindly provided by Dr. Robert Wheeler (*C. albicans* CAF2-yCherry and CAN34-yCherry). An overview of all the strains used in this study and their corresponding genotype are summarized in table 2.

Table 2: Overview of *Candida* strains used for *in vitro* and *in vivo* experiments

<i>Candida</i> strains	Genotype	source	Description in thesis
SC5314	Wild-type	Gillum et.al (1984)	WT
CJN702 (<i>bcr1Δ/bcr1Δ</i>)	<i>ura3Δ::λimm434 arg4::hisG his1::hisG::pHIS1 bcr1::ARG4 ura3Δ::λimm434 arg4::hisG his1::hisG bcr1::URA3</i>	Nobile et al. (2006)	<i>bcr1Δ/bcr1Δ</i>
CAN34 (<i>efg1Δ/Δ cph1Δ/Δ</i>)	<i>cph1::hisG}cph1::hisG, efg1 : :hisG}efg1::hisG : :URA3: :hisG</i>	Dieterich et al. (2002)	<i>efg1Δ/Δ cph1Δ/Δ</i>
MLR62-GFP (WT- GFP)	<i>ura3Δ::λimm434 ARG4:URA3::arg4::hisG his1::hisG::pHIS1-TEF1-GFP ura3Δ::λimm434 arg4::hisG his1::hisG</i>	Nobile et al. (2005)	WT-GFP
CJN750-GFP (<i>bcr1Δ/bcr1Δ</i>-GFP)	<i>ura3Δ::λimm434 arg4::hisG his1::hisG::pHIS1-TEF1-GFP bcr1::ARG4/ ura3Δ::λimm434 arg4::hisG his1::hisG bcr1::URA3</i>	Nobile et al. (2005)	<i>bcr1Δ/bcr1Δ</i> -GFP
CAF2-yCherry (WT- yCherry)	<i>ura3Δ::imm434/URA3 PADH1- yCherry_NATR</i>	Brothers et al. (2011)	WT-yCherry
CAN34-yCherry (<i>efg1Δ/Δ cph1Δ/Δ</i>- yCherry)	<i>ura3Δ::imm434/ura3Δ::imm434 efg1Δ::hisG efg1Δ::hisG cph1Δ::hisG cph1Δ::URA3 PADH1- yCherry_NATR</i>	Brothers et al. (2011)	<i>efg1Δ/Δ cph1Δ/Δ</i> - yCherry

1.3.2. Preparation of *C. albicans* strains for *in vitro* experiments

C. albicans strains were grown on YPD plates at 37 °C, overnight. Next, *Candida* cells were scrapped off the plate and submerged in 1mL of PBS, diluted 100 x and counted using a Bürker chamber. Final concentration of *Candida* cells was adjusted to 1x10⁷ cells/ml (for 96-well biofilm development) or 1x10⁵ cells/ml (for biofilm formation on polyethylene discs).

1.3.3. Preparation of *C. albicans* strains for *in vivo* experiments

C. albicans strains were grown on YPD plates at 37 °C, overnight. The next day, a single colony was transferred to 2 ml of liquid YPD medium and incubated at 30 °C, overnight, 200 rpm. Overnight cultures were washed twice with PBS (2 min, 22°C at 8 000 rpm). *Candida* suspension was diluted 1 000 x. The amount of cells in suspension was counted using a Bürker chamber.

1.4. Detection of fluorescence signal intensity of microspheres and *C. albicans* strains

Microspheres (10 µm) and *Candida* strains were prepared as described in section 1.2.2 and 1.3.2., respectively. Next, 100 µl of *Candida* cells (1×10^6 cells/well) was added to a 96-well polystyrene plate (Greiner plate, flat bottom) in triplicate. Subsequently, microspheres (1×10^3 spheres/well) were introduced to *Candida* cells and plates were incubated at 37 °C for 24 h. Afterwards, the plates were shortly (approximately 10 s) centrifuged at 1000 rpm. Next, the remaining medium was removed very gently (except the control condition that contains only microspheres and no *Candida* cells) and 100 µl of PBS was added to each well. Consequently the fluorescence signal was measured by the spectrofluorometer (H1 hybrid reader, Synergy). Wells containing only PBS were considered as a blank.

1.5. *In vitro* *C. albicans* biofilm formation on borosilicate chambers and on polyethylene discs in the presence or absence of microspheres

Microspheres (10 µm) and *Candida* cells were prepared as previously described in sections 1.2.2 and 1.3.2, respectively. Next, red or green/yellow microspheres (1×10^4 spheres/well) were combined with 1 ml of *Candida* cells (1×10^5 cells/well). This suspension was introduced to a UV sterilized borosilicate chamber and to tissue culture polyethylene coverslips (13 mm diameter, Sarstedt) placed in a 24- well plate. Both set ups were incubated for 24h at 37°C (biofilm formation). Biofilm formation and biofilm thickness were visualized by confocal laser scanning microscopy.

2. *In vivo* experimental procedure

2.1. Zebrafish lines

In this study, WT zebrafish lines (AB line) were kindly provided by the zebrafish facility (UZ Gasthuisberg, KU Leuven, Belgium). This line was used for the majority of experiments. For one preliminary experiment, a transgenic *fli:GFP* reporter fish line with GFP-expressing macrophages and endothelium was used (Brothers et al., 2011).

2.2. Zebrafish maintenance and care

Zebrafish lines are housed in aquaria systems in transparent cages. It is of great importance to keep the water in a good condition. If the water is not cleaned properly, then the fish could

suffer from the toxicity of their own excretion products. The simplest way to keep the water clean is to keep fish at very low densities and to change the water regularly (10- 20 % of the total fish water volume should be exchanged on a daily basis) (Brand, et. al, 1999).

In the aquatic facility at UZ Gasthuisberg, KU Leuven, Belgium the animals are kept in recirculating systems from Marine biotech (Figure 8).



Figure 8: Marine biotech recirculating system. Water is moved from the housing tank through a series of components that reduce or remove the waste products. These components include mechanical, biological and chemical filtering units.

In these systems, the water is moved from the housing tank through the series of components that include mechanical, biological and chemical filtering. Mechanical filtration is responsible for the removal of un-eaten food, feces and algal debris. Medications, chemicals and coloring agents are removed by activated carbon present in the central space of a cartridge filter. Equipping the aquaria with biological filters, aids the purification process of the water as they contain a large surface area on which bacteria can grow and degrading the toxic ammonia into less toxic nitrates. Substances like ammonia, chlorine, nitrite and copper must be kept as low as possible, if possible zero (water must be checked 2-3 times per week). An ultraviolet sterilizer will neutralize mold, spores, protozoa, bacteria and even some viruses (Brand et. al, 1999). The pH and conductivity probes, which are present in the water reservoir of the system, gather information and relay it to the controller (iks aquastar) for processing. To maintain these parameters in defined ranges, the controller directs automated dosing units for pH and conductivity. The temperature is also measured by the controller, but the regulation is done by a separate water heating system. To maintain the conductivity, a sea salt mixture is added to

the automated dosing unit. The conductivity set point is programmed at 480 μS (microSiemens) $\pm 10 \mu\text{S}$. The pH should remain between 6.9 and 7.5 (pH set point is 7.15 ± 0.05) and this is achieved by the addition of sodium bicarbonate (CAS 144-55-8) to the automated dosing unit for pH. When the buffering capacity of the water is not efficient, the pH could drop below 6.0, which is toxic. This problem can be solved by adding bicarbonate. On the other hand, when the capacity of the biological filters is too low, the pH may rise to values above 8 and this prevents the growth of the denitrifying bacteria resulting in the production of ammonium compounds. Frequent water changes and the addition of hydrochloric acid could circumvent this problem. Zebrafish require a water temperature between 26 and 28°C (temperature set point is 27°C $\pm 0.15^\circ\text{C}$). Usually, the room temperature must be slightly higher to prevent condensation and mold growth (Brand et al., 1999).

In the aquatic facility, the larvae are raised in transparent tanks of 4 liter. Adults used for spawning are kept in 2 liter tanks at a density of 6 females or 8 males per tank. Females and males are kept separately. Cage enrichment is achieved by housing the fishes in groups (to promote shoaling behavior) and by feeding them daily with living brine shrimp (this induces chasing behavior). When fish are ready to spawn, they receive green plastic plants and a shallow spawning area mimicking a natural environment.

Zebrafish are kept in a laboratory where the light is provided for 14-hour and the dark cycle for 10 h. Zebrafish start to spawn when the light is turned on in the morning. By changing the day-night rhythm, embryos of different development stages can be obtained (Brand et al., 1999). In the aquatic facility, the 'static-tank strategy' is used to breed zebrafish. First, fish are removed from their original housing tank and placed in breeding tanks that are disconnected from the water circulation (static). The day before mating, a plastic mating tank is placed into a larger container filled with system water. Six females are added to the top compartment and three to four males (one set-up) are placed in the bottom compartment. Green plastic plants are added to each compartment. The next day, all set-ups are protected from light by placing them in a cupboard. When embryos are required, the breeding tanks are taken out of the cupboard and the presence of light induces spawning. The males and females are added together and the fertilized eggs fall through a grid to protect them from cannibalism. After 30 minutes, the eggs are collected by pouring the tank water through a non-abrasive tea strainer and transferred into a Petri dish containing clean fish water.

Zebrafish are omnivorous, feeding primarily on zooplankton and insects. Adult fish are fed three times a day and the surplus of feed must be removed one hour after feeding (Brand et al., 1999). In the morning and evening, they receive small amounts of dry powder from SDS (Special Diet Services, Technilab). In the afternoon, the fish receive Great Salt Lake Brine shrimps (*Artemia*). The artemia suspension is made fresh every day starting from cysts bought from Technilab.

There are a number of diseases that can affect the entire fish colony. The most common ones are velvet disease, fish tuberculosis and nematode infection. To minimize the risk of entry of new pathogens, imported fish will be housed in a quarantine zone. Any sick fish should be discarded as quickly as possible. To avoid spreading of diseases, it is very important to keep the containers and the tools clean and remove everything what could have been in a contact with the infected fish. After the experiment it is important to clean and decontaminate the work area with a disinfectant (Ummonium38).

Fish that are younger than 7 days are euthanized in 1% Ummonium38 solution (5 min incubation at room temperature). Fish older than 7 days, are euthanized with an overdose of benzocaine hydrochloride until the opercular movements stop (approximately 5 min incubation at room temperature).

Most of the info was obtained by internal communication with Dr. Lambaerts, K., aquatic facility, UZ Gasthuisberg, KU Leuven, Belgium).

2.3. Zebrafish injection

All the preparatory work regarding the animal handling, preparation of needles and the zebrafish injection was demonstrated by Dr. Kathleen Lambaerts (manager of the aquatic facility, UZ Gasthuisberg, KU Leuven, Belgium).

2.3.1. Pulling the capillaries

Before any *in vivo* experiment it is advisable to prepare needles in advance. Needles are made from glass capillaries (KWIK – FIL™ Borosilicate glass capillaries, World precision instruments, Inc.) by making use of the p-87 needle puller (flaming/brown micropipette puller, Sutter instrument co.) (figure 9).



Figure 9: Needle puller. Close-up of the p-87 needle puller.

Next, it is very important to establish the correct settings on the needle puller in order to create a good needle. The settings optimized for pulling needles for zebrafish injections, are fixed on program 8 on the p-87. A RAMP test (for the needle resistance) was performed before pulling the first needle. The heat value (ramp test value + 5 units) was compared with the ramp test and adjusted if needed (maximum heat value is the ramp test value + 25 units). Subsequently, the needles were kept in a Petri dish containing clay. It is important to mention that after this procedure capillaries remained closed and before injection must be opened.

2.3.2. Open the capillaries

Before the capillaries could be used for injection, they were cut to have an open tip. The needle tip was visualized by light microscope (Zeiss) and the tip of the needle was gently ticked against a scalpel so that only a small part of the needle was broken off. It was crucial to create a needle that was narrow enough to facilitate the piercing of the chorion and the yolk. Needles were always cut in a straight way to avoid damage of the embryos during injection.

2.3.3. Calibration of the needles

To estimate the injection volume and assure a consistent injection volume, the needles had to be calibrated.

First, the needles were filled with 2-3 μl of injection material using a microloader tip (Eppendorf). Consequently, the needle was inserted into the microinjector (World precision instruments) (figure 10, picture on the right).

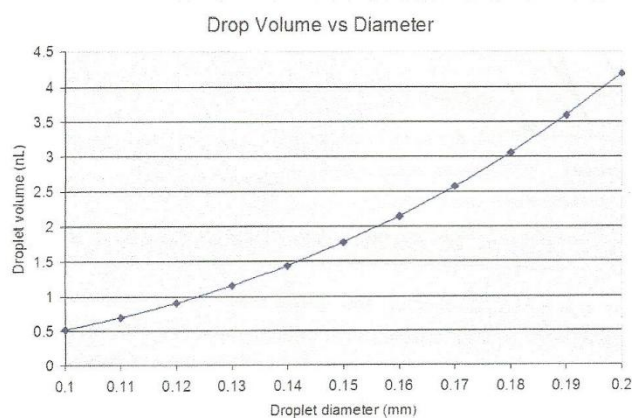


Figure 10: A calibration graph showing the relation between droplet size and injected volume (left) and a photograph demonstrating a set-up of the microinjector (right).

Next, a drop of mineral oil was pipetted on a calibration micrometer slide (Pyser-SGI limited) that contains a scale, which divides 1 mm into 100 units. The needle was introduced into the

mineral oil and by pressing the foot pedal of the injector (Eppendorf Femtojet) the size of the drop on the oil was observed. When injected into the oil, the drop had to create a round shaped sphere. Figure 10 (graph on the left side) shows the relation between droplet size and the injection volume.

Since the injection volume of 2 nl was typically used for zebrafish embryos, the drop had to have a diameter of 0.16 mm. To achieve a droplet size of 0.16 mm, the injection pressure (p_i) was adjusted until the desired volume was reached. This step was crucial for the reproducibility of the microinjection experiment. Preferentially, the p_i should be between 200 and 300 hPa. The compensation pressure (p_c), which is applied counter to the forces of capillary suction, was set on 15 hPa and ensures that no liquid flows into the injection capillary. The injection time (t_i) was set on 0.1-0.2 seconds and gave the period for which the p_i was maintained (Biocompare, 2006). Once the desired injection volume was reached, there was a transfer to the injection of zebrafish embryos.

2.3.4. Injection of *C. albicans* cells and microspheres into zebrafish embryos

During the injection of *Candida* cells into the yolk of zebrafish embryos, the injection material contained either *Candida* strains alone, microspheres alone or a combination of both. The strains and microspheres (4 μ m) were prepared as described above (section 1.2.3 and 1.3.3). In the morning, the embryos were collected by the employee of the aquatic facility and injection occurred in the one-cell, maximum two- cell stage. To uniformly label the embryos, injections must be performed before the four-cell stage (1hpf). After injection, the embryos were kept in Petri dishes containing egg water at 28 °C.

Red microspheres were combined with WT-GFP and/or *bcr1 Δ /bcr1 Δ* -GFP, whereas yellow-green microspheres were combined with WT-yCherry and/or *efg1 Δ / Δ cph1 Δ / Δ* -yCherry prior to injection.

First, a microscope slide was placed in an inverted lid of a Petri dish and zebrafish embryos were lined up against the side of the slide using a Pasteur pipette creating a single row. During the positioning of the embryos, the needle tip was submerged in the mineral oil to prevent drying out and clogging of the needle. Next, the excess of egg water was removed and the needle was lowered towards the row of aligned eggs

Consequently, 2 nl (0.16mm) of injection material was injected into the yolk of zebrafish embryos (figure 11) under an angle of 45°.

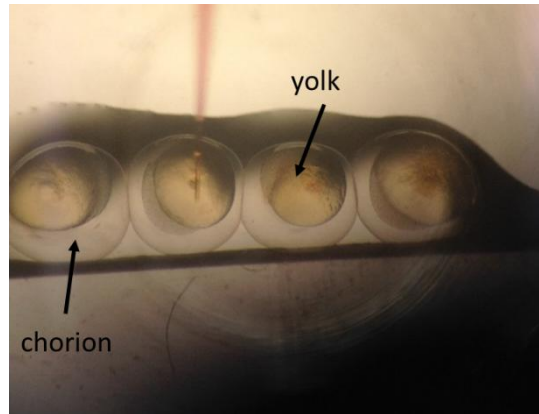


Figure 11: A suspension injected into the yolk of zebrafish embryos.

During the injection, the needle must pass through a first membrane, called the chorion before entering the yolk. Tables 3 and 4 give an overview of the *Candida* and microsphere concentrations used during this project and the corresponding amount of cells and microspheres for 2 nl injection volume.

Table 3: Relationship between microspheres concentration in a microcentrifuge tube and the corresponding amount of microspheres injected per embryo in a final volume of 2 nl.

Microspheres concentration in microcentrifuge tube	Microspheres injected/embryo (2 nl final volume)
12.5×10^7 microspheres/ml	250 microspheres
5×10^7 microspheres /ml	100 microspheres
2.5×10^7 microspheres /ml	50 microspheres
1.25×10^7 microspheres /ml	25 microspheres
1×10^7 microspheres /ml	20 microspheres
0.5×10^7 microspheres /ml	10 microspheres
0.25×10^7 microspheres /ml	5 microspheres

Table 4: Relationship between *Candida* cells concentration and the corresponding amount of *Candida* cells injected per embryo in a final volume of 2 nl.

<i>Candida</i> concentration in microcentrifuge tube	<i>Candida</i> cells injected/embryo (2 nl final volume)
5x10⁷cells/ml	100 cells
2.5x10⁷cells/ml	50 cells
1.25x10⁷cells/ml	25 cells
1x10⁷cells/ml	20 cells
0.5x10⁷cells/ml	10 cells
0.25x10⁷cells/ml	5 cells

After the injection, a stream of egg water was used to transfer the injected embryos into a clean Petri dish containing fresh egg water and incubated at 28 °C.

2.3.5. Survival of zebrafish larvae

A few hours after injection, the dead, unfertilized and damaged embryos were removed and the egg water was refreshed to reduce the chance of infection. This procedure was repeated at several time points (usually 20 h, 24 h, 48 h, 72 h and 144 h) to follow up the survival of the zebrafish larvae. Afterwards, a data sheet was generated with the number of death and alive embryos and survival curves were constructed with Graphpad Prism 6.

3. *In vitro* biofilm quantification methods

3.1. Biofilm formation on 96-well plate

Candida cells were prepared as previously described (section 3.2.1). Next, 100 µl of *Candida* cells (1x10⁶ cells/well) was added to a flat-bottom 96-well polystyrene plate (6 wells per strain). After 90 min (period of adhesion), the wells containing the *Candida* strains (in RPMI- MOPS) were washed with 1X PBS and further incubated at 37°C for 24h (biofilm formation). After 24h, the wells were washed twice with 1X PBS and further quantified.

3.2. XTT

In vitro *C. albicans* biofilms were developed on the bottom of a 96-well microtiter plate and quantified by XTT reduction assay. This assay represents a rapid and a robust method for the semi-quantitative measurement of *C. albicans* biofilm formation. It determines the metabolic activities of biofilm-forming cells and the colorimetric change is based on the reduction of 2, 3-bis (2-methoxy-4-nitro-5-sulfophenyl)-2H-tetrazolium-5-carboxanilide (XTT, a tetrazolium dye).

Metabolically active cells are able to process XTT, yielding an in water-soluble colored product that can be measured by the spectrophotometer (Kuhn et al., 2003; Pierce et al., 2008).

A fresh XTT solution was prepared in sterile PBS (final concentration 1 mg/ml), stored in the dark until use. Just before the use, menadione solution (prepared in sterile water, concentration of 1M) was added to the XTT solution, so that the final menadione concentration was 1 μ M.

After biofilm formation, the wells were supplemented with 100 μ l XTT working solution (Sigma Aldrich). The plates were incubated at 37°C for 1 h in the dark and the intensity of the colorimetric change was measured by the spectrophotometer at 490 nm. As a blank, a well with only XTT solution was added.

3.3. Confocal laser scanning microscopy (CLSM)

C. albicans biofilms formed inside the borosilicate chambers and on the tissue culture coverslips in the presence of absence of microspheres were visualized by CLSM. Prior to microscopy, biofilms were washed with 1 mL of PBS. Biofilms formed by non-fluorescently-tagged *C. albicans* strains were stained with concanavalin A conjugated to Alexa Fluor 488 (final concentration 50 μ g/ml) (Invitrogen). Biofilms were stained for 20 min at 37°C, gentle shaking (100 rpm) in the dark. Biofilms formed by GFP- and yCherry – tagged *Candida* strains were only washed and immediately visualized. Subsequently, after 30 min, the samples were imaged using the confocal microscope (LSM510/ ConfoCor2 system, Carl Zeiss, Jena, Germany). The software used for image analyses was Olympus FV10-ASW.

Biofilm thickness was measured by capturing successive z-images through the biofilm structure.

4. *In vivo* biofilm quantification methods

4.1. Confocal laser scanning microscopy

Embryos injected with microspheres and/or fluorescently labeled *Candida* strains, were positioned on a thin glass slide (Indigo instruments) and the excess of egg water was removed to avoid the movement of the embryo. In some cases, the embryos were placed between two glass slides as the spherical form of the embryo could hide the observation of *Candida* cells and/or microspheres. Next, the embryos were analyzed under the CLSM.

4.2. Homogenization and CFUs

Embryos or larvae, devoided from egg water, were added to cryovials containing 100 μ l PBS. Next, the animals were homogenized (to check the dissemination) for few seconds by using a homogenizer (Proscientific). Between different embryos, the homogenizer was always cleaned

with 70% ethanol and sterile water. Consequently, the vials containing *Candida* strains, were sonicated for 10 min at 40 000 Hz in a water bath sonicator (Branson 2210) to fragment hyphal structures. Next, all samples were vigorously vortexed and the original samples, 1/100 and 1/1000 dilutions were plated on penicillin/streptomycin YPD agar plates. Plates were incubated at 37°C for 24 h and CFUs were enumerated.

4.3. Statistics

For the *in vitro* *C. albicans* biofilm formation on microspheres, statical significance was determined with a two-tailed Student's t-test. $P \leq 0.05$ was considered as statistically significant difference. *In vivo* survival experimental curves were generated using GraphPad Prism 6. Statistical analyses were performed with Kaplan Meier test. The calculations of the Kaplan-Meier survival fractions take into account censored observations, such as animals that were excluded from the particular experiment, for example for microscopy or homogenization. To test statistically significant differences between curves, a Logrank test was used. The P-value tests the null hypothesis that the survival curves are identical in the overall population or in other words, that the treatment did not change survival.

Table 5 gives an overview of the experimental set-up.

Table 5: An overview of different *C. albicans* strains, fluorescently labeled microspheres and zebrafish lines used for various experimental set up.

Aim 1: device-associated infection	Aim 2: explore innate immunity
Microspheres	
Red or yellow/green	Yellow/green
<i>C. albicans</i> strains	
GFP-tagged strains (WT-GFP <i>bcr1Δ/bcr1Δ</i> -GFP), yCherry strains (WT-yCherry, <i>efg1Δ/Δ cph1Δ/Δ</i> -yCherry)	yCherry strains (WT-yCherry, <i>efg1Δ/Δ cph1Δ/Δ</i> -yCherry)
Zebrafish lines	
AB	Transgenic fish line <i>fli1:GFP</i> (GFP expressing macrophages and endothelium)
Imaging methods	
Confocal scanning laser microscopy	Confocal scanning laser microscopy
Colony forming units	Colony forming units

Results

1. Determination of the fluorescence signal of red and green microspheres

In this study, we employed the use of fluorescently labeled microspheres for *C. albicans* device-associate infections. Before executing *in vivo* experiments, we first assessed the intensity of the fluorescence signal of microspheres (red and green, 10 μm). The fluorescence of the microspheres was validated by measuring their signal intensity. Results are demonstrated in figure 12.

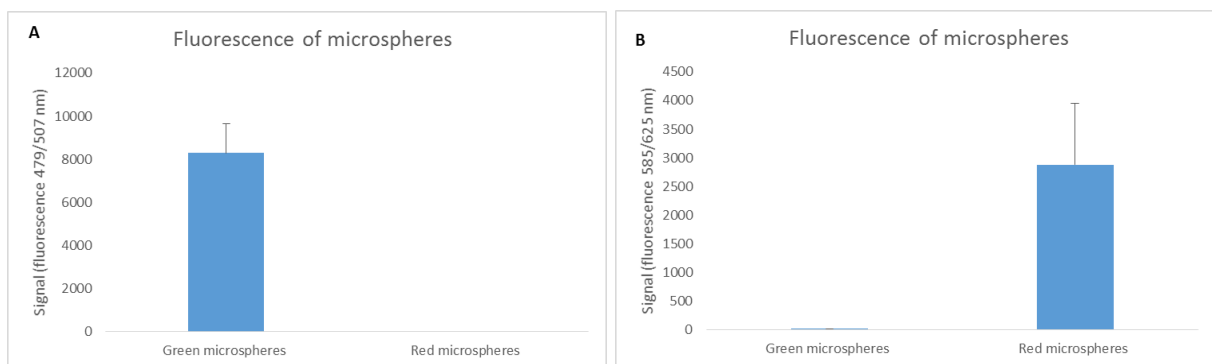


Figure 12: Fluorescence signal of microspheres. Red and green microspheres (10 μm) were dissolved in PBS at a concentration of 1×10^3 spheres/well. (A) Green fluorescence was measured at 479/507 nm, whereas (B) red fluorescence at 585/625 nm. Error bars represent standard deviation (SD). This experiment was repeated twice.

As it is shown in figure 12, green microspheres expressed high green fluorescence signal and red microspheres exhibited an intense response to the red fluorescence. Importantly, red microspheres did not express green fluorescence and green microspheres did not display red fluorescence, indicating no cross reactivity with different fluorescent signals and high quality of fluorescence microspheres.

2. Characterization of the fluorescence signal of *C. albicans* GFP- and yCherry- tagged strains with and without microspheres

Next to microspheres alone, we additionally examined the fluorescent intensity of GFP- and yCherry - tagged strains in the presence or absence of red and green microspheres. Non-fluorescently tagged strains, such as *C. albicans* SC5314, *bcr1 Δ /bcr1 Δ* and *efg1 Δ / Δ cph1 Δ / Δ* were used as controls. *C. albicans* GFP- or yCherry- tagged strains were incubated in the presence with red microspheres (10 μm) and yCherry strains were mixed with green

microspheres (10 μm) and incubated at 37 $^{\circ}\text{C}$. Fluorescence signal intensity was measured by spectrofluorometer after 24 h of device-associated infections. The results are demonstrated in figure 13.

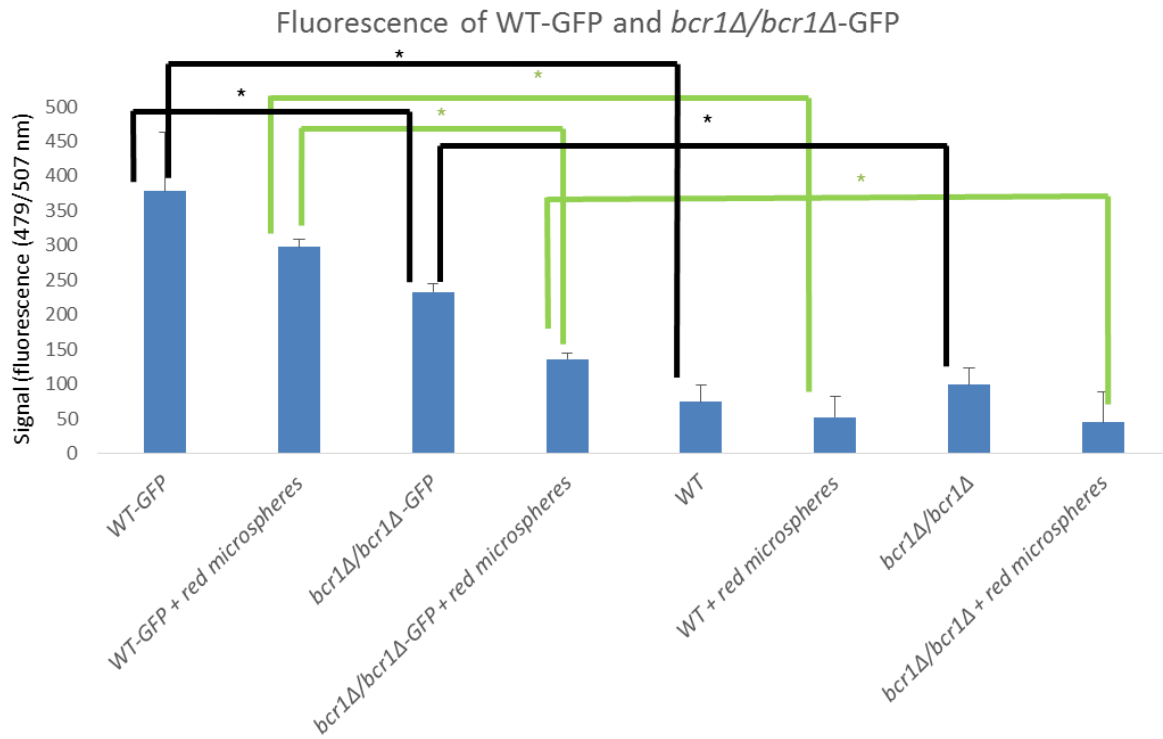


Figure 13: Fluorescence signal of *C. albicans* GFP-tagged strains with and without red microspheres. Fluorescence signal of *C. albicans* WT, *bcr1* Δ /*bcr1* Δ , WT-GFP and *bcr1* Δ /*bcr1* Δ - GFP- tagged strains in the absence and in the presence of red microspheres (10 μm). *C. albicans* cells (1×10^6 cells/well) were combined with microspheres (1×10^3 spheres/well) and incubated for 24 h in a 96- well polystyrene plate. The green fluorescence signal was measured with spectrofluorometer. PBS was used as a blank. Error bars represent SD. This experiment was repeated twice. Statistical significance was considered when $*p < 0.05$.

Figure 13, demonstrated statistically significant difference in fluorescence signal between GFP-tagged strains and non-GFP - tagged strains ($p < 0.05$). Moreover, the WT-GFP strain displayed significantly increased signal in comparison with the *bcr1* Δ /*bcr1* Δ -GFP strain ($p < 0.05$), indicating that the mutant strain failed to colonize the substrate. However, there was no higher signal in the conditions where the strains were combined with the polystyrene microspheres compared to the conditions without microspheres and this was against the expectations.

The same experiment was performed with the WT – yCherry and *efg1Δ/Δ cph1Δ/Δ* – yCherry - tagged strains. During this experiment, strains were incubated at 37 °C in the presence or absence of green/yellow microspheres (10 μm). After 24 h of infection process, fluorescent signal was measured by spectrofluorometer (figure 14).

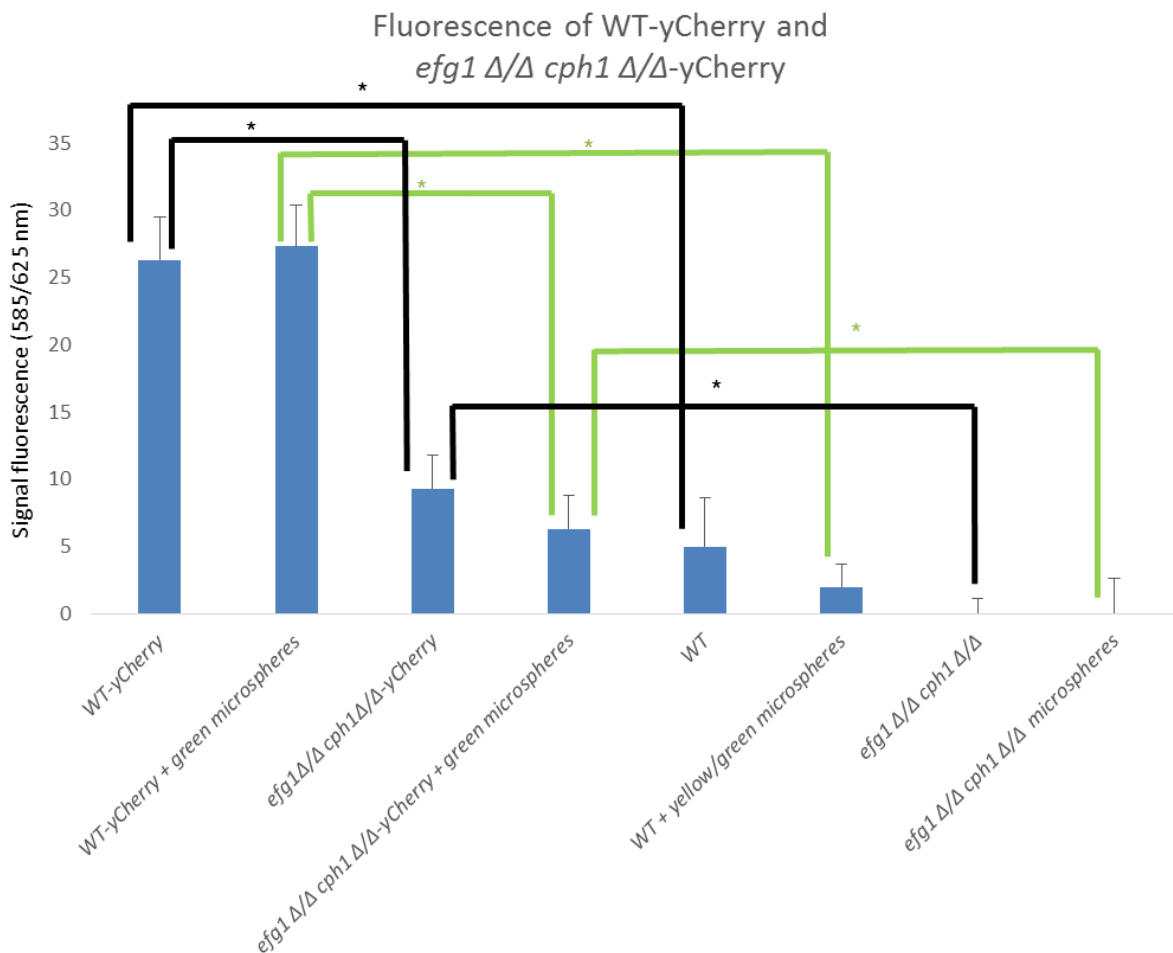


Figure 14: Fluorescence signal of *C. albicans* yCherry-tagged strains with and without green microspheres. Fluorescence signal of *C. albicans* WT, *efg1Δ/Δ cph1Δ/Δ*, WT-yCherry and *efg1Δ/Δ cph1Δ/Δ*- yCherry- tagged strains in the absence and in the presence of green microspheres (10 μm). *C. albicans* cells (1×10^6 cells/well) were combined with microspheres (1×10^3 spheres/well) and incubated for 24 h in 96- well polystyrene plate. The green fluorescence signal was measured with spectrofluorometer. PBS was used as a blank. Error bars represent SD. This experiment was repeated at twice. Statistical significance was considered when $*p < 0.05$.

As it is shown in figure 13, yCherry-tagged strains expressed significantly higher fluorescence in comparison with non-yCherry-tagged WT and mutant ($p < 0.05$). The mutant strain *efg1Δ/Δ cph1Δ/Δ*-yCherry expressed less fluorescent signal compared to the WT-yCherry strain,

indicating decreased amount of cells attached on the surface. In general, yCherry-tagged strains expressed lower fluorescence signal in comparison with the GFP-tagged strains.

It is noteworthy to mention that experiments demonstrated above were also performed without the centrifugation step. This resulted in *Candida* cells and microspheres detachment from the bottom of 96-well plates. When using these conditions, the intensity of fluorescence was significantly lower (data not shown).

3. *In vitro* biofilm formation on 96 well polystyrene plate

Before *in vitro* and *in vivo* experiments we first analyzed the WT strains (WT-GFP and WT-yCherry) and deletion strains (*bcr1Δ/bcr1Δ*-GFP and *efg1Δ/Δ cph1Δ/Δ*-yCherry) for their ability to develop biofilms *in vitro*. *Candida* cells were inoculated into a 96- well polystyrene plate. Biofilms (24 h old) were quantified by XTT reduction assay, which is based on the determination of the metabolic activity of device-associated cells. The results are displayed in figure 15.

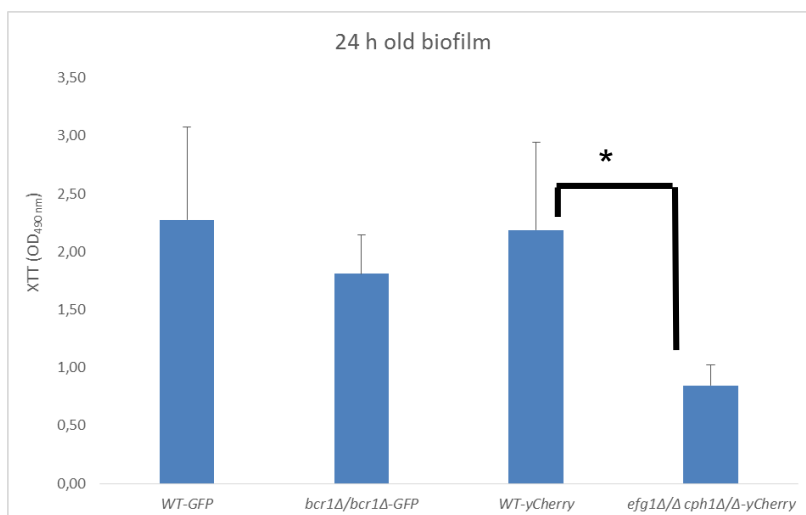


Figure 15: Biofilm formation of fluorescently tagged *C. albicans* strains. The metabolic activity of biofilm-forming cells was quantified using the XTT reduction assay measured at 490 nm. Biofilms were grown in a 96-well polystyrene plate. Error bars represent standard deviation (SD). Statistical significance was considered when $*p < 0.05$. This experiment was repeated at twice, always using six wells per strain.

As it is shown in figure 15, *C. albicans* WT-GFP tagged strain exhibited relatively higher metabolic activity of biofilm-forming cells in comparison with the *bcr1Δ/bcr1Δ*-GFP tagged strain. Although, this difference was not statistically significant, there is a decreased signal measured in *bcr1Δ/bcr1Δ*-GFP substrate-associated cells. *C. albicans* WT-yCherry strain demonstrated high XTT measurements indicating strong biofilm development. As it was

expected, *C. albicans efg1Δ/Δ cph1Δ/Δ*-yCherry device-associated cells exhibited much lower metabolic activity, in comparison with the WT-yCherry tagged strain ($p < 0.05$).

4. *In vitro* biofilm formation of *C. albicans* strains on polyethylene discs in the presence or absence of fluorescent microspheres

In the next step, we investigated the ability of *C. albicans* strains to develop device-associated infections in the presence of fluorescently-labelled microspheres *in vitro*. Herewith, we aimed at investigating the behavior of *Candida* cells in the presence of microspheres, their biofilm architecture including their biofilm thickness.

Biofilms were first studied in borosilicate chambers, which are specifically manufactured to study samples by CLSM. The biofilm formation of *Candida* strains alone was compared to the biofilm development of *Candida* strains in combination with microspheres. Moreover the WT-strain was always compared to a mutant strain, which served as a control. Unfortunately, experiments using borosilicate chambers were not successful, because biofilm-forming cells detached from the bottom, indicating that this substrate does not represent a preferable material for *Candida* attachment. Therefore, exactly the same experiments were executed on highly adhesive tissue culture round discs that were placed into a polystyrene 24-well plate. Biofilm formation of the fluorescently tagged strains was done in parallel with biofilm formation of the non-fluorescent strains.

The non-fluorescent strains were stained with concanavalin A conjugated to Alexa Fluor 488 prior to imaging. This dye binds to glucose and mannose residues of cell wall polysaccharides (Chandra, 2001). The thickness of the *C. albicans* WT-GFP and *bcr1Δ/bcr1Δ*-GFP biofilm structure was measured by capturing individual slices. The results are demonstrated in figure 16.

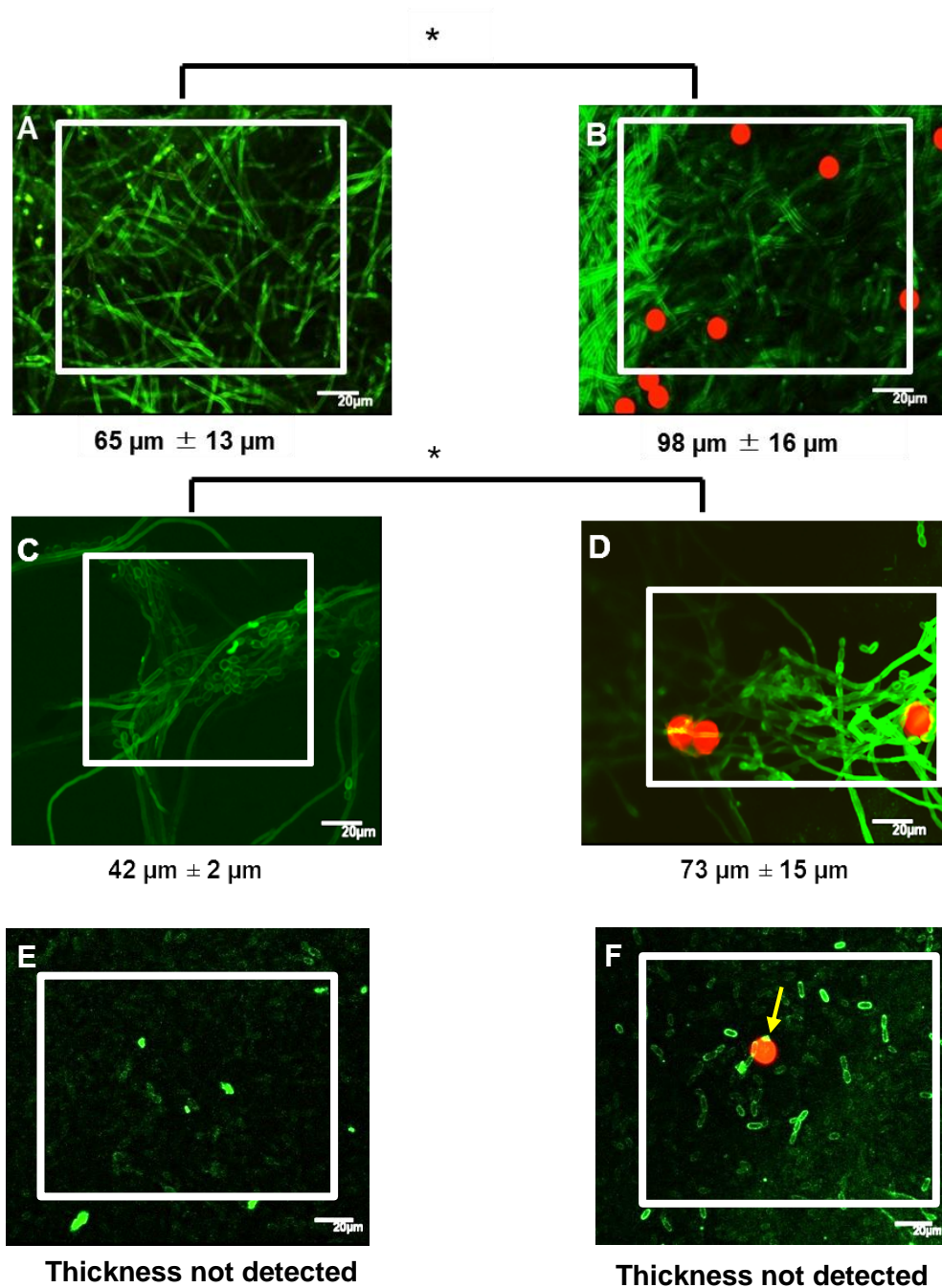


Figure 16: Confocal laser scanning images of 24 h old biofilm formation of non-GFP tagged WT *C. albicans* SC5314 without (A) and with microspheres (B), *bcr1Δ/bcr1Δ* without (C) and with microspheres (D) and *efg1Δ/Δ cph1Δ/Δ* without (E) and with microspheres (F) on highly adhesive plastic discs. These substrates were challenged with *Candida* cells (1×10^5 cells/well) and red microspheres (1×10^4 spheres/well). Mature biofilms (24 h old) were stained with concanavalin A conjugated to Alexa Fluor 488 (green fluorescence). The thickness was measured by acquiring z-images (indicated below the figures). Two independent experiments were performed. Statistical significance was considered when $*p < 0.05$. White frames indicate the scanned area. Magnification 60x. Scale bar= 20 μm

Architecturally speaking, the WT strain developed thick biofilms as characterized by the presence of hyphal cells alongside the substrate. The *bcr1Δ/bcr1Δ* strain, on the contrary, formed only rudimentary biofilm displaying the scattered amount of hyphal cells attached on the substrate. *C. albicans efg1Δ/Δ cph1Δ/Δ* strain failed to form biofilms, as documented by the presence of yeast cells spread on the substrate. Importantly, *Candida* cells were able to develop an infection around the microspheres. When measuring biofilm thickness, there was a significant difference ($p < 0.05$) between the WT strain without microspheres ($65 \mu\text{m} \pm 13 \mu\text{m}$, figure 16 A) and the WT strain in the presence of microspheres ($98 \mu\text{m} \pm 16 \mu\text{m}$, figure 16 B). Essentially, this assumes that the addition of polystyrene microspheres enhances biofilm formation. Similarly, the *C. albicans bcr1Δ/bcr1Δ* strain formed a thicker biofilm structure in the presence of the microspheres ($73 \mu\text{m} \pm 15 \mu\text{m}$, figure 16 D) than in the condition without the microspheres ($42 \mu\text{m} \pm 2 \mu\text{m}$, figure 16 C) ($p < 0.05$). For the *efg1Δ/Δ cph1Δ/Δ* strain, we observed no biofilm formation but figure 16 F demonstrates the adherence of yeast cells on the red microspheres as indicated by the yellow arrow. In addition, the WT strain forms a thicker structure compared to the mutant strains (*bcr1Δ/bcr1Δ* and *efg1Δ/Δ cph1Δ/Δ*) and this is the case for the conditions with and without microspheres. The biofilm structure of the WT strain in the absence of microspheres ($65 \mu\text{m} \pm 13 \mu\text{m}$, figure 16 A) is significantly ($p < 0.05$) thicker than the *bcr1Δ/bcr1Δ* strain without microspheres ($42 \mu\text{m} \pm 2 \mu\text{m}$, figure 16 E). Equivalently, the biofilm of the WT strain in combination with microspheres ($98 \mu\text{m} \pm 16 \mu\text{m}$, figure 16 B) is significantly ($p < 0.05$) thicker than of the *bcr1Δ/bcr1Δ* strain with microspheres ($73 \mu\text{m} \pm 15 \mu\text{m}$, figure 16 D). The biofilm thickness of the WT and the *bcr1Δ/bcr1Δ* strains was significantly ($p < 0.05$) higher than for the *efg1Δ/Δ cph1Δ/Δ* as this strain failed to form a biofilm in the condition with (figures 16 F) as well as the condition without microspheres (figure 16 E).

In the next step, we were curious whether fluorescently-labelled microspheres will influence the biofilm thickness of GFP-tagged strains (WT-GFP and *bcr1Δ/bcr1Δ*-GFP). These results are represented in figure 17.

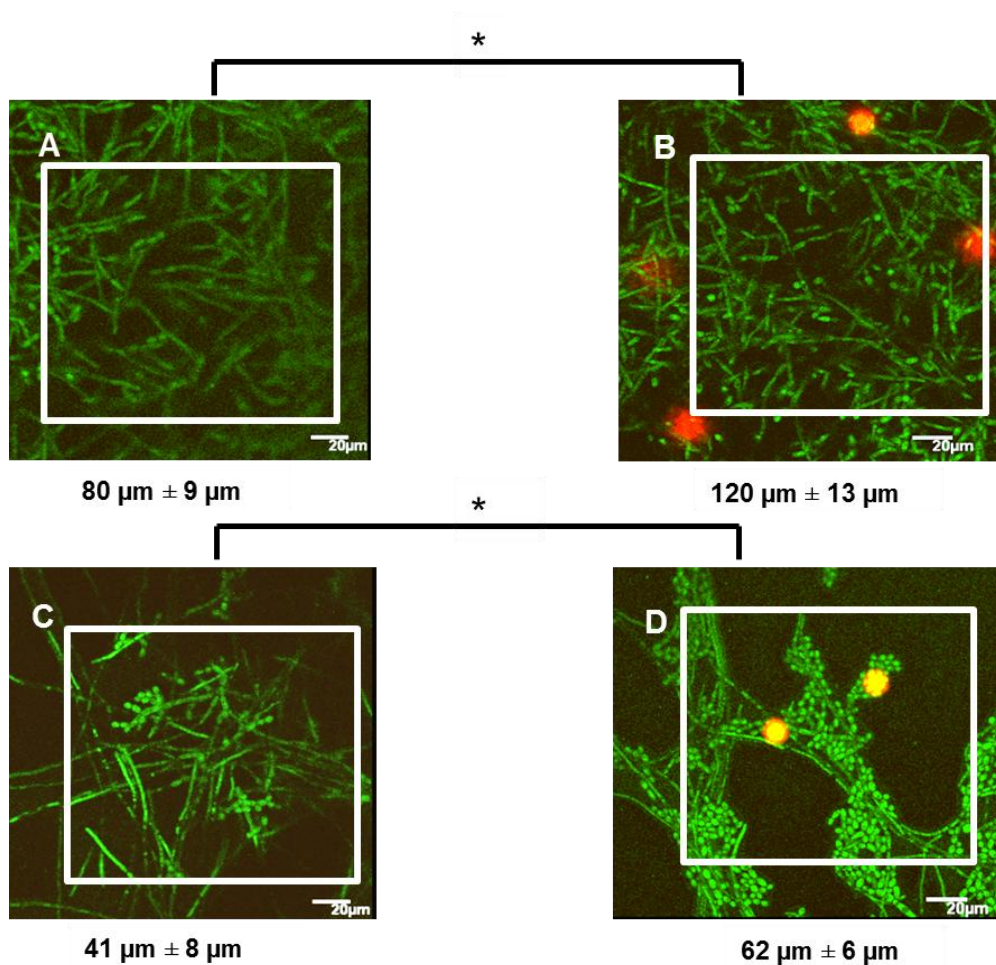


Figure 17: Confocal laser scanning images of 24 h old biofilm formation of GFP tagged WT *C. albicans* without (A) and with microspheres (B), *bcr1Δ/bcr1Δ*-GFP without (C) and with microspheres (D) on highly adhesive plastic discs. These substrates were challenged with *Candida* cells (1×10^5 cells/well) and red microspheres (1×10^4 spheres/well). The thickness was measured by acquiring z-images (indicated below the figures). Two independent experiments were performed. Statistical significance was considered when $*p < 0.05$. White frames indicate the scanned area. Magnification 60x. Scale bar= 20 μm .

The biofilm architecture of GFP-tagged strains was in agreement with the biofilm structure observed with non-GFP-tagged strains. Importantly, the biofilm thickness of the WT-GFP strain with microspheres ($120 \mu\text{m} \pm 13 \mu\text{m}$, figure 17 B) was again higher than the condition without microspheres ($80 \mu\text{m} \pm 9 \mu\text{m}$, figure 17 A). Moreover, there was a significant difference ($p < 0.05$) between the biofilm thickness of the *bcr1Δ/bcr1Δ*-GFP strain in the presence of microspheres ($62 \mu\text{m} \pm 6 \mu\text{m}$, figure 17 D) compared to the condition where microspheres were absent ($41 \mu\text{m} \pm 8 \mu\text{m}$, figure 17 C). Also in this case, the biofilm structure of the WT-GFP strain in the absence of microspheres ($80 \pm 9 \mu\text{m}$, figure 17 A) is significantly ($p < 0.05$) thicker than the *bcr1Δ/bcr1Δ*-GFP strain without microspheres ($41 \mu\text{m} \pm 8 \mu\text{m}$, figure 17 C). Similarly, the biofilm of the WT-GFP strain in combination with microspheres ($120 \mu\text{m} \pm 13 \mu\text{m}$, figure 17

B) is significantly ($p < 0.05$) thicker than of the *bcr1Δ/bcr1Δ*-GFP strain with microspheres ($62 \mu\text{m} \pm 6 \mu\text{m}$, figure 17 D).

Following the biofilm formation by GFP-tagged strains, next, we analyzed the ability of *C. albicans* yCherry-tagged strains to develop biofilms on highly adhesive tissue culture round discs in the presence and absence of microspheres. On figure 18, the results are demonstrated from the experiment with the yCherry-tagged strains. Biofilm formation of the WT-yCherry strain was compared to the *efg1Δ/Δ cph1Δ/Δ*-yCherry deletion strain.

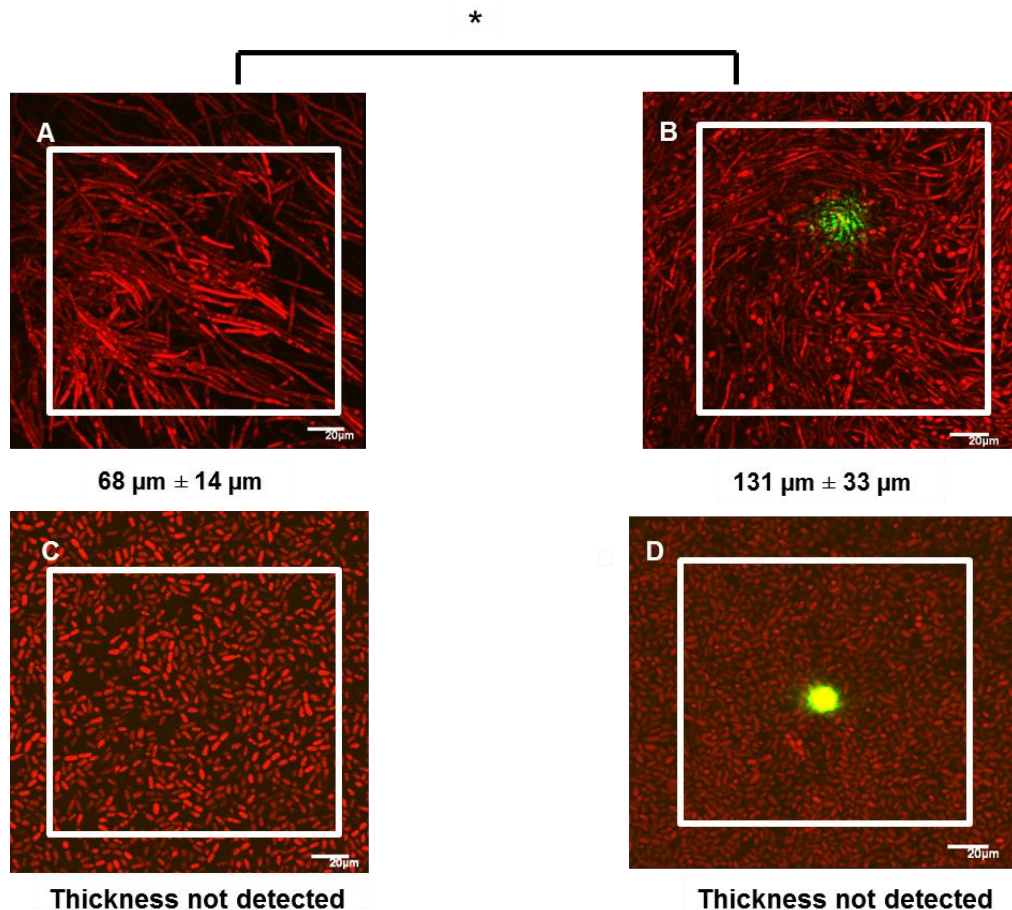


Figure 18: Confocal laser scanning images of 24 h old biofilm formation of yCherry-tagged WT *C. albicans* without (A) and with microspheres (B), *efg1Δ/Δ cph1Δ/Δ*-yCherry without (C) and with microspheres (D) on highly adhesive plastic discs. These substrates were challenged with *Candida* cells (1×10^5 cells/well) and green microspheres (1×10^4 spheres/well). The thickness was measured by acquiring z-images (indicated below the figures). Two independent experiments were performed. Statistical significance was considered when $*p < 0.05$. White frames indicate the scanned area. Magnification 60x. Scale bar= 20 μm

As it is shown in figure 18, the WT-yCherry strain formed thick biofilms characterized by a strong network of hyphal cells spread alongside the substrate. More importantly, the presence of microspheres significantly enhanced the biofilm formation, as the biofilm thickness was $131 \mu\text{m} \pm 33 \mu\text{m}$ when microspheres were added in comparison with the biofilms without the microspheres $68 \mu\text{m} \pm 14 \mu\text{m}$ ($p < 0.05$). *C. albicans efg1Δ/Δ cph1Δ/Δ*-yCherry was not able to develop biofilms and only scattered amount of yeast cells was present on the substrate as documented by CLSM. Because of this reason, the biofilm thickness could not be measured.

These findings indicated that the presence of microspheres during the biofilm development significantly increased the biofilm thickness of the WT strains. Moreover, *Candida* WT strains were able to form a thick network of hyphal cells embedded within the polystyrene microspheres. The mutant strains showed a defect in mature biofilm formation. These data are in agreement with the results obtained by Nobile et al., (2005).

In the next steps we asked ourselves whether *Candida* cells will form a hyphal network embedded within the microspheres *in vivo*, as this situation would mimic a device-associated infection. Also we were curious whether the mutant strains will show the same phenotype as during the *in vitro* experiments. To achieve this we performed *in vivo* experiments in zebrafish embryos and larvae since this model organism provides several advantages as already discussed in section 5.2.

5. Unravel the injection volume and the size of microspheres

In literature, typical injection volumes used for the development of *Candida* infection in the hindbrain of zebrafish larvae are 5 to 10 nl (approximately 20 yeast cells/fish for a *Candida* suspension at $1 \times 10^7/\text{ml}$) (Brothers & Wheeler, 2012). In our study, which is based on the injection of *Candida* cells into the yolk of zebrafish embryos, a typical injection volume was 2 nl what corresponds to 20 yeast cells (droplet size of 0.16 mm). Injection into the yolk during the 1 – 4 -cell stage allowed for a free delivery of the injection material from the yolk to the cells that will become the embryo. If injection would occur during higher cell stages, then the possibility of destroying the embryos during the injection may eventually happen. During the initial steps, yolk injection required intensive practicing.

As one of our main goals was to investigate *Candida* device-associated infections, we first examined whether the microspheres could be injected into the zebrafish embryos and what size of the substrate is optimal to allow passage through the injection needle. To our knowledge, this has never been done before and therefore several microsphere sizes were tested, namely 1 μm , 4 μm and 10 μm size. Injection with 10 μm microspheres into the yolk of

zebrafish embryos immediately after the fertilization was not successful, because the needle clogged even at high dilutions. Injection of 1 μm and 4 μm microspheres did not cause any problems. However, the size of 1 μm microspheres could have been too small for microscopic evaluation. Secondly, the size of one *Candida* cell is approximately 3 to 7 μm (depending on the *Candida* cells morphology), therefore the usage of such small microspheres would not allow *Candida* to develop infection around the microspheres. Therefore, in our next experiments we decided to continue with the 4 μm microspheres. The size and fluorescent signal of 4 μm microspheres is shown in figure 19.

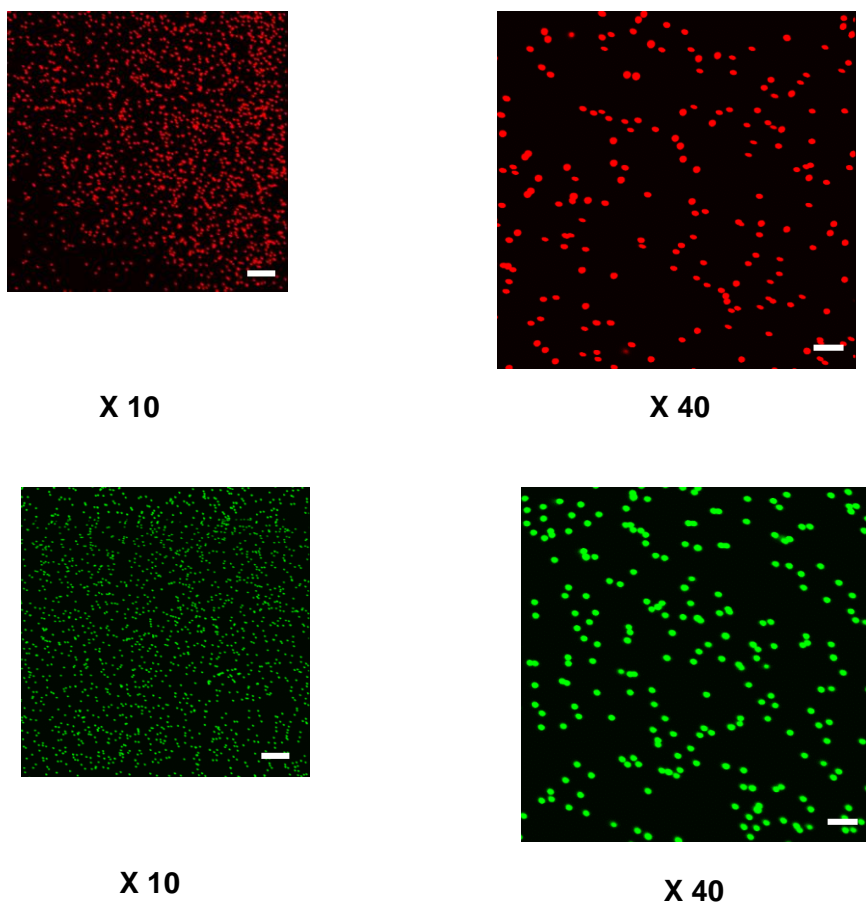


Figure 19: Confocal laser scanning electron images of red and yellow/green microspheres of 4 μm size. Magnification 10x and 40x. Bars= 20 μm for 40x objective and 100 μm for 10x objective.

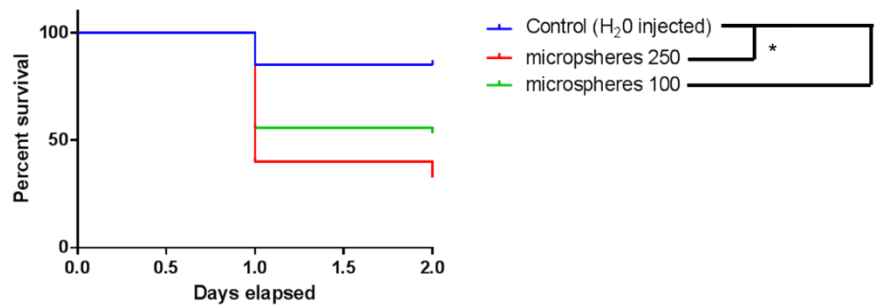
6. Zebrafish survival upon injection of microspheres at different concentrations into the yolk

Our first *in vivo* experiments were based on the survival of zebrafish embryos upon injection of microspheres into the yolk. The embryos at 1– 4- cell stage were injected with 250, 100, 50, 25, 10, 5 and 2 microspheres/embryo. Red microspheres (4 μm) were used for this experiment.

Water-injected embryos were considered as controls. The survival was followed for 24 h and 48 h. The survival curves are demonstrated in figure 20.

A

Survival of zebrafish embryos upon microspheres injection



B

Survival of zebrafish embryos upon microspheres injection

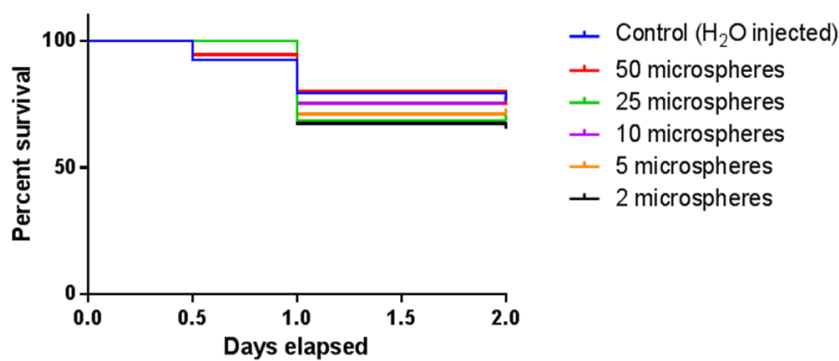


Figure 20: Survival of zebrafish embryos upon microspheres (4 μ m) injection into the yolk at different concentrations. Microspheres at **(A)** high (250 and 100 microspheres) and **(B)** lower (50, 25, 10, 5 and 2 microspheres) concentrations were injected into the yolk of 1-cell stage zebrafish embryos (2 nl injection volume). Fifty embryos were injected per condition. The survival of the zebrafish larvae was checked at two different time points (24 h and 48 h). Statistical significance was considered when $*p < 0.05$.

As it is demonstrated in figure 20 (A) zebrafish died significantly faster when higher concentrations of microspheres were injected in comparison to water-injected embryos ($p < 0.05$). Despite of that, zebrafish survived and developed further when lower amounts of microspheres were injected (B) in comparison with the control ($p > 0.05$). Some of the embryos were also subjected to confocal microscopy (figure 21).

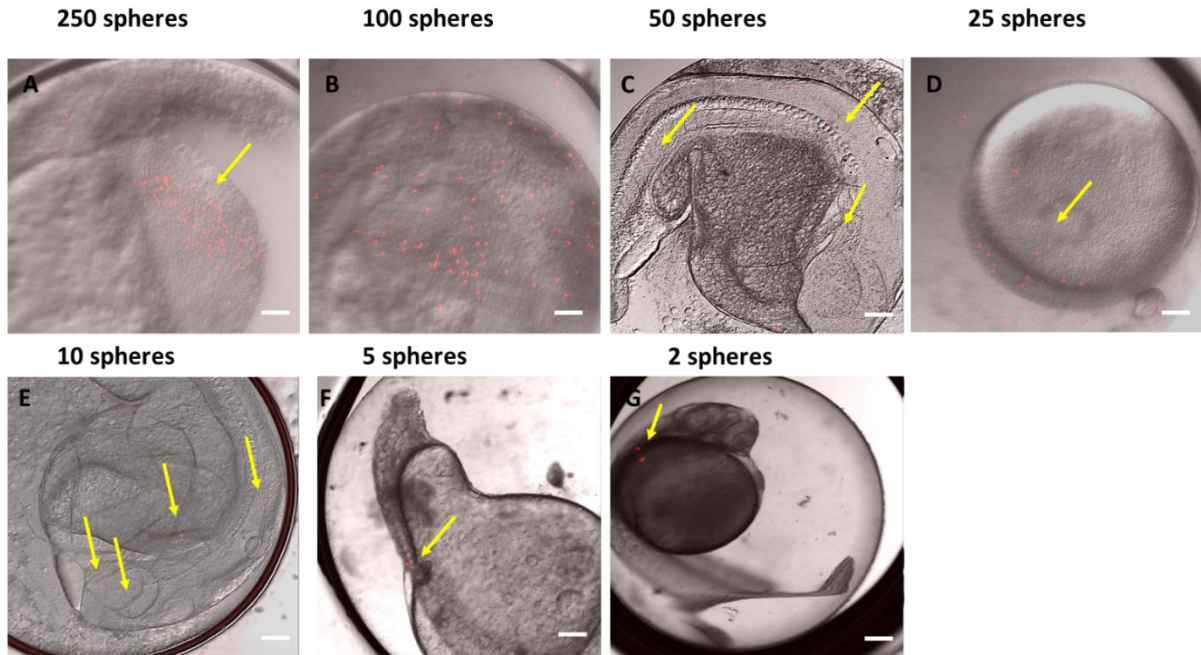


Figure 21: Confocal laser scanning microscopy demonstrating microspheres inside the yolk of zebrafish embryos. Embryos were injected with different numbers (250, 100, 50, 25, 10, 5 and 2) of microspheres into the yolk of 1-cell stage zebrafish embryos. Embryos were imaged at 4 hpi (A, B and D) and 24 hpi (C, E, F and G). Yellow arrows indicate the location of the microspheres inside the yolk. Magnification 10 x. Scale bar= 100 μ m. Arrows indicate the location of the microspheres.

As it is demonstrated in figure 21, the microspheres were located inside the yolk of the zebrafish embryos (A, B, D and F). Although a certain concentration of microspheres was injected, it seemed that the embryo didn't always contain the desired amount. Most of the time, there were less microspheres present as compared to the initial injection volume. This might have been due to an artefact of the needle because the gravity causes the microspheres to sink to the tip of the needle and this sometimes led to inconsistent injection volumes.

However, even though the injections were done in the yolk, some microspheres were also dispersed into other parts of the embryo (such as the tail, head, etc.) (C, E and G). It is important to mention that within the following hours of development of embryo, microspheres disseminated into different organs. A more detailed overview of microspheres dissemination after 48 hpi is demonstrated in figure 22.

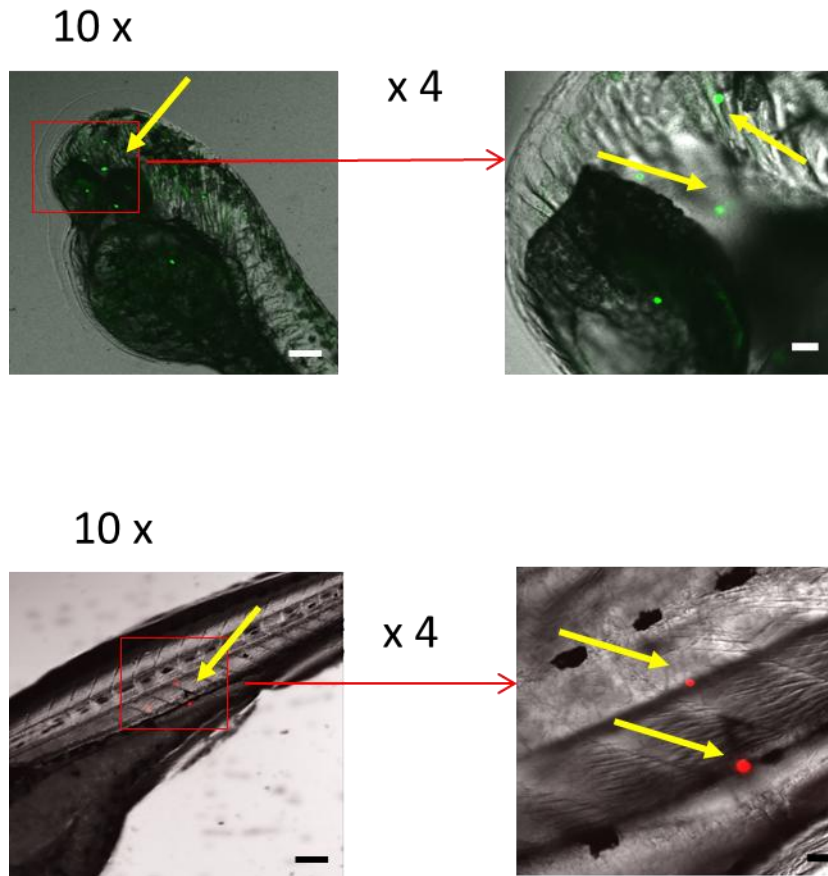


Figure 22: Dissemination of microspheres throughout the larvae. Pictures represent 48 h old zebrafish larvae. Magnifications 10X (for left pictures) and 40X (for right pictures). Scale bar= 100 μ m (for left pictures) and 20 μ m (for right pictures).

For the future experiments, we decided to use a concentration of 50 spheres injected per embryo, because this amount yielded in high survival percentages and a sufficient amount of spheres per animal.

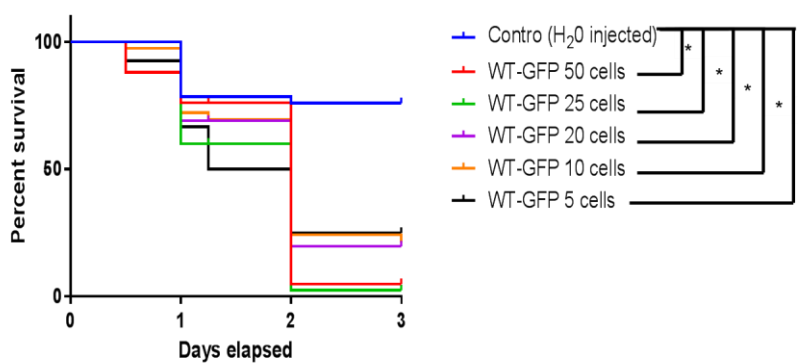
7. *C. albicans* injection and follow-up of the survival of zebrafish embryos

In our previous experiments, we have determined the survival of zebrafish after the injection of microspheres. In the next step, we tested the effect of different concentrations of *Candida* cells injected into the yolk on the survival of embryos. On one hand, high concentrations of *Candida* might cause that the embryos succumb the infection at early time points, but on the other hand, too low injection concentration could result in the absence of an infection. As such, there is a trade-off between injecting enough *Candida* cells and the survival of the embryos. For a first experiment, a concentration gradient, ranging from 50 to 5 *Candida* cells injected per embryo was used. The WT-GFP and *bcr1* Δ /*bcr1* Δ -GFP strains were injected at 0-1 hpf

into the yolk of zebrafish embryos. Per condition, 50 embryos were injected. The survival of the zebrafish embryos was monitored after 4h, 24h, 48h and 72h. After 24h and 48h, five embryos per condition were analyzed under the confocal microscope to detect the infection. The survival curves for the WT-GFP and *bcr1Δ/bcr1Δ*-GFP strains and representative figures demonstrating an infection inside the embryos are demonstrated in figures 23 and 24 respectively. In order to determine whether the differences between the survival curves of the WT-GFP strain and the mutant *bcr1Δ/bcr1Δ*-GFP strain were statistically significant, a Logrank test was performed in Graphpad Prism (Table 6).

A

Survival of zebrafish embryos upon WT-GFP injection



B

Survival of zebrafish embryos upon *bcr1Δ/bcr1Δ*-GFP injection

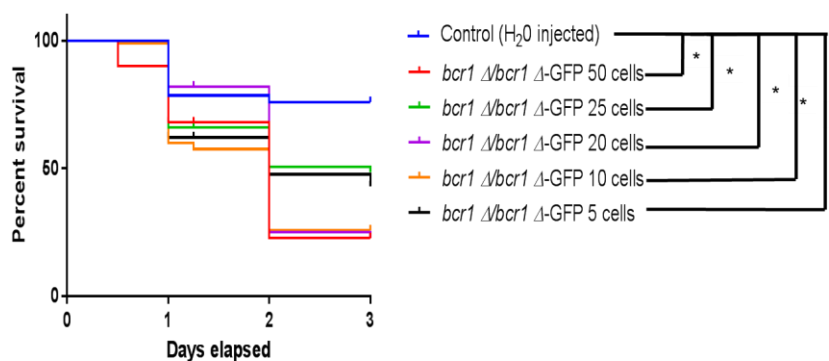


Figure 23: Survival curves of zebrafish embryos upon *Candida* injection. WT-GFP (A) and *bcr1Δ/bcr1Δ*-GFP (B) were injected at various concentrations into the yolk of one-cell stage zebrafish embryos. The survival of zebrafish embryos was monitored after 4, 24, 48 and 72 h post injection. Statistically significant when * $p < 0.05$ (Logrank test). Data are from one particular experiment.

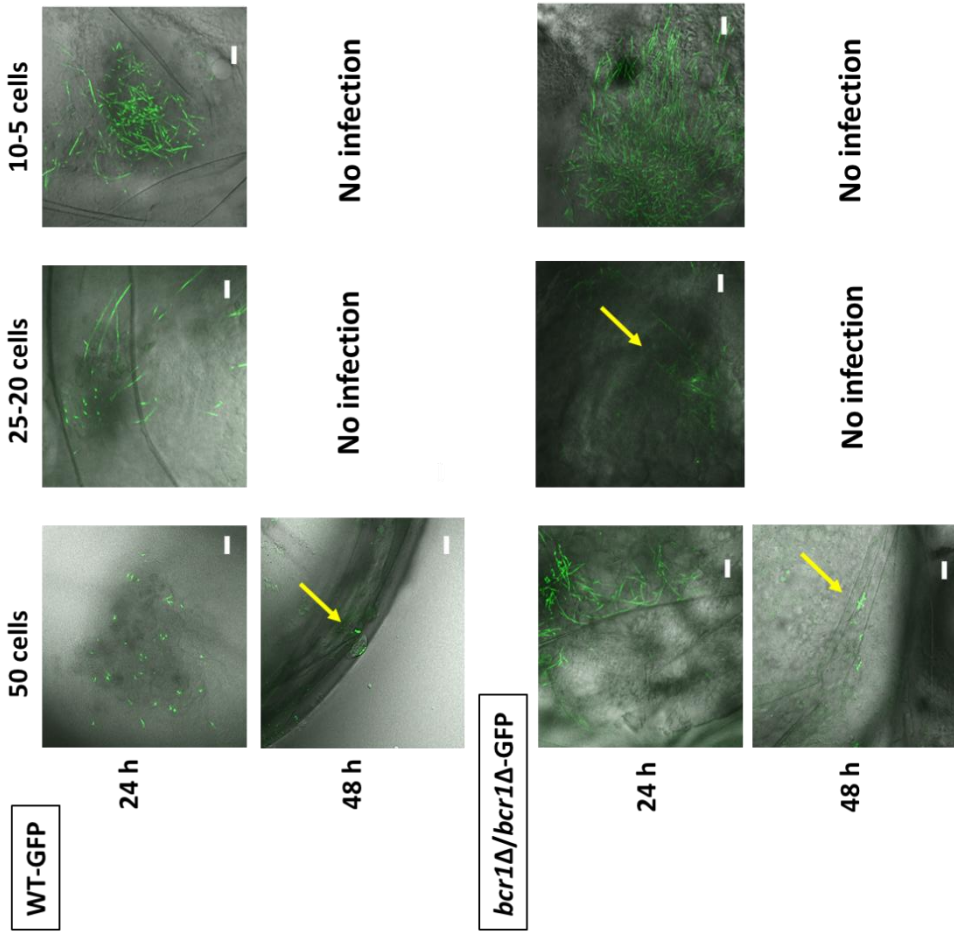


Figure 24: Confocal laser scanning images demonstrating *Candida* infection inside the yolk of zebrafish embryos. WT-GFP and *bcr1Δ/bcr1Δ*-GFP were injected into yolk of zebrafish embryos at different concentrations (50, 25, 20, 10 and 5 cells). The embryos were screened under the confocal microscope after 24 and 48 h post injection. Scale bar= 20 μm. Magnification 40 x.

Table 6: A summary displaying the statistically significant difference in the survival of zebrafish embryos upon different concentrations of *C. albicans* WT-GFP strain and *bcr1Δ/bcr1Δ*-GFP strain injection. Survival was monitored for 3 days. Statistical analyses were performed after 3 days. Significant difference when $p < 0.05$ (Logrank test).

Comparison of strains	Statistically significant ($p < 0.05$)
WT-GFP 50 cells <i>bcr1Δ/bcr1Δ</i> -GFP 50 cells	No
WT-GFP 25 cells <i>bcr1Δ/bcr1Δ</i> -GFP 25 cells	Yes
WT-GFP 20 cells <i>bcr1Δ/bcr1Δ</i> -GFP 20 cells	No
WT-GFP 10 cells <i>bcr1Δ/bcr1Δ</i> -GFP 10 cells	No
WT-GFP 5 cells <i>bcr1Δ/bcr1Δ</i> -GFP 5 cells	No

As it is demonstrated in figure 23 A, injection of the embryos with water showed minor effect on the survival of the zebrafish (survival rate 75-80%). After 24 h of infection with the WT-GFP strain approximately 30% - 40% of embryos died regardless of the different concentrations of *Candida* cells/embryo injected. This was documented by the presence of hyphal cells in the yolk of the embryos infected with the WT-GFP. After 48 h of infection, embryos injected with the highest concentrations of WT-GFP *Candida* cells (50 and 25) died (figure 23 A). In comparison with the water-injected embryos this difference was statistically significant ($p < 0.05$). However, embryos challenged with the lower concentrations of WT-GFP *Candida* cells (20, 10 and 5 cells) survived the infection for 2 days and were even still alive 3 days after the injection. These findings were in agreement with the representative confocal images as no infection was observed after 2 days (figure 24) for the WT-GFP strains injected with lower concentrations of cells. Despite of this, the dead embryos (addendum B, figure B1) demonstrated massive *Candida* infection after 48h. The embryos were damaged by *Candida* hyphae.

In general, there was a higher amount of embryos, which survived when injected with the *bcr1Δ/bcr1Δ*-GFP as compared to the embryos injected with the WT-GFP strain (figure 23 B). However, there was a significant difference ($p < 0.05$) between the survival of the embryos that were treated with *Candida* cells (*bcr1Δ/bcr1Δ*-GFP) compared to the control condition (water injected). After 2 days, there was a huge drop in the survival of the embryos injected with the highest concentration (50) of *bcr1Δ/bcr1Δ*-GFP (figure 23 B) and the embryos injected with 10

and 20 cells. When observing the representative confocal images, there was no infection visible for the live embryos that were injected with average (25-20) and lower amounts of *bcr1Δ/bcr1Δ*-GFP cells (5-10) after 48 h, but when examining the dead embryos (addendum B, figure B1), there was again a massive infection (which correlated with the reduced survival percentage after 48 h for the embryos injected with all the concentrations of *bcr1Δ/bcr1Δ*-GFP). Table 6 shows that, although the survival of the embryos injected with the mutant strain seemed to be higher, there were overall no statistical differences between the survival curves of the WT-GFP and the *bcr1Δ/bcr1Δ*-GFP. Only Injection of 25 *Candida* cells per embryo, resulted in a significant difference between the survival curves of WT-GFP and *bcr1Δ/bcr1Δ*-GFP. Next, we followed the survival of embryos upon injection with the WT-yCherry and *efg1ΔΔ cph1ΔΔ*-yCherry strains. For this experiment, 30 embryos were injected per *Candida* concentration. The survival curves and representative confocal images are represented in figures 25 and 26, respectively. Figure 27 demonstrates the dissemination of WT-yCherry into a zebrafish larvae. An overview of the significant differences is given in table 7.

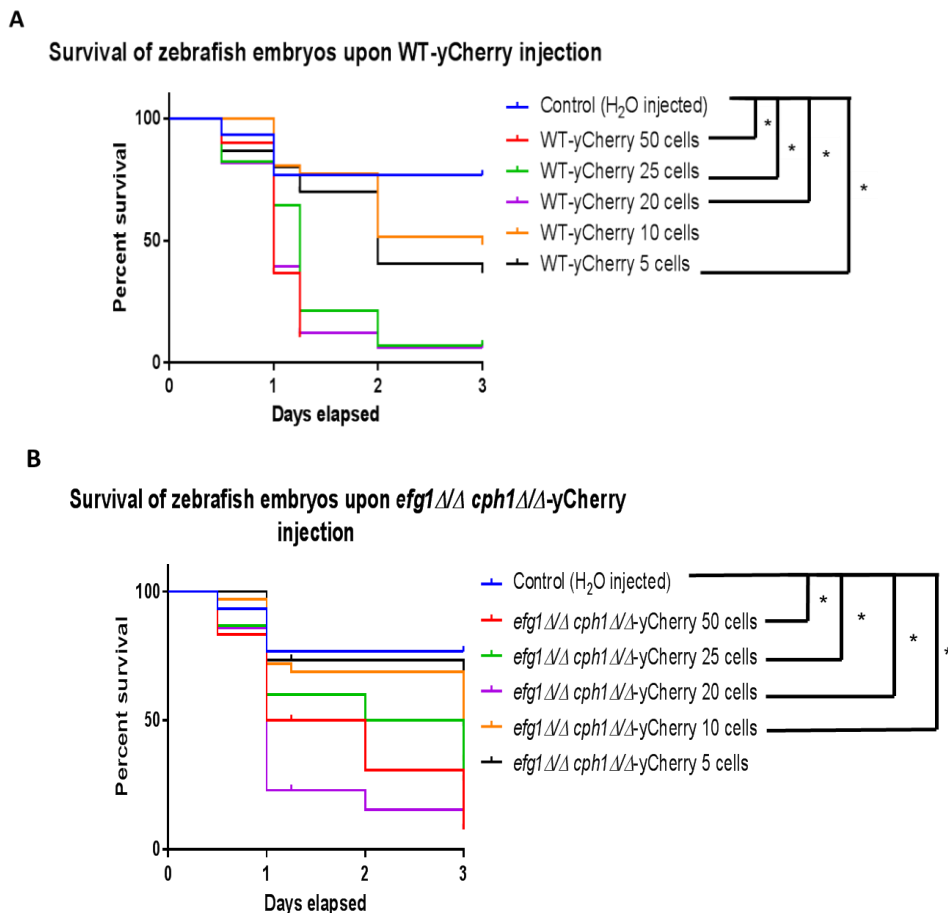


Figure 25: Survival curves of zebrafish embryos upon *Candida* injection. WT-yCherry (A) and *efg1ΔΔ cph1ΔΔ*-yCherry (B) were injected at various concentrations into the yolk of one-cell stage zebrafish embryos. The survival of zebrafish embryos was monitored after 4, 24, 30, 48 and 72 h post injection. Statistically significant when * $p < 0.05$ (Logrank test). Data are from one particular experiment.

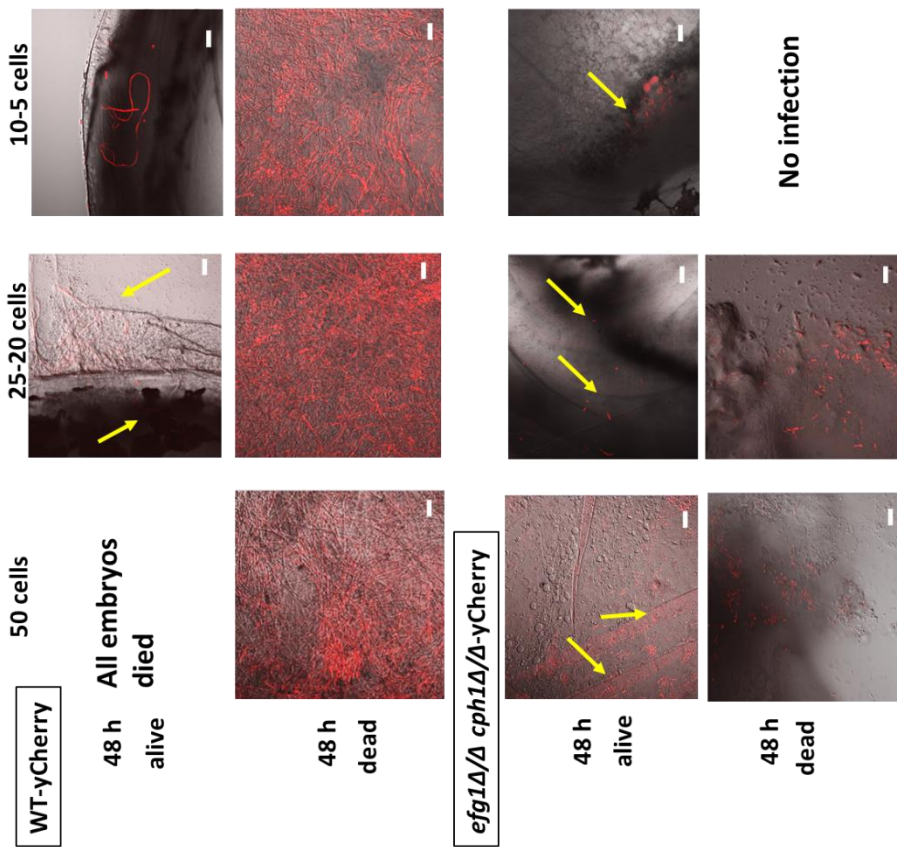


Figure 26: Confocal laser scanning images demonstrating *Candida* infection inside the yolk of zebrafish embryos. WT-yCherry and *efg1Δ/Δ cph1Δ/Δ*-yCherry were injected into the yolk of zebrafish embryos (one-cell stage) at different concentrations (50, 25, 20, 10 and 5 cells). The embryos were screened under the confocal microscope after 48h post injection. Scale bar= 20 μm. Magnification 40 x.

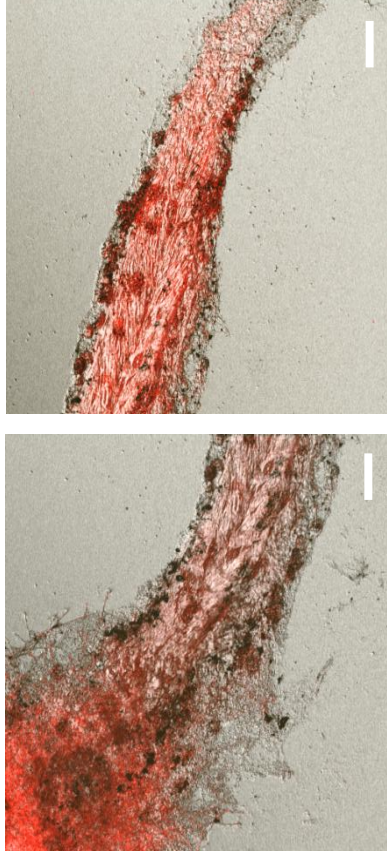


Figure 27: Dissemination of WT-yCherry into a zebrafish larvae. WT-yCherry (20 cells) was injected into the yolk of zebrafish embryos. After 72 h, *Candida* disseminated throughout the whole larvae and the larvae succumbed the infection. Scale bar= 100μm. Magnification 10 x

Table 7: A summary displaying the statistically significant difference in the survival of zebrafish embryos upon different concentrations of *C. albicans* WT-yCherry strain and *efg1Δ/Δ cph1Δ/Δ*-yCherry strain injection. Survival was monitored for 3 days and statistics were done after 3 days. Significant when $p < 0.05$ (Logrank test).

Comparison of strains	Statistically significant ($p < 0.05$)
WT-yCherry 50 cells <i>efg1Δ/Δ cph1Δ/Δ</i> -yCherry 50 cells	Yes
WT-yCherry 25 cells <i>efg1Δ/Δ cph1Δ/Δ</i> -yCherry 25 cells	Yes
WT-yCherry 20 cells <i>efg1Δ/Δ cph1Δ/Δ</i> -yCherry 20 cells	No
WT-yCherry 10 cells <i>efg1Δ/Δ cph1Δ/Δ</i> -yCherry 10 cells	No
WT-yCherry 5 cells <i>efg1Δ/Δ cph1Δ/Δ</i> -yCherry 5 cells	No

For this experiment, there was a significant difference (< 0.05) between the embryos injected with 50, 25, 20 and 5 WT-yCherry cells per embryo and the embryos injected with water. After 1 day, there was a strong reduction in the survival of the embryos injected with the highest concentration (50 cells per embryo) of WT-yCherry and after that day all embryos died. After 2 days, there was a strong reduction in the survival of embryos injected with all the concentrations of WT-yCherry. These observations were in accordance with the confocal images. After 48 h, all dead embryos showed a massive infection (figure 26). In these embryos, the WT-yCherry strain formed a hyphal network and in some cases the strain disseminated into other parts of the larvae such as head and tail (figure 27). Around 50% of the embryos that were injected with a low amount of WT-GFP (10 and 5 cells), were able to overcome the infection. The embryos that stayed alive after 2 days, showed almost no infection for injections of 5 to 10 cells. After 3 days, all the embryos that were injected with 25 or 20 cells, succumbed the infection (figure 25 A). The embryos injected with the mutant strain (*efg1Δ/Δ cph1Δ/Δ*-yCherry) had significant differences in survival compared to the embryos injected with water and this was the case for all the concentrations of *efg1Δ/Δ cph1Δ/Δ*-yCherry, except for injections with 5 cells. The embryos that were injected with the *efg1Δ/Δ cph1Δ/Δ*-yCherry strains seemed to survive for longer time points, compared to injections with the WT-yCherry strain (figure 25 B). This was also noted when the embryos were visualized under the microscope as the *efg1Δ/Δ cph1Δ/Δ*-yCherry strain stayed in the yeast form inside the animals

and behaved less virulent compared to the WT-strain. Significant differences between the survival of embryos injected with WT-yCherry and the mutant strain were obtained for the two highest concentrations (50 and 25 cells) indicating that the animals die faster when injecting 50 and 25 cells of the WT-yCherry strain than injecting the same amount of the mutant strain.

Based on the previous two experiments, it could be concluded that embryos succumb the infection at earlier time points when they are injected with 25 cells of the WT strains compared to the mutant strains. These differences were considered significant ($p < 0.05$). Moreover, for future experiments, the embryos will be injected with 20-25 cells per embryo because this concentration gave the best trade-off between survival of the embryos and the development of an infection.

8. *C. albicans* device-associated infection in zebrafish embryos

In the following step of this study, we finally infected zebrafish embryos with *Candida* cells together with the microspheres. Embryos were injected with microspheres (4 μm) or *Candida* cells alone, or with a combination of both. To verify that the correct amount of *Candida* cells was injected, few embryos were homogenized immediately after the injection and the CFUs were counted (data not shown). The survival of the embryos after the injection of WT-GFP and *bcr1* Δ /*bcr1* Δ -GFP alone or in a combination with the red microspheres (4 μm) are shown in figure 28. Around 30 embryos were injected per condition. Representative images displaying the infection inside the yolk are displayed in figure 29. Statistically significant differences are demonstrated in table 8.

Table 8: A summary displaying the statistically significant difference in the survival of zebrafish embryos upon WT-GFP, *bcr1* Δ /*bcr1* Δ -GFP (20 cells) and microspheres (50) injection. Survival was monitored for 6 days and statistics was done after 6 days. Significant when $p < 0.05$ (Logrank test).

Comparison of strains	Statistically significant ($p < 0.05$)
WT-GFP + spheres WT-GFP alone	No
<i>bcr1</i> Δ / <i>bcr1</i> Δ -GFP + spheres <i>bcr1</i> Δ / <i>bcr1</i> Δ -GFP alone	Yes
WT-GFP + spheres <i>bcr1</i> Δ / <i>bcr1</i> Δ + spheres	No
WT-GFP alone <i>bcr1</i> Δ / <i>bcr1</i> Δ -GFP alone	Yes

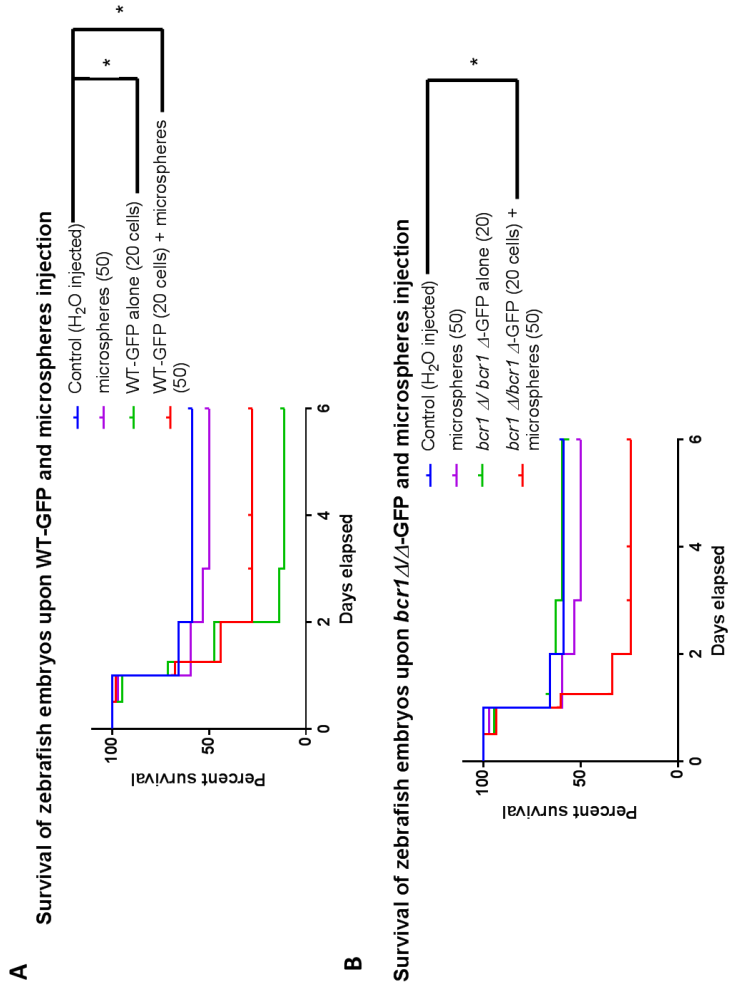


Figure 28: Survival curves of zebrafish embryos upon *Candida* and microspheres injection. Embryos were injected with 20 cells of WT-GFP (A) or *bcr1*Δ/*bcr1*Δ-GFP (B) and in the presence or absence of spheres (50) into the yolk of one-cell stage zebrafish embryos. The survival of zebrafish embryos was monitored after 4, 24, 30, 48, 72 h and 6 days post injection. Statistically significant when *p<0.05 (Logrank test). Data are shown from a single experiment.

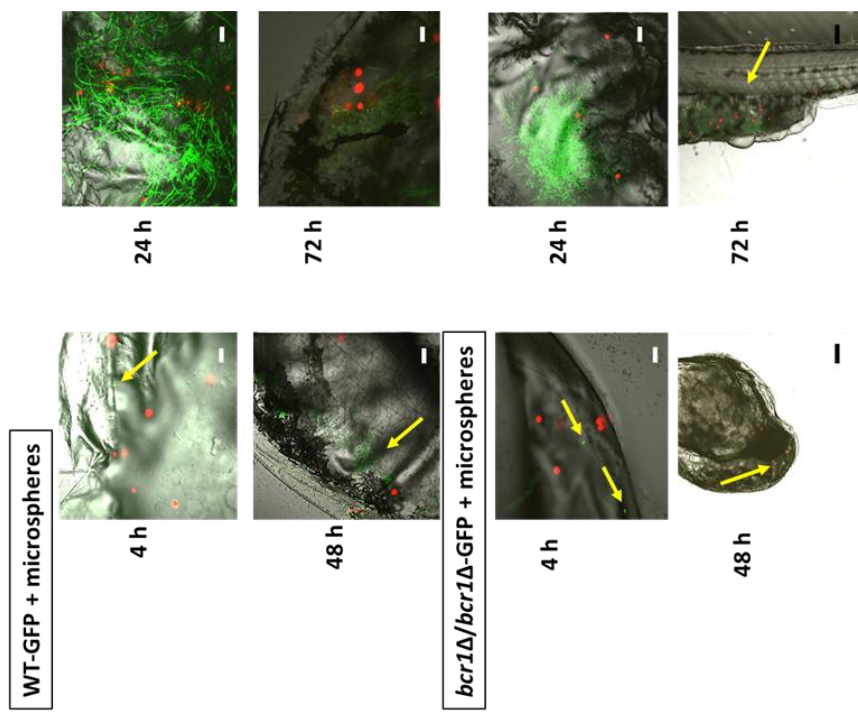
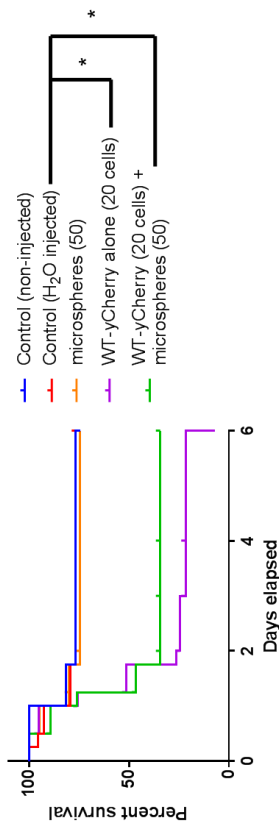


Figure 29: Confocal laser scanning images demonstrating *Candida* and microspheres infection inside the yolk of zebrafish embryos. Zebrafish embryos (at one-cell stage) were injected into the yolk with WT-GFP or *bcr1*Δ/*bcr1*Δ-GFP (20 cells) in combination with microspheres (50). The embryos were screened under the confocal microscope after 4 h, 24 h, 48 h and 72 h post injection. Scale bars= 20 μm and 100 μm (for *bcr1*Δ/*bcr1*Δ-GFP and microspheres 48 h and 72 h). Magnifications 10 x and 40 x.

As it is demonstrated in figure 28 A and B, no statistically significant difference was observed between the control condition and the condition where only microspheres were injected, indicating that microspheres did not influence the growth and the development of zebrafish embryos. After 4 hpi, almost all embryos that were injected with WT-GFP were still alive and corresponding confocal images showed the presence of only some small spots of *Candida* cells in the yolk of the zebrafish embryos (figure 29). After 24h, around 60 % of the embryos injected with WT-GFP, died (figure 28 A). This was also documented by the hyphae formation in the zebrafish embryo and these hyphal cells seemed to be embedded within the microspheres. After 48 hpi, a lot of embryos died especially in the conditions where WT-GFP alone was injected. This was not a surprise considering the massive infection after 24 h. The remaining embryos that stayed alive after 48 h and that were injected with WT-GFP (alone or in combination with spheres), developed no infection (figure 29). These embryos survived even up to 6 days. Around 70 % of the embryos injected with *bcr1Δ/bcr1Δ*-GFP in combination with microspheres, died after day 1 (figure 28 B). The corresponding confocal images demonstrated that this might have been caused by the presence of hyphae in these embryos. From day 2 onwards, there was a constant survival of the embryos injected with *bcr1Δ/bcr1Δ*-GFP alone or in combination with microspheres. There was indeed no big infection documented in the alive *bcr1Δ/bcr1Δ*-GFP injected animals after 48 h (figure 29). One larva out of the three that were visualized after 72 h, showed an increased infection and although the injections were performed into the yolk, we noticed that *Candida* disseminated throughout the larvae and even dragged along the microspheres. An important observation was that, in combination with the microspheres, the mutant strain seemed to behave like a WT-GFP strain. This is shown by the fact that overall, there was no statistically significant difference between survival of embryos injected with WT-GFP and the mutant strain in the presence of the microspheres (table 6). However, in the absence of the microspheres, the mutant strain showed the same behavior as the control condition (water injected) and this difference was significant from day 2 (addendum C, table C1). This suggested that the mutant strain is somehow less virulent compared to the WT-strain and we already observed this in the previous experiment. Interestingly, the mutant strain seemed to cause more death in the combination with microspheres (figure 27 B) than without. This difference was considered statically significant from day 2 (addendum C, table C1). Taken together, these results suggested that the mutant stain alone is less virulent compared to WT-GFP alone. However, when the microspheres were present, there was no difference between the survival of the embryos injected with *bcr1Δ/bcr1Δ*-GFP and WT-GFP. In addition, the *bcr1Δ/bcr1Δ*-GFP strain seemed to cause significantly more death in the presence of microspheres. The same experiment was also performed with the yCherry tagged strains and green microspheres (4 μm). The survival curves are exhibited on figure 29 and the representative figures are shown in figure 30. Table 9 gives an overview of the statically significant differences between the WT strain and the mutant strain.

A Survival of zebrafish embryos upon WT-yCherry and microspheres injection



B Survival of zebrafish embryos upon *efg1Δ/Δ cph1Δ/Δ*-yCherry and microspheres injection

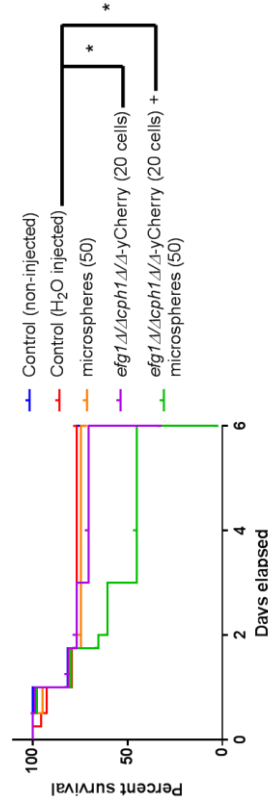


Figure 29: Survival curves of zebrafish embryos upon *Candida* and microspheres injection. Embryos were injected with 20 cells WT-yCherry (A) or *efg1Δ/Δ cph1Δ/Δ*-yCherry (B) in the presence or absence of spheres (50). The survival of zebrafish embryos was monitored after 4, 24, 30, 48, 72 h and 6 days post injection. Data represent two individual experiments. Statistically significant when * $p < 0.05$ (Logrank test).

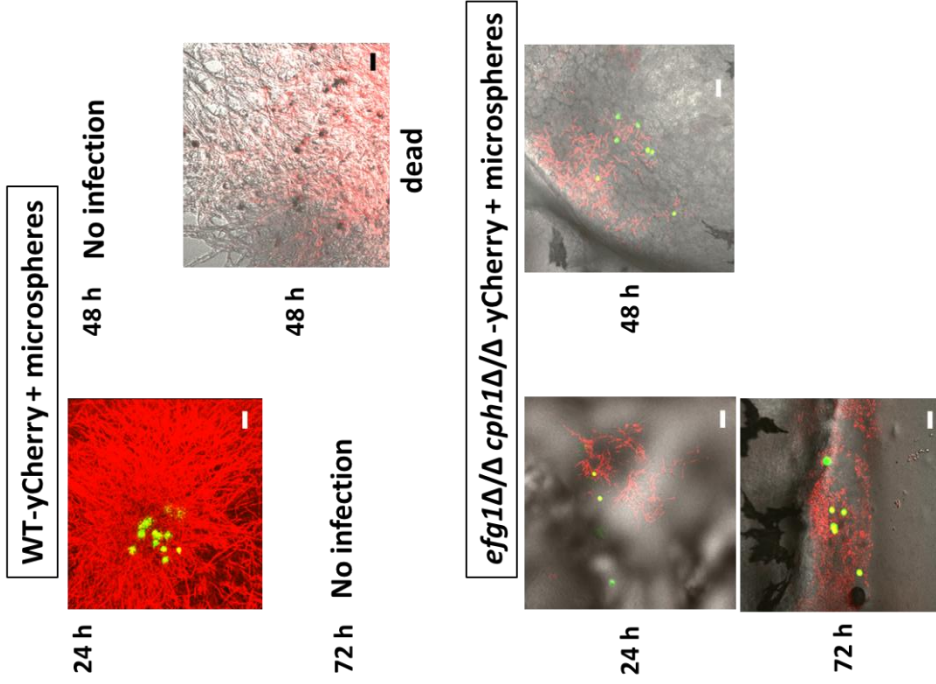


Figure 30: Confocal laser scanning images demonstrating *Candida* and microspheres infection inside the yolk of zebrafish embryos. Zebrafish embryos (at one-cell stage) were injected into the yolk with WT-yCherry or *efg1Δ/Δ cph1Δ/Δ*-yCherry (20 cells) in combination with microspheres (50). The embryos were screened under the confocal microscope after 24 h, 48 h and 72 h post injection. Scale bar= 20 μm . Magnification 40 x.

Table 9: A summary displaying the statistically significant difference in the survival of zebrafish embryos upon WT-yCherry, *efg1Δ/Δ cph1Δ/Δ*-yCherry (20 cells) strain and microspheres (50) injection. Survival was monitored for 6 days and statistics were done after 6 days. Significant when $p < 0.05$ (Logrank test).

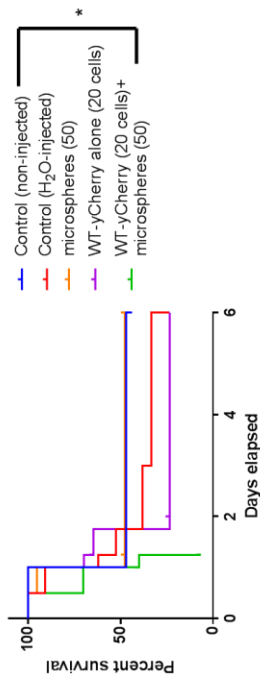
Comparison of strains	Statistically significant (p<0.05)
WT-yCherry + spheres WT-yCherry alone	No
<i>efg1Δ/Δ cph1Δ/Δ</i> -yCherry + spheres <i>efg1Δ/Δ cph1Δ/Δ</i> -yCherry alone	Yes
WT-yCherry + spheres <i>efg1Δ/Δ cph1Δ/Δ</i> -yCherry + spheres	No
WT-yCherry alone <i>efg1Δ/Δ cph1Δ/Δ</i> -yCherry alone	Yes

At 1 day post injection, around 50 % of the embryos that were injected with WT-yCherry died (figure 29 A). This was demonstrated on the confocal images by the presence of a massive infection after 24 h in the embryos injected with WT-yCherry. This was the case for the embryos that were injected with WT-yCherry alone (data not shown), as well as in combination with the microspheres (figure 30). At day 2, the survival curves of the embryos injected with WT-yCherry again dropped to 20 – 30 %. The embryos that were injected with WT-yCherry and that were still alive, showed no infection during visualization after 2 days (figure 30). The embryos that died after 2 days, contained a massive infection and were damaged. After 48 h, the survival curves of the embryos injected with WT-yCherry stayed more or less constant. The confocal images of embryos that survived after 72 h, showed no infection. For the mutant strain, only around 20 % of the embryos injected with *efg1Δ/Δ cph1Δ/Δ*-yCherry alone or *efg1Δ/Δ cph1Δ/Δ*-yCherry in combination with spheres, died at 24 h. This was also documented by a small infection of yeast cells in the yolk of the embryos (figure 30). After 1 day, more embryos survived injected with *efg1Δ/Δ cph1Δ/Δ*-yCherry alone compared to embryos injected with *efg1Δ/Δ cph1Δ/Δ*-yCherry and microspheres together. After 3 days, around 50 % of the embryos injected with *efg1Δ/Δ cph1Δ/Δ*-yCherry and microspheres, died. At this time point (72 h), the confocal images of survived fishes showed a bigger infection compared to the infection after 24 and 48 h. However it seems that the embryos are able to cope with this infection, as they were still alive during imaging. After 3 days, the survival curves of the embryos injected with *efg1Δ/Δ cph1Δ/Δ*-yCherry (in the presence or absence of spheres), remained constant. After 6 days, all embryos that were injected with *efg1Δ/Δ cph1Δ/Δ*-yCherry and microspheres, died. Table 9 shows that there was no significant

difference between the survival of embryos injected with WT alone compared to embryos injected with WT and microspheres. Notably, after 6 days, there was a significant difference between the survival of embryos that were injected with the mutant strains alone and the mutant strain combined with spheres (Table 9). This suggests that in the presence of the spheres, the *efg1Δ/Δ cph1Δ/Δ*-yCherry is more virulent than in the absence of spheres. This is in compliance with what we observed before during the experiment with the GFP-tagged strains. There, we also noticed that embryos succumbed the infection at earlier time points when they were injected with a combination of spheres and *bcr1Δ/bcr1Δ*-GFP compared to injections with the *bcr1Δ/bcr1Δ*-GFP strain alone. In addition, there was overall no significant difference between the survival of embryos injected with WT-yCherry and microspheres and *efg1Δ/Δ cph1Δ/Δ*-yCherry and microspheres again suggesting that the microspheres contribute to the virulence of the mutant strain. We also compared if there was a difference between the survival of the embryos injected with WT-yCherry or *efg1Δ/Δ cph1Δ/Δ*-yCherry (in the presence or absence of microspheres) for day 1 and day 2 separately. These results are demonstrated in table C2, addendum C. First, there was little to no difference ($p>0.05$) between the survival curves of the embryos injected with either the WT-yCherry or the mutant strain (*efg1Δ/Δ cph1Δ/Δ*-yCherry) in the presence or absence of microspheres at day 1, except for the control condition (see also figures 29 A and B). From two days onwards, there was a significant difference between the survival of embryos injected with the WT-yCherry strain alone and the mutant strain alone (so without microspheres). This means that from this time point, more embryos survived when they were injected with the mutant compared to the embryos injected with WT-yCherry. This experiment was also executed with 5 and 10 *Candida* cells that were combined with the green microspheres (addendum D). Also for this experiment, we found that overall, more embryos survived when they were injected with 10 cells of *efg1Δ/Δ cph1Δ/Δ*-yCherry alone compared to WT-yCherry alone.

As we already stated it several times, most of the embryos that survived the first day post injection and that were visualized under the microscope after 48 h, showed almost no infection. In addition, more embryos survived when they were injected with the mutant strains (without microspheres), compared to the WT strains. All these observations made us suspect that the innate immune system could be an important key player during the development of a device-associated infection. As a preliminary experiment, we wanted to explore the role of macrophages during infection. Therefore we made use of a transgenic *fli:GFP* zebrafish line expressing green fluorescent macrophages and endothelium (Brothers et al., 2011). This zebrafish line allowed us to co-image fungi and innate immune cells. We applied the exact same conditions as the previous experiment but this time we used *fli:GFP* zebrafish embryos. The survival curves and corresponding confocal images are exhibited in figures 32 and 33 respectively. Table 10 gives an overview of the statically significant differences between the WT strain and the mutant strain (*efg1Δ/Δ cph1Δ/Δ*-yCherry).

A Survival of zebrafish embryos upon WT-yCherry and microspheres injection (fli:GFP line)



B Survival of zebrafish embryos upon *efg1Δ/Δ cph1Δ/Δ*-yCherry and microspheres injection (fli:GFP line)

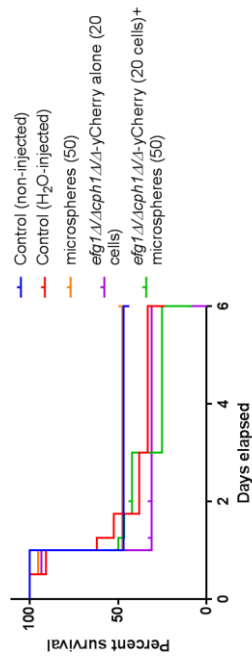
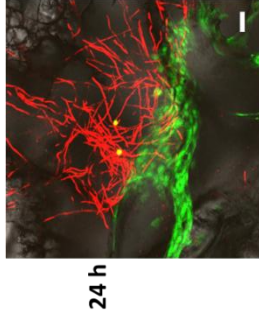


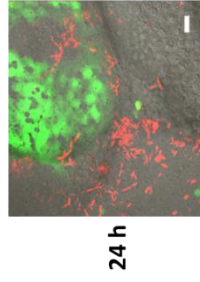
Figure 32: Survival curves of zebrafish embryos (*fli:GFP*) upon *Candida* and microspheres injection. Zebrafish embryos (at one-cell stage) were injected with 20 cells WT-yCherry (A) or *efg1Δ/Δ cph1Δ/Δ*-yCherry (B) in the presence or absence of spheres (50). The survival of zebrafish embryos was monitored after 4, 24, 30, 48, 72 h and 6 days post injection. Data are from one particular experiment. Statistically significant when * $p < 0.05$ (Logrank test).

WT-yCherry + microspheres



48 h No infection

***efg1Δ/Δ cph1Δ/Δ*-yCherry + microspheres**



48 h

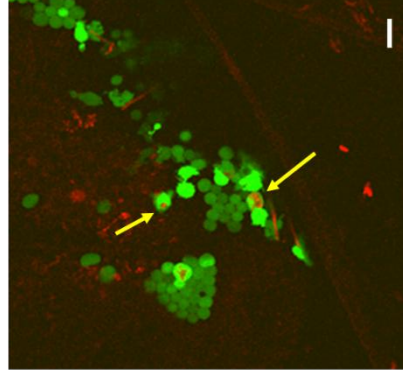


Figure 33: Confocal laser scanning images demonstrating *Candida* and microspheres infection inside the yolk of zebrafish embryos (*fli:GFP*). Zebrafish embryos (at one-cell stage) were injected into the yolk with WT-yCherry or *efg1Δ/Δ cph1Δ/Δ*-yCherry (20 cells) in combination with microspheres (50). The embryos were screened under the confocal microscope after 24 h, 48 h and 72 h post injection. Magnification 40 x. Scale bar = 20 μm.

Table 10: A summary displaying the statistically significant difference in the survival of zebrafish embryos upon WT-yCherry, *efg1Δ/Δ cph1Δ/Δ*-yCherry (20 cells) strain and microspheres (50) injection in a *fli:GFP* zebrafish line. Survival was monitored for 6 days and statistics was done after 6 days. Significant when $p < 0.05$ (Logrank test).

Comparison of strains	Statistically significant ($p < 0.05$)
WT-yCherry + spheres WT-yCherry alone	Yes
<i>efg1Δ/Δ cph1Δ/Δ</i> -yCherry + spheres <i>efg1Δ/Δ cph1Δ/Δ</i> -yCherry alone	No
WT-yCherry + spheres <i>efg1Δ/Δ cph1Δ/Δ</i> -yCherry + spheres	Yes
WT-yCherry alone <i>efg1Δ/Δ cph1Δ/Δ</i> -yCherry alone	No

In general, the survival of the transgenic embryos was low as it was indicated by a strong reduction in the survival for the control embryos (non-injected and water injected) (figure 32). With this fish line, all the embryos that were injected with WT-yCherry and microspheres, died after 24 h. On figure 33, it is clearly shown that after 24 h, the embryos showed a massive infection for the WT-yCherry injection. After 2 days, there was a strong reduction in the survival of embryos injected with WT-yCherry alone but the following days, the survival remained constant. This time, there was no significant difference observed between the embryos injected with *efg1Δ/Δ cph1Δ/Δ*-yCherry alone and *efg1Δ/Δ cph1Δ/Δ*-yCherry combined with microspheres (table 10).

More importantly, the embryos that were injected with *efg1Δ/Δ cph1Δ/Δ*-yCherry and microspheres survived longer compared to embryos injected with WT-yCherry and microspheres and this difference was considered significant (table 10) and contradictory to previous results. The confocal images indeed showed that the infection was less extensive for the embryos injected with *efg1Δ/Δ cph1Δ/Δ*-yCherry and microspheres compared to WT-yCherry and microspheres. The vacuolar-like structures shown in figure 33 represent early macrophage-like cells and these cells seemed to be capable of engulfing the yeast cells formed by the *efg1Δ/Δ cph1Δ/Δ*-yCherry strain (indicated by yellow arrows). This suggests that the innate immune system of the host is provoked upon *Candida* injection and that the immune cells are trying to combat the infection. This preliminary experiment already gave a good onset for further research concerning the role of the innate immune system during *C. albicans* device-associated infections.

Discussion

C. albicans is a commensal fungal species colonizing human mucosal surfaces (Kim & Sudbery, 2011). However, in cases of immune dysfunction, *Candida* can become a pathogen causing infections, which might be life-threatening (Shirliff et al., 2009). *C. albicans* is able to form biofilms on a variety of medical devices and can gain access to the bloodstream resulting in disseminated infections. Among fungal species, *C. albicans* is responsible for the majority of device-associated infections (Peters et al., 2012). In addition, *C. albicans* biofilm-forming cells exhibited increased tolerance of biofilms towards known antifungals, such as azoles and polyene classes (Nett et al., 2010b; Mitchell et al., 2015). Therefore, it is important to get more insight into the mechanisms underlying these infections. As *in vitro* assays can't mimic the situation in the human body (Brothers & Wheeler, 2012), mainly due to the absence of the immune system, there is a need for novel *in vivo* models to study *C. albicans* device-associated infections. In the past, a number of *in vivo* models have been introduced (Andes et al., 2004; Lazzell, et al., 2009; Rიციcova, et al., 2010; Kucharikova et al., 2010). These models, though advantageous, require fungal analyses *post mortem*. Therefore researchers try to look for novel approaches to study *C. albicans* infection in real time.

The present study aimed to use zebrafish larvae as a host model to investigate *C. albicans* device-associated infections. Both adult zebrafish (Chao et al., 2010) as well as the transparent larvae (Brothers et al., 2011), have been used as a host for *C. albicans* disseminated infection. These studies clearly showed *C. albicans* colonization and invasion at multiple anatomical sites and killing of the zebrafish in a dose-dependent manner. Notably, both studies showed the importance of yeast-to-hyphae transition, as a crucial phenomenon in the disease development and further killing of the host organism. The innovative character of this study was the demonstration of the different stages of *C. albicans* infections on polystyrene microspheres.

A second part of this project consisted of the exploration of the role of the innate immune system during initial host-pathogen interactions. Invading and disseminating *Candida* cells primarily encounter phagocytic cells such as macrophages and neutrophils which efficiently phagocytose *C. albicans* yeast cells and short hyphae. While neutrophils can kill the fungus and strongly inhibit growth (including the yeast-to-hyphae transition), yeast cells undergoing phagocytosis by macrophages may survive and even produce hyphae rapidly resulting in killing of the phagocyte and allowing *C. albicans* to escape (Jacobsen et al., 2012). Apart from this, not so much is known about the response of the host immune system during early stages of infection. We wanted to investigate the role of these macrophages during the combat of the infection. For this, we used a transgenic *fli:GFP* zebrafish line with GFP expressing macrophages and endothelium.

Characterization of the fluorescent signal

In this work, we first tested the fluorescence signal intensity of the red and green polystyrene microspheres and the GFP- and yCherry- tagged *C. albicans* strains in comparison with non-fluorescently tagged strains. It is noteworthy to mention that all strains for the *in vitro* work were prepared in RPMI-MOPS because RPMI promotes the development of mature biofilms and induces the yeast-to-hyphae transition in *C. albicans* (Kucharikova et al., 2011). The results indicated that the microspheres were highly fluorescent and each at their appropriate wavelength. Consequently, these microspheres could be used for the further *in vivo* experiments. So far, microspheres have been used in other applications such as blood flow determination, tracing, *in vivo* imaging etc. Herewith, we used them for the first time as a substrate for *C. albicans* colonization under *in vitro* conditions. We observed that the fluorescently tagged strains showed a significantly higher fluorescence signal compared to the non-fluorescent strains. In addition, the signal of the WT-GFP strain was higher than the *bcr1Δ/bcr1Δ*-GFP strain. This was as expected because the latter strain has a deletion in a transcription factor that is responsible for mature *in vitro* and *in vivo* biofilm development and only forms a rudimentary biofilm *in vitro* (Nobile et al., 2006). Microscopic analyses revealed the failure of the mutant strain to colonize the substrate. However, the expectation that there would be more biofilm formation for the WT strain containing microspheres was not fulfilled. Because the microspheres are made of polystyrene, we expected that *Candida* would be more attracted by these latter because of hydrophobic interactions (Shinde et al., 2012) and thus a thicker biofilm would be formed. Although the plate was centrifuged before the wells were washed, we still noticed that during the washing step, some of the biofilm containing the microspheres was removed. Another explanation might be that even though the microspheres were washed before incubation with *Candida* cells, there were still some traces of the solution present (0.02% thimerosal) in which the microspheres were maintained. Thimerosal is a mercury based preservative and mercury based compounds might cause failure of *Candida* growth (Yannai et al., 1991). Similar results were obtained with the yCherry-tagged strains. The fluorescently tagged strains demonstrated a higher fluorescent signal and the WT-yCherry strain displayed significantly increased signal in comparison with *efg1Δ/Δ cph1Δ/Δ*-yCherry. *EFG1* and *CPH1* are two transcription factors required for the expression of genes involved in morphogenesis, a key step in biofilm formation (Chao et al., 2010). The mutant strain containing deletions in both transcription factors, only appears in the yeast form. The ability of the WT-strains to form hyphae and a biofilm versus the yeast cells of the mutant strain explains the significant increased fluorescent signal of WT-yCherry.

In vitro biofilm formation on 96-well polystyrene plate

Next to the characterization of the fluorescent signal, we also performed an XTT assay in a 96-well polystyrene plate, to assess the ability of the WT-strains (WT-GFP and WT-yCherry) and the mutant strains (*bcr1Δ/bcr1Δ*-GFP and *efg1Δ/Δ cph1Δ/Δ*-yCherry) to develop biofilms. The results indicated that the WT-GFP tagged strain exhibited relatively higher metabolic activity of biofilm-forming cells in comparison with the *bcr1Δ/bcr1Δ*-GFP tagged strain. Unlike, the previous experiment, this difference was not considered statistically significant. It should be noted that although the mutant strain is not capable of forming a mature biofilm, it still can form hyphae but to a less extent compared to the WT-GFP strain (Nobile & Mitchell, 2005). To verify this result, we could have determined CFUs or checked the strains under the confocal microscope for biofilm development. This different outcome might have been due to the use of different conditions such as one extra washing step after the period of adhesion (90 min.), no centrifugation of the plate or an artefact of the assay. For the yCherry strains, on the contrary we saw a significant higher metabolic activity of the WT-yCherry strain compared to the *efg1Δ/Δ cph1Δ/Δ*-yCherry strain.

Biofilm formation and characterization on polyethylene tissue culture discs

As our goal was to establish an *in vivo* host model for device-associated infections, we first had to investigate the behavior of *Candida* cells in the presence of microspheres, their biofilm architecture including their biofilm thickness. Therefore, we developed biofilms of fluorescently tagged and non-fluorescent strains on tissue culture polyethylene discs in a polystyrene 24-well plate. The fluorescently tagged and non-fluorescently tagged mutant strains were used as controls. The polyethylene discs provide a good surface for the adherence of the *Candida* cells and subsequent visualization under the microscope. Moreover, polystyrene seemed to support the adhesion of *Candida* cells (Shinde et al., 2012). The results demonstrated that the WT strain developed thick biofilms as characterized by the presence of hyphal cells along the substrate. The *bcr1Δ/bcr1Δ* strain, on the contrary, formed only rudimentary biofilm on the substrate including yeast cells interspersed with a few hyphal filaments and the surrounding medium appeared more turbid compared to the WT strains. These results were earlier observed by Nobile & Mitchell (2005) where they used silicone substrates for the development of biofilms. Their study also indicated that the WT strain produced a biofilm with typical bilayer structure whereas the *bcr1Δ/bcr1Δ* mutant strain produces a less thick biofilm structure. Thus, Bcr1p was indicated to be required for the formation of biofilms, but not hyphae (Nobile & Mitchell, 2005). On the other hand, *C. albicans efg1Δ/Δ cph1Δ/Δ* strain failed to form biofilms, as documented by the presence of yeast cells spread on the substrate. Importantly, *Candida* cells were able to develop infection around the microspheres. We also observed that the fluorescently and non-fluorescently tagged WT and *bcr1Δ/bcr1Δ* strains with microspheres

demonstrated a significantly thicker biofilm compared to the conditions without microspheres (figures 16, 17 and 18). Moreover, the fluorescent and non-fluorescent WT strains had a significant higher biofilm thickness compared to the fluorescent and non-fluorescent mutant strains. Altogether, these results indicate that the presence of microspheres during biofilm development significantly increased the biofilm thickness of the WT strains and the *bcr1Δ/bcr1Δ* mutant strains. Moreover, *Candida* WT strains were able to form a thick network of hyphal cells embedded within the polystyrene microspheres. The mutant strains showed a defect in mature biofilm formation.

Injections into the yolk of zebrafish embryos

During this project, all injections were performed into the yolk of 1-cell stage zebrafish embryos. The yolk is an oily, fat- and protein rich structure and is consumed by the zebrafish as the embryo grows. The yolk is the biggest organ and easiest structure for injections compared to structures such as the swim bladder or the hindbrain which are much more labor intensive and low throughput (Veneman et al., 2013). Moreover, all injections occurred in the 1 - 4-cell stage because at that point, the cytoplasmic flow and diffusion will bring the working solution into cells that will become an embryo. If injections would occur into later stages, the further development of the embryo could be influenced. In addition, injections into the first stages of development facilitate the experimental reproducibility. For injections into the yolk, a typical injection volume of 2 nl was used. By adjusting the final concentration of *Candida* cells and microspheres, we obtained different amounts of *Candida* cells and microspheres that were injected per embryo (table 3 and 4, section 2.3.4). According to literature, approximately 20 yeast cells per fish were injected (Brothers et al., 2011) which corresponded to a *Candida* concentration of 1×10^7 cells/ml for 2 nl injection volume.

Injection of microspheres

Our first *in vivo* experiments had to unravel what concentration of microspheres yielded the best survival of the zebrafish larvae. To our knowledge, this has never been before. Therefore, a concentration gradient (ranging from 250 to 2 microspheres per embryo) was injected into yolk of 1- cell stage zebrafish embryos. The survival graphs (figure 20) indicated that a concentration of 50 spheres injected per embryo, resulted in high survival percentages and the corresponding pictures (figure 21) showed the presence of a sufficient amount of spheres per animal. We noticed that injections of a high amount of spheres caused significant mortality compared to the control condition (water-injected). This suggests that although the microspheres were not harmful for the embryo, the injection of a high concentration of foreign material has an influence on the survival rate of the zebrafish embryos. Moreover, the injection

procedure itself is also causes some stress for the embryos and this is shown by the slight decrease in survival of the embryos injected with water. For several experiments, we also included a condition where we just punched the zebrafish embryos with the needle (data not shown), without injecting any material. The survival of these embryos was comparable to those of the water injected ones.

We also noticed that although we injected into the yolk of zebrafish embryos, the microspheres also dispersed throughout the whole larvae (figure 22). This was because when the injections occur in the 1-cell stage, there is a free delivery from the yolk to cells that will become the embryo.

Injection of *Candida* cells

As already stated above, previous studies of *C. albicans* infection into the zebrafish indicated that injections of around 10 to 20 *Candida* cells per embryo gave the most consistent results (Brothers et al., 2011; Brothers & Wheeler, 2012). These injections however occurred in the hindbrain ventricle or the swim bladder and may result in a different outcome compared to injections into the yolk. Gratacap et al. (2014), established a zebrafish infection model where *C. albicans* infects the swim bladder and according to their study the inoculum dose was limited to 5×10^7 cells/ml (or 250 cells/embryo for a 5 nl bolus) due to the clogging of the needle caused by the size of *C. albicans* cells (3 – 4 μm). Injections into the yolk of zebrafish embryos have been done before with bacteria (Veneman et al., 2013) using a concentration gradient. Therefore we decided to first inject the zebrafish embryos with a gradient of *Candida* cells as we first did with the microspheres. We injected WT-GFP, WT-yCherry strains at different concentrations (50, 25, 20, 10 and 5 cells) into the yolk of 1-cell stage zebrafish embryos. Two mutant strains (*bcr1Δ/bcr1Δ* –GFP and *efg1Δ/Δ cph1Δ/Δ*-yCherry) were used as control strains.

First of all, it should be emphasized that Brothers et al. (2011) also tried to inject WT-GFP *Candida* cells into the yolk of zebrafish embryos. However, their attempt at infection of the yolk resulted into universal lethality within 24 h.

Our results showed that that there was a correlation between the concentrations of cells that were injected and the death of the embryos. Embryos that were injected with higher concentrations of WT cells, died earlier than the embryos injected with lower amounts of cells. Moreover, the embryos injected with the WT-strains (WT-GFP and WT-yCherry) already succumbed the infection at early time points (after 1 day already 30 – 40 % death). This was in accordance with the data from Brothers et al. (2011), as they also noticed a preliminary death of the embryos injected with WT-GFP after 24 h. During this 24 h time point, the WT

strains formed hyphae inside the yolk of zebrafish embryos. Embryos that were massively infected after 24 h, were expected to die within the next 24 h. Indeed, when we looked at the survival curves, we saw a huge drop in survival between 24 and 48 h. The embryos that were still surviving after 48 h, were almost not infected. This was also documented by Brothers et al. (2011) as they saw a precipitous drop in fungal burden in surviving fish after 48 h. This made us suspect that within this context, the immune system could play a role. So either the immune system is able to combat the initial infection resulting in survival of fishes after 48 h, or the immune system is not able to control proliferation and morphogenesis leading to moribund larvae with extensive fungal hyphae (as documented by the confocal images of the dead embryos, addendum B).

In contrast to the study of Brothers et al. (2011), we also included a *bcr1Δ/bcr1Δ*-GFP mutant. Notably, we found that there was a significant difference between the survival of embryos injected with 25 cells of WT-GFP and 25 cells of *bcr1Δ/bcr1Δ*-GFP, indicating that embryos injected with 25 cells of WT-GFP died earlier than embryos injected with 25 cells of *bcr1Δ/bcr1Δ*-GFP. This would suggest that this mutant strain, which only forms rudimentary biofilms, is less virulent. For this however, we found contradictory results in a mouse model for disseminated candidiasis (Nobile et al., 2006; Gutiérrez-Escibano et al., 2012). Gutiérrez-Escibano et al. (2012) found that mutation of the Bcr1p transcription factor, indeed resulted into an impaired virulence of the strain. On the other hand, Nobile et al. (2006) documented that for a rat venous catheter model, the *bcr1Δ/bcr1Δ* mutant yielded only few adherent to the catheter surface compared to the WT strain (Nobile et al., 2006) but that for a disseminated mouse model, the WT strain and *bcr1Δ/bcr1Δ* mutant grew comparably.

Also for the yCherry-tagged strain, we saw that injection of 25 cells of WT-yCherry into zebrafish embryos resulted into a significant higher death of the embryos compared to *efg1Δ/Δ cph1Δ/Δ*-yCherry injection. This attenuation in virulence of *efg1Δ/Δ cph1Δ/Δ*-yCherry was already demonstrated by Brothers et al. (2011) and Chao et al. (2010). Although *efg1Δ/Δ cph1Δ/Δ* is a hypofilamentous strain *in vitro*, it still can form pseudohyphae *in vivo*, as demonstrated on figure 34 and this was in accordance with the data from Brothers et al. (2011).

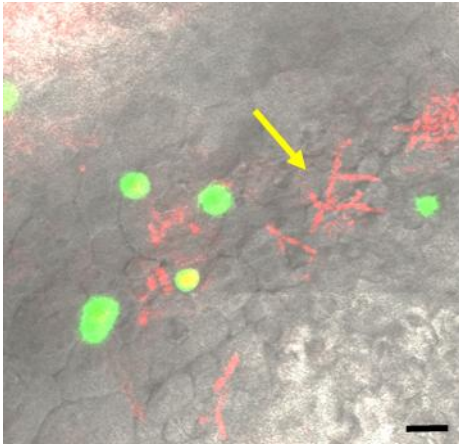


Figure 34: Confocal laser scanning image, demonstrating injection of *efg1* Δ/Δ *cph1*-yCherry Δ/Δ (20 cells) and microspheres (50) into the yolk of zebrafish embryos. Visualization of the embryo was done 48 h post injection Magnification 60 X. Scale bar= 10 μ m.

Injection of *Candida* and microspheres

The final step of this project was the injection of *Candida* together with microspheres. Importantly, we were the first ones injecting *Candida* in combination with microspheres into the yolk of 1-cell stage zebrafish embryos. Based on the previous experiments, we decided to inject around 20-25 *Candida* cells because this yielded the best trade-off between survival of the embryos and the development of an infection. We injected around 20-25 *Candida* cells of different strains (WT-GFP, *bcr1* Δ /*bcr1* Δ -GFP, WT-yCherry and *efg1* Δ/Δ *cph1* Δ/Δ -yCherry) together with 50 microspheres into the yolk of zebrafish embryos.

Here it should be noted that for each experiment, we also always confirmed the injected amount of cells by homogenizing the embryos and counting CFUs. This was not very successful as the WT strains almost yielded no colonies in comparison with the mutant strains. This was due to the formation of hyphal cells, formed by the WT strains, which are difficult to disrupt and hence resulting in a wrong interpretation and enumeration of the CFUs. Sonication of the samples did not completely overcome this problem.

During these experiments, we found one very important observation. We noticed that both mutant strains (*bcr1* Δ /*bcr1* Δ -GFP and *efg1* Δ/Δ *cph1* Δ/Δ -yCherry) caused more death of the embryos when they were injected together with microspheres than in the absence of microspheres. Moreover, when the mutant strains were injected together with the microspheres into the zebrafish embryos, they showed the same behaviour as the WT strains combined with microspheres. On the contrary, when the mutant strains were injected alone into the embryos, there was a significant difference in the survival of the embryos compared

to injections with the WT strain alone. For this phenomenon, there are several explanations possible. One might be that the mutant strains are able to proliferate faster in the presence of the microspheres because the polystyrene might enhance this latter. Another option is that the mutant cells produce something in response to the spheres, which enhances their growth and even maybe enables the cells to escape the immune system. These are all questions that will need to be answered in further research.

Secondly, we also found that after a few days post injection, *Candida* was able to disseminate throughout the whole larva, mainly due to its ability to switch from yeast to hyphal form, and to drag along the microspheres indicating again the strong interaction between the *Candida* and the microspheres which we also observed during the *in vitro* experiments. This means that morphogenesis is one of the crucial phenomena for the development of the infection.

From the results it was clear that some of the embryos were able to overcome the infection and therefore we wanted to explore the role of the immune system during a device-associated infection. We performed one preliminary experiment where we used a transgenic fish line (*fli:GFP*) with GFP expressing macrophages and endothelium (Brothers et al., 2011). The first macrophage precursors are already present as early as 20 hours post fertilization and this allowed us to look at initial host-pathogen interactions. We noticed that the macrophages (which resemble vacuolar-like structures) were able to phagocytose the yeast cells but that the hyphal like cells were not subjected to the macrophages and could circumvent the immune system. However, further research, using this device-associated infection model, will be needed to explore the role of the immune system during a device-associated infection. It would for example be interesting, to use a fish line devoid of immune cells to determine the role of these latter during a device-associated infection.

In general, we can say that we were able to establish a successful device-associated infection model, which can be used for high-throughput screens. In the future, bioluminescence or fluorescence imaging might make this model system even more high –throughput. Moreover, this model is cheap and easy to maintain. Furthermore, there are microspheres available with different surface modifications enabling the possibility to couple certain compounds to the beads. This might provide a tool to test the effect of certain antifungals on a device-associated infection.

Finally, it should also be emphasized that although we were able to establish a proper model for the development of device-associated infections, it remains unknown how far this situation is reflected in the mammalian host, since the ectothermic zebrafish differ from mammals by their high body temperature, which is an important hypha-inducing factor (Brunke & Hube, 2013).

References

- Alby, K., & Bennett, R. J. (2009). Stress-induced phenotypic switching in *Candida albicans*. *Molecular biology of the cell*, 20(14), 3178-3191.
- Andes, D., Nett, J., Oschel, P., Albrecht, R., Marchillo, K., & Pitula, A. (2004). Development and characterization of an in vivo central venous catheter *Candida albicans* biofilm model. *Infection and immunity*, 72(10), 6023-6031.
- Berman, J. (2012). *Candida albicans*. *Current biology*, 22(16), 620-622.
- Bink, A., Kucharikova, S., Neirinck, B., Vleugels, J., Van Dijck, P., Cammue, B. P., & Thevissen, K. (2012). The nonsteroidal antiinflammatory drug diclofenac potentiates the in vivo activity of caspofungin against *Candida albicans* biofilms. *Journal of infectious diseases*, 206(11), 1790-1797.
- Biocompare*. (2006, November 28). Retrieved May 12, 2015, from <http://www.biocompare.com/Product-Reviews/40541-FemtoJet-Microinjector-From-Eppendorf/>
- Bonhomme, J., & d'Enfert, C. (2013). *Candida albicans* biofilms: building a heterogeneous, drug-tolerant environment. *Current opinion in microbiology*, 16(4), 398-403.
- Bopp, S. K., Minuzzo, M., & Lettieri, T. (2006). *The Zebrafish (Danio rerio): an Emerging model organism in the environmental field*. European Commission, Joint Research Centre.
- Brand, M., Granato, M., & Nüsslein-Volhard, C. (2002). Keeping and raising zebrafish. In *Zebrafish* (Vol. 261, pp. 7-37). Oxford University Press.
- Brothers, K. M., & Wheeler, R. T. (2012). Non-invasive imaging of disseminated candidiasis in zebrafish larvae. *Journal of visualized experiments: JoVE*, 65.
- Brothers, K. M., Newman, Z. R., & Wheeler, R. T. (2011). Live imaging of disseminated candidiasis in zebrafish reveals role of phagocyte oxidase in limiting filamentous growth. *Eukaryotic cell*, 10(7), 932-944.
- Brunke, S., & Hube, B. (2013). Two unlike cousins: *Candida albicans* and *C. glabrata* infection strategies. *Cellular microbiology*, 15(5), 701-708.
- Calderone, A. R., & Fonzi, W. A. (2001). Virulence factors of *Candida albicans*. *Trends in microbiology*, 9(7), 327-335.
- Chao, C.-C., Hsu, P.-C., Jen, C.-F., Chen, I.-H., Wang, C.-H., Chan, H.-C. et al. (2010). Zebrafish as a model host for *Candida albicans* infection. *Infection and immunity*, 78(6), 2512-2521.
- Christensen, L. D., Moser, C., Jensen, P. O., Rasmussen, T. B., Christophersen, L., Kjelleberg, S. et al. (2007). Impact of *Pseudomonas aeruginosa* quorum sensing on biofilm persistence in an in vivo intraperitoneal foreign-body infection model. *Microbiology*, 153(7), 2312-2320.

- Coenye, T., & Nelis, H. J. (2010). In vitro and in vivo model systems to study microbial biofilm formation. *Journal of microbiological methods*, 83(2), 89-105.
- de Groot, P. W., Bader, O., de Boer, A. D., Weig, M., & Chauhan, N. (2013). Adhesins in human fungal pathogens: glue with plenty of stick. *Eukaryotic cell*, 12(4), 470-481.
- Demuyser, L., Jabra-Rizk, M., & Van Dijck, P. (2014). Microbial cell surface proteins and secreted metabolites involved in multispecies biofilms. *Pathogens and disease*, 70(3), 219-230.
- Dieterich, C., Schander, M., Noll, M., Johannes, F.-J., Brunner, H., Graeve, T., & Rupp, S. (2002). In vitro reconstructed human epithelia reveal contributions of *Candida albicans* *EFG1* and *CPH1* to adhesion and invasion. *Microbiology*, 148(2), 497-506.
- Dooley, K., & Zon, L. I. (2000). Zebrafish: a model system for the study of human disease. *Current opinion in genetics & development*, 10(3), 252-256.
- Douglas, J. L. (2003). *Candida* biofilms and their role in infection. *Trends in microbiology*, 11(1), 30-36.
- EOL *Encyclopedia of life*. (2015). Retrieved from Danio rerio zebrafish: <http://eol.org/pages/204011/overview>
- Fan, Y., He, H., Dong, Y., & Pan, H. (2013). Hyphae-Specific Genes *HGC1*, *ALS3*, *HWP1*, and *ECE1* and relevant signaling pathways in *Candida albicans*. *Mycopathologia*, 176(5-6), 329-335.
- Fashion Cloud. (2015). Retrieved from <http://fashions-cloud.com/pages/z/zebrafish-embryo-stages/>
- Forche, A., Alby, K., Schaefer, D., Johnson, A. D., Berman, J., & Bennett, R. J. (2008). The Parasexual Cycle in *Candida albicans* provides an alternative pathway to meiosis for the formation of recombinant strains. *PLoS biology*, 6(5), e110.
- Fu, Y., Ibrahim, A. S., Sheppard, D. C., Chen, Y.-C., French, S. W., Cutler, J. E. et al. Edwards, J. E. (2002). *Candida albicans* Als1p: an adhesin that is a downstream effector of the *EFG1* filamentation pathway. *Molecular Microbiology*, 44(1), 61-72.
- Gillum, A. M., Tsay, E. Y., & Kirsch, D. R. (1984). Isolation of the *Candida albicans* gene for orotidine-5'-phosphate decarboxylase by complementation of *S. cerevisiae* *ura3* and *E. coli* *pyrF* mutations. *Molecular and General Genetics MGG*, 198(1), 179-182.
- Gow, N. A., van de Veerdonk, F. L., Brown, A. J., & Netea, M. G. (2012). *Candida albicans* morphogenesis and host defence: discriminating invasion from colonization. *Nature reviews microbiology*, 10(2), 112-122.
- Gratacap, R. L., Bergeron, A. C., & Wheeler, R. T. (2014). Modeling mucosal candidiasis in larval zebrafish by swimbladder injection. *JoVE (Journal of Visualized Experiments)*, 93, e52182-e52182.

- Gutiérrez-Escibano, P., Zeidler, U., Suárez, M., Bachellier-Bassi, S., Clemante-Blanco, A., Bonhomme, J. et al. (2012). The NDR/LATS kinase Cbk1 controls the activity of the transcriptional regulator Bcr1 during biofilm formation in *Candida albicans*. *PLoS pathogens*, 8(5), e1002683.
- Howe, K., Clark, M. D., Torroja, C. F., Tarrance, J., Berthelot, C., Muffato, M. et al. (2013). The zebrafish reference genome sequence and its relationship to the human genome. *Nature*, 496(7446), 498-503.
- Jacobsen, I. D., Wilson, D., Wächtler, B., Brunke, S., Naglik, J. R., & Hube, B. (2012). *Candida albicans* dimorphism as a therapeutic target. *Expert review of anti-infective therapy*, 10(1), 85-93.
- Keppler-Ros, S., Noffz, C., & Dean, N. (2008). A New Purple Fluorescent Color Marker for Genetic Studies in *Saccharomyces cerevisiae* and *Candida albicans*. *Genetics*, 179(1), 705-710.
- Kim, J., & Sudbery, P. (2011). *Candida albicans*, a major human fungal pathogen. *The journal of microbiology*, 49(2), 171-177.
- Kimmel, C. B., Ballard, W. W., Kimmel, S. R., Ullmann, B., & Schilling, T. F. (1995). Stages of Embryonic Development of the Zebrafish. *Developmental dynamics*, 203(3), 253-310.
- Kucharikova, S., Sharma, N., Spriet, I., Maertens, J., Van Dijck, P., & Lagrou, K. (2013). Activities of systemically administered echinocandins against in vivo mature *Candida albicans* biofilms developed in a rat subcutaneous model. *Antimicrobial agents and chemotherapy*, 57(5), 2365-2368.
- Kucharikova, S., Tournu, H., Holtappels, M., Van Dijck, P., & Lagrou, K. (2010). In vivo efficacy of anidulafungin against mature *Candida albicans* biofilms in a novel rat model of catheter-associated Candidiasis. *Antimicrobial agents and chemotherapy*, 54(10), 4474-4475.
- Kucharikova, S., Tournu, H., Lagrou, K., Van Dijck, P., & Bujdakova, H. (2011). Detailed comparison of *Candida albicans* and *Candida glabrata* biofilms under different conditions and their susceptibility to caspofungin and anidulafungin. *Journal of medical microbiology*, 60(9), 1261-1269.
- Kucharikova, S., Vande Velde, G., Himmelreich, U., & Van Dijck, P. (2015). *Candida albicans* biofilm development on medically-relevant foreign bodies in a mouse subcutaneous model followed by bioluminescence imaging. *Journal of visualized experiments*.
- Kuhn, D. M., Balkis, M., Chandra, J., Mukherjee, P. K., & Ghannoum, M. A. (2003). Uses and limitations of the XTT assay in studies of *Candida* growth and metabolism. *Journal of clinical microbiology*, 41(1), 506-508.
- Kuo, Z.-Y., Chuang, Y.-J., Chao, C.-C., Liu, F.-C., Lan, C.-Y., & Chen, B.-S. (2012). Identification of infection-and defense-related genes via a dynamic host-pathogen interaction network using a *Candida albicans*-zebrafish infection model. *Journal of innate immunity*, 5(2), 137-152.

- LaFleur, M. D., Kumamoto, C. A., & Lewis, K. (2006). *Candida albicans* biofilms produce antifungal-tolerant persister cells. *Antimicrobial agents and chemotherapy*, *50*(11), 3839-3846.
- Lazzell, A. L., Chaturvedi, A. K., Pierce, C. G., Prasad, D., Uppuluri, P., & Lopez-Ribot, J. L. (2009). Treatment and prevention of *Candida albicans* biofilms with caspofungin in a novel central venous catheter murine model of candidiasis. *Journal of antimicrobial chemotherapy*, *64*(3), 567-570.
- Levraud, J.-P., Palha, N., Langevin, C., & Boudinot, P. (2014). Through the looking glass: witnessing host-virus interplay in zebrafish. *Trends in microbiology*, *9*, 490-497.
- Liu, Y., & Filler, S. G. (2011). *Candida albicans* Als3, a multifunctional adhesin and invasin. *Eukaryotic Cell*, *10*(2), 168-173.
- Lo, H.-J., Kohler, J. R., DiDomenico, B., Loebenberg, D., Cacciapuoti, A., & Fink, G. R. (1997). Nonfilamentous *C. albicans* mutants are avirulent. *90*(5), 939-949.
- Mayer, F. L., Wilson, D., & Hube, B. (2013). *Candida albicans* pathogenicity mechanisms. *Virulence*, *4*(2), 119-128.
- McBain, A. J. (2009). *In Vitro* biofilm models: an overview. In *Advances in applied microbiology* (Vol. 69, pp. 99-132).
- Meijer, A. H., & Spaink, H. P. (2011). Host-pathogen interactions made transparent with the zebrafish model. *Current drug targets*, *12*(7), 1000-1017.
- Mitchell, K. F., Zarnowski, R., Sanchez, H., Edward, J. A., Reinicke, E. L., Nett, J. E. et al. (2015). Community participation in biofilm matrix assembly and function. *PNAS*, *112*(13), 4092-4097.
- Mohandas, V., & Ballal, M. (2011). Distribution of *Candida* species in different clinical samples and their virulence : biofilm formation, proteinase and phospholipase production: a study on hospitalized patients in Southern India. *Journal of global infectious diseases*, *3*(1), 4.
- Nett, J. E., Brooks, E. G., Cabezas-Olcos, J., Sanchez, H., Zarnowski, R., Marchillo, K., & Andes, D. R. (2014). Rat indwelling urinary catheter model of *Candida albicans* biofilm. *Infection and immunity*, *82*(12), 4931-4940.
- Nett, J. E., Marchillo, K., Spiegel, C. A., & Andes, D. R. (2010a). Development and validation of an *in vivo* *Candida albicans* biofilm denture model. *Infection and immunity*, *78*(9), 3650-3659.
- Nett, J. E., Sanchez, H., Cain, M. T., & Andes, D. R. (2010b). Genetic basis of *Candida* biofilm resistance due to drug-sequestering matrix glucan. *Journal of Infectious Diseases*, *202*(1), 171-175.
- Nobile, C. J., & Mitchell, A. P. (2005). Regulation of cell-surface genes and biofilm formation by the *C. albicans* transcription factor Bcr1p. *Current Biology*, *15*(12), 1150-1155.

- Nobile, C. J., Andes, D. R., Nett, J. E., Smith, Jr, F. J., Yue, F., Phan, Q.-T. et al. (2006). Critical role of Bcr1-dependent adhesins in *C. albicans* biofilm formation in vitro and in vivo. *PLoS pathogens*, 2(7), e63.
- Nobile, C. J., Schneider, H. A., Nett, J. E., Sheppard, D. C., Filler, S. G., Andes, D. R., & Mitchell, A. P. (2008). Complementary adhesin function in *C. albicans* biofilm formation. *Current biology*, 18(14), 1017-1024.
- Pande, K., Chen, C., & Noble, S. M. (2013). Passage through the mammalian gut triggers a phenotypic switch that promotes *Candida albicans* commensalism. *Nature genetics*, 45(9), 1088-1091.
- Peters, B. M., & Noverr, M. C. (2013). *Candida albicans*-*Staphylococcus aureus* polymicrobial peritonitis modulates host innate immunity. *Infection and immunity*, 81(6), 2178-2189.
- Peters, B. M., Ovchinnikova, E. S., Krom, B. P., Schlecht, L., Zhou, H., Hoyer, L. L. et al. (2012). *Staphylococcus aureus* adherence to *Candida albicans* hyphae is mediated by the hyphal adhesin Als3p. *Microbiology*, 158(Pt 12), 2975-2986.
- Pierce, C. G., Uppuluri, P., Tristan, A. R., Wormley Jr., F. L., Mowat, E., Ramage, G., & Lopez-Ribot, J. L. (2008). A simple and reproducible 96 well plate-based method for the formation of fungal biofilms and its application to antifungal susceptibility testing. *Nature protocols*, 3(9), 1494-1500.
- Ramage, G., Jose, A., Sherry, L., Lappin, D., Jones, B., & Williams, C. (2013). Liposomal amphotericin B displays rapid dose-dependent activity against *Candida albicans* biofilms. *Antimicrobial agents and chemotherapy*, 57(5), 2369-2371.
- Reed, B., & Jennings, M. (2011). *Guidance on the housing and care of zebrafish Danio rerio*. Research Animals Department, Science Group, RSPCA.
- Renshaw, S. A., & Trede, N. S. (2012). A model 450 million years in the making: zebrafish and vertebrate immunity. *Disease models & mechanisms*, 5(1), 38-47.
- Renshaw, S. A., Loynes, C. A., Trushell, D. M., Elworthy, S., Ingham, P. W., & Whyte, M. K. (2006). A transgenic zebrafish model of neutrophilic inflammation. *Blood*, 108(13), 3976-3978.
- Ricicova, M., Kucharikova, S., Tournu, H., Hendrix, J., Budjakova, H., Van Eldere, J. et al. (2010). *Candida albicans* biofilm formation in a new in vivo rat model. *Microbiology*, 156(3), 909-919.
- Schaller, M., Borelli, C., Korting, H. C., & Hube, B. (2005). Hydrolytic enzymes as virulence factors of *Candida albicans*. *Mycoses*, 48(6), 365-377.
- Shinde, R. B., Raut, J. S., & Karuppayil, M. S. (2012). Biofilm formation by *Candida albicans* on various prosthetic materials and its fluconazole sensitivity: a kinetic study. *Mycoscience*, 53(3), 220-226.
- Shirliff, M. E., Peters, B. M., & Jabra-Rizk, M. (2009). Cross-kingdom interactions: *Candida albicans* and bacteria. *FEMS microbiology letters*, 299(1), 1-8.

- Staveley, B. E. (2015). *Molecular & developmental biology*. Retrieved May 13, 2015, from http://www.mun.ca/biology/desmid/brian/BIOL3530/DEVO_03/devo_03.html
- Sudbery, P., Gow, N., & Berman, J. (2004). The distinct morphogenic states of *Candida albicans*. *Trends in microbiology*, 12(7), 317-324.
- Sullivan, C., & Kim, C. H. (2008). Innate immune system of the zebrafish, *Danio rerio*. In *Innate immunity of plants, animals, and humans* (Vol. 21, pp. 113-133). Springer.
- Tobin, D. M., May, R. C., & Wheeler, R. T. (2012). Zebrafish: A see-through host and a fluorescent toolbox to probe host–pathogen interaction. *PLoS pathogens*, 8(1), e1002349.
- Torraca, V., Masud, S., Spaink, H. P., & Meijer, A. H. (2014). Macrophage-pathogen interactions in infectious diseases: new therapeutic insights from the zebrafish host model. *Disease models & mechanisms*, 7(7), 785-797.
- Tournu, H., & Van Dijck, P. (2011). *Candida biofilms* and the host: models and new concepts for eradication. *International journal of microbiology*, 2012.
- van der Sar, A. M., Stockhammer, O. W., van der Laan, C., Spaink, H. P., Wilbert, B., & Meijer, A. H. (2006). MyD88 innate immune function in a zebrafish embryo infection model. *Infection and immunity*, 74(4), 2436-2441.
- Vande Velde, G., Kucharikova, S., Schrevens, S., Himmelreich, U., & Van Dijck, P. (2014). Towards non-invasive monitoring of pathogen–host interactions during *Candida albicans* biofilm formation using in vivo bioluminescence. *Cellular microbiology*, 16(1), 115-130.
- Veneman, W. J., Stockhammer, O. W., de Boer, L., Zaat, S. A., Meijer, A. H., & Spaink, H. P. (2013). A zebrafish high throughput screening system used for *Staphylococcus epidermidis* infection marker discovery. *BMC genomics*, 14(1), 255.
- Yannai, S., Berdicevsky, I., Duek, L. (1991). Transformations of inorganic mercury by *Candida albicans* and *Saccharomyces cerevisiae*. *Applied and environmental microbiology*, 57(1), 245-247.
- Zhu, W., & Filler, S. G. (2010). Interaction of *Candida albicans* with epithelial cells. *Cellular Microbiology*, 12(3), 273-282.

Addendum A: Risk analysis

Risks for chemical substances

- Menadione is hazardous when swallowing and is irritating for skin and eyes and respiratory system. This substance should be discarded in waste category 3.
- RPMI-1640, though not hazardous, might be irritating for the eyes, skin and respiratory system. Contact with the eyes should be avoided and a lab coat and gloves should be worn.
- Thimerosal (solution in which microspheres are maintained) is classified as non-hazardous but might be irritating for the eyes and skin. Contact with the eyes should be avoided and a lab coat and gloves should be worn. Swallowing can cause damage to the person's health.
- Tricaine (CAS 886-86-2), which is used to anesthetize the zebrafish, contains 3-aminobenzoic acid ethyl ester (MS-222), and is categorized as an irritant. It is necessary to wear gloves and any spills should be wiped up promptly and completely. In the case that tricaine comes into contact with skin or the eyes, it should be rinsed with copious amount of water (Chemical safety: E1 – waste category 5).
- Sodium azide (solution in which microspheres are maintained) is classified as non-hazardous but might be irritating for the eyes. Swallowing can cause damage to the person's health.
- XTT is not classified as a hazardous substance but protective clothing such as a lab coat and gloves should be worn.

General precautions

During each experiment, a lab coat and gloves should be worn. All experiments with microorganisms should be carried out under the laminar flow to avoid cross contamination. All glass work, tips and media should be sterile (this is done by autoclaving). All waste should be discarded in the biological waste bin.

Caution must be taken when using flammable products such as ethanol, Alcolgel.

Precautions for the researcher:

All experiments were executed in a L2 laboratory because *C. albicans* is classified in risk class 2 for both humans and animals. The *C. albicans* SC5314 WT strain is a clinical isolate and is known to be highly virulent. Extra precautions must be taken for people with an impaired immune system. All work with this organism should be executed under the laminar flow class II. After each experiment, the surface must be cleaned with 70% ethanol or 5% Dettol and hands must be washed, followed by the application of Alcolgel.

Precautions for zebrafish work:

- Injection of the zebrafish embryos was executed in the aquatic facility at Gasthuisberg, Leuven. The care and housing of the animals was done according to the Standard Operating Procedures.
- After the experiment it is important to clean and decontaminate the work area with a disinfectant (Ummonium38)
- Needles should be discarded into specific containers after use.
- Scalpels need to be cleaned regularly and precautions must be taken when using these objects.

Risks due to physical handlings

- Sonication:

While sonicating, two hazards must be taken into account. The first hazard is the hearing damage caused by the high frequency sound. The second hazard is aerosol formation during the sonication. These aerosols are generated by cavitations of the sonicator horn in the sample media and mechanical mixing. During the sonication process a number of precautions must be taken; wear sound mufflers to protect from hearing, do not sonicate in a room with people not wearing ear protection and shut the doors of the room where the sonication takes place.

- Precautions for confocal laser microscope:

There is a risk that the reflected light may enter the eyes when the laser beam is being output from the objective mount hole. In this case, there might never be looked at the specimen while the laser is scanning. Hands might never be exposed to the laser beam output otherwise the skin can be damaged. Specimens should always be placed horizontally on the stage, otherwise the laser beam may reflect around the microscope. Do never put a flammable object near the air outlet of the laser cooling fan. Take precautions when using ethanol to clean the optics, as ethanol is highly flammable. Always wait 10 minutes to switch the reflected light power ON again after it is switched off, if not the life of the mercury bulb will be shortened. Avoid condensation of dew of the laser tube by preventing that heat enters the room, as this will lead to explosion of the latter.

Source: safety guide Olympus confocal laser scanning microscope, sonicator safety lab manager, HSE service KU Leuven.

Addendum B: Additional figures of dead embryos upon WT-GFP and *bcr1Δ/bcr1Δ*-GFP injection into the yolk of 1-cell stage zebrafish embryos.

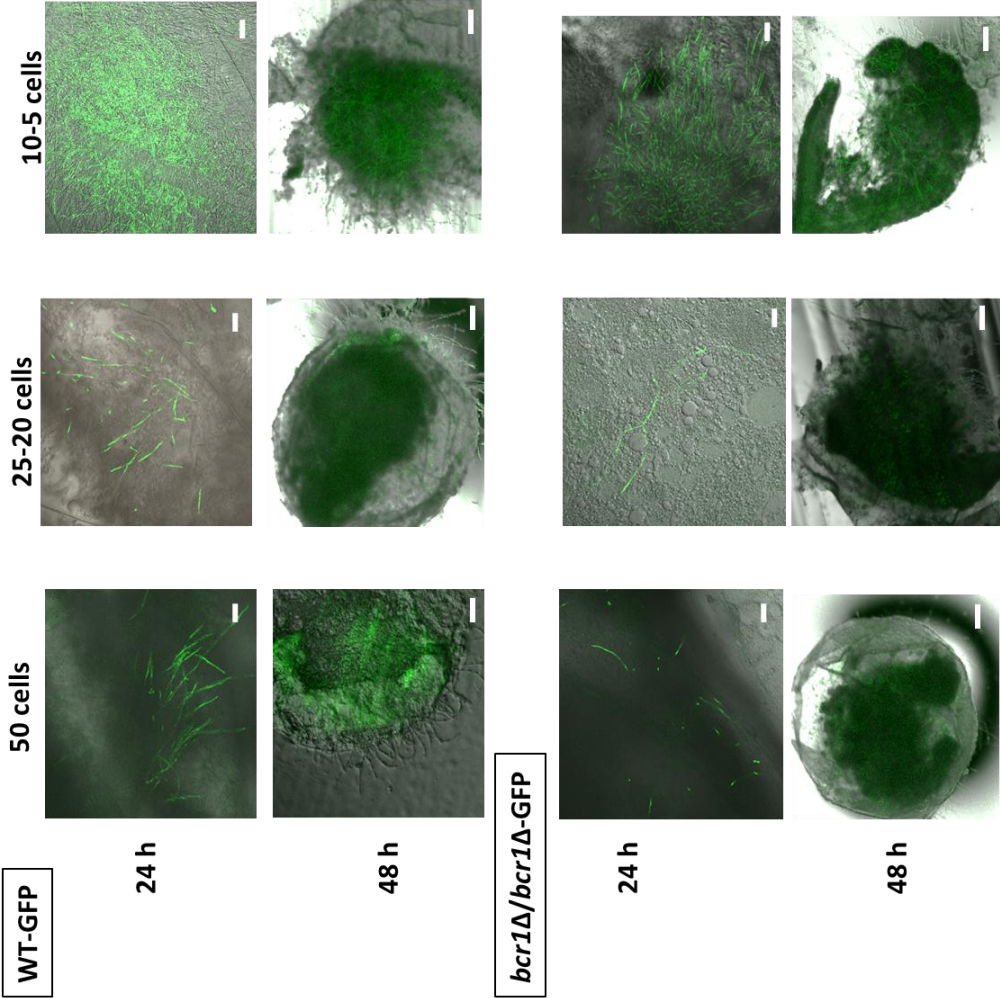


Figure B1: Confocal laser scanning images demonstrating *Candida* infection inside the yolk of zebrafish embryos. Zebrafish embryos were injected with WT-GFP or *bcr1Δ/bcr1Δ*-GFP into the yolk of 1-cell stage zebrafish embryos. The embryos were screened under the confocal microscope after 24 and 48 h post injection. Scale bar= 20 μm (pictures of 24h) and 100 μm (pictures of 48 h). Magnifications 10 x and 40 x.

Addendum C: Statistical significance after 1 and 2 days of *Candida*-yCherry and spheres and *Candida*-GFP and spheres injection into 1- cell stage zebrafish embryos.

Table C1: A summary displaying the statistically significant difference in the survival of zebrafish embryos upon WT-GFP, *bcr1Δ/bcr1Δ*-GFP (20 cells) and microspheres (50) injection. Survival was monitored for 6 days and statistics was done after 1 and 2 days. Significant when $p < 0.05$ (Logrank test).

Comparison of strains	Statistically significant ($p < 0.05$)	
	DAY 1	DAY 2
WT-GFP (20 cells) + 50 spheres WT-GFP (20 cells) alone	No	No
<i>bcr1Δ/bcr1Δ</i> -GFP (20 cells) + 50 spheres <i>bcr1Δ/bcr1Δ</i> -GFP (20 cells) alone	No	Yes
WT-GFP (20 cells) + 50 spheres <i>bcr1Δ/Δ</i> (20 cells) + 50 spheres	No	No
WT-GFP (20 cells) alone <i>bcr1Δ/bcr1Δ</i> -GFP (20 cells) alone	No	Yes

Table C2: A summary displaying the statistically significant difference in the survival of zebrafish embryos upon WT-yCherry, *efg1Δ/Δ cph1Δ/Δ*-yCherry (20 cells) strain and microspheres (50) injection. Survival was monitored for 6 days and statistics was done after 1 and 2 days. Significant when $p < 0.05$ (Logrank test).

Comparison of strains	Statistically significant ($p < 0.05$)	
	DAY 1	DAY 2
WT-yCherry + spheres WT-yCherry alone	No	No
<i>efg1Δ/Δ cph1Δ/Δ</i> -yCherry + spheres <i>efg1Δ/Δ cph1Δ/Δ</i> -yCherry alone	No	No
WT-yCherry + spheres <i>efg1Δ/Δ cph1Δ/Δ</i> -yCherry + spheres	No	Yes
WT-yCherry (20 cells) alone <i>efg1Δ/Δ cph1Δ/Δ</i> -yCherry alone	No	Yes

Addendum D: Survival experiment of *Candida*-yCherry and microspheres injection

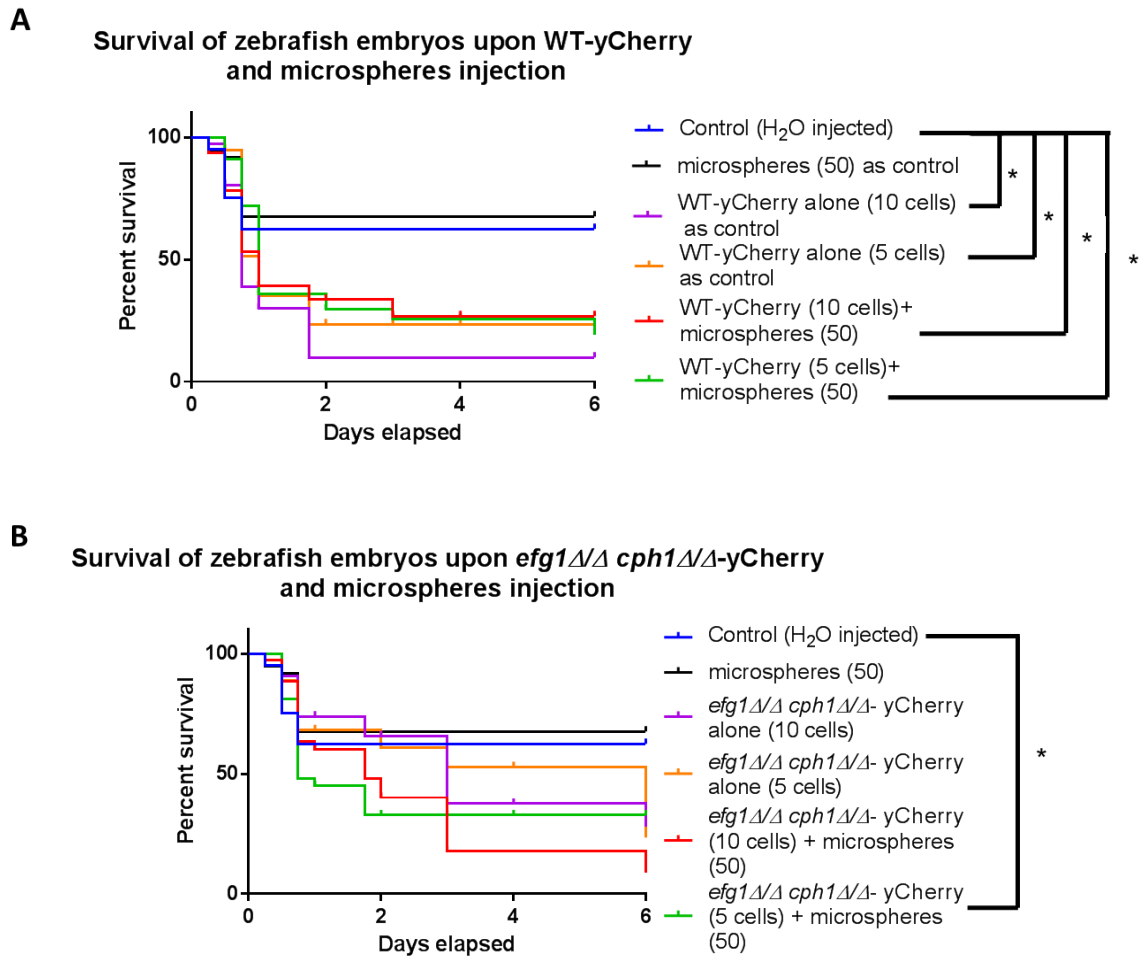


Figure D1: Survival curves of zebrafish embryos upon *Candida* and microspheres injection. Zebrafish embryos (at one-cell stage) were injected with 5 or 10 cells WT-yCherry (A) or *efg1Δ/Δ cph1Δ/Δ*-yCherry (B) in the presence or absence of spheres (50). The survival of zebrafish embryos was monitored after 4, 24, 30, 48, 72 h and 6 days post injection. Data represent a single experiment. Statistically significant when * $p < 0.05$ (Logrank test).

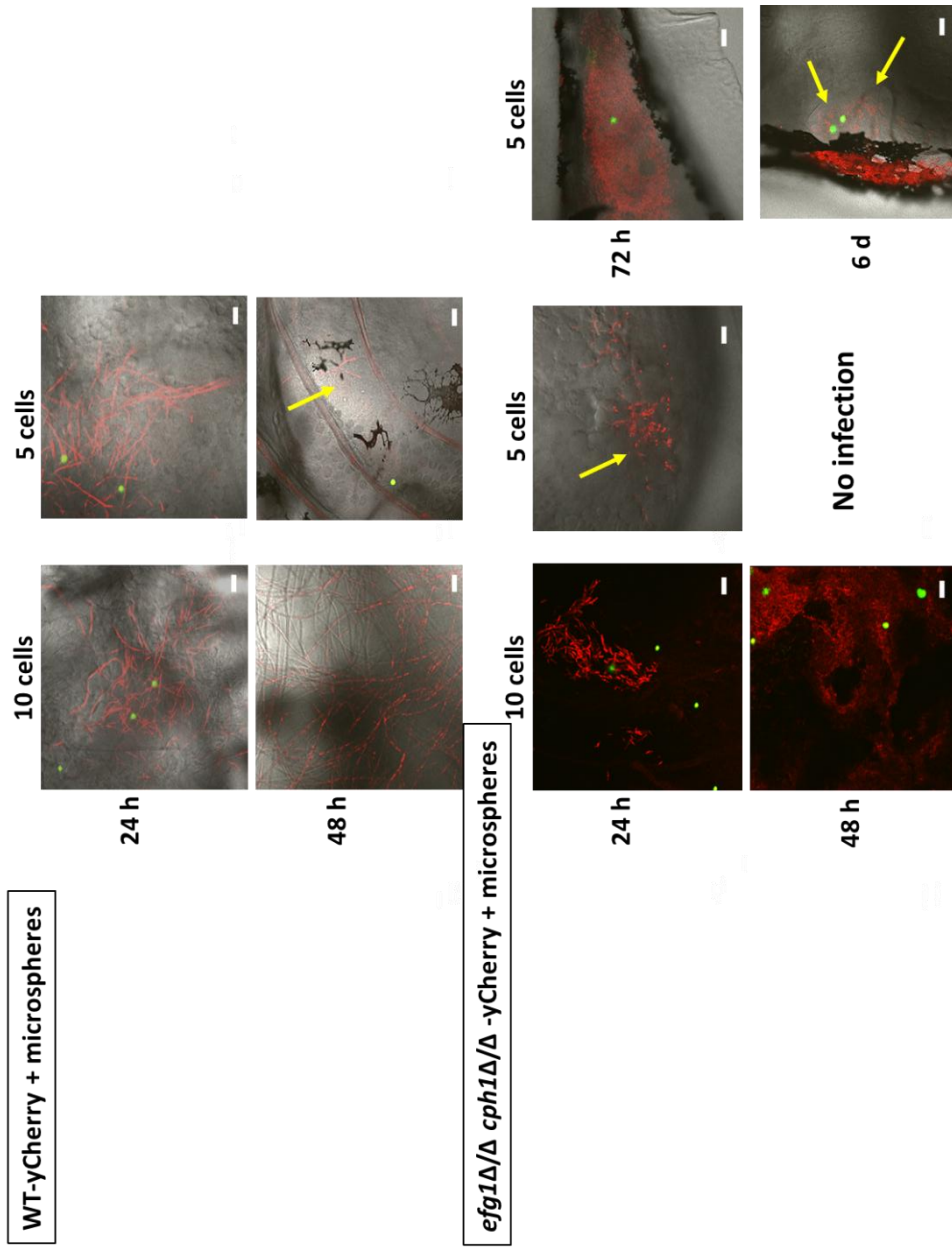


Figure D2: Confocal laser scanning images demonstrating *Candida* and microspheres infection inside the yolk of zebrafish embryos. Zebrafish embryos (at one- cell stage) were injected into the yolk with WT-yCherry or *efg1Δ/Δ cph1Δ/Δ*-yCherry (10 or 5 cells) in combination with microspheres (50). The embryos were screened under the confocal microscope after 24 h, 48 h and 72 h and 6 days post injection. Magnification 40 x. Scale bar= 20µm.

Table D1: A summary displaying the statistically significant difference in the survival of zebrafish embryos upon *C. albicans* WT-yCherry strain (5 and 10 cells) and *efg1Δ/Δ cph1Δ/Δ*-yCherry strain (5 and 10 cells) and microspheres (50) injection. Survival was monitored for 6 days and statistics was done after 6 days. Significant when $p < 0.05$ (Logrank test).

Comparison of strains	Statistically significant ($p < 0.05$)
WT-yCherry (10 cells) + spheres WT-yCherry (10 cells) alone	No
WT-yCherry (5 cells) +spheres WT-yCherry (5 cells) alone	No
<i>efg1Δ/Δ cph1Δ/Δ</i> -yCherry (10 cells) + spheres <i>efg1Δ/Δ cph1Δ/Δ</i> -yCherry (10 cells) alone	No
<i>efg1Δ/Δ cph1Δ/Δ</i> -yCherry (5 cells) +spheres <i>efg1Δ/Δ cph1Δ/Δ</i> -yCherry (5 cells) alone	No
WT-yCherry (10 cells) + spheres <i>efg1Δ/Δ cph1Δ/Δ</i> -yCherry (10 cells) + spheres	No
WT-yCherry (5 cells) + 50 spheres <i>efg1Δ/Δ cph1Δ/Δ</i> -yCherry (5 cells) + spheres	No
WT-yCherry (10 cells) alone <i>efg1Δ/Δ cph1Δ/Δ</i> -yCherry (10 cells) alone	Yes
WT-yCherry (5 cells) alone <i>efg1Δ/Δ cph1Δ/Δ</i> -yCherry (5 cells) alone	No

**AFDELING MOLECULAIRE MICROBIOLOGIE EN BIOTECHNOLOGIE
LABORATORIUM MOLECULAIRE CELBIOLOGIE**

Kasteelpark Arenberg 31 bus 2438
3001 LEUVEN, BELGIË
tel. + 32 16 32 15 12
fax + 32 16 32 19 79
patrick.vandijck@mmbio.vib-kuleuven.be

